Novel Artificial Urinary Sphincter for Stress Urinary Incontinence Treatment

A Thesis
SUBMITTED TO THE FACULTY OF
UNIVERSITY OF MINNESOTA
BY

Avishek Mishra

IN PARTIAL FULFILLMENT OF THE REQUIREMENTS
FOR THE DEGREE OF
MASTER OF SCIENCE

Gerald W. Timm, Ph.D.

September 2017

Acknowledgements

I would like to thank all the people who contributed material towards this research directly or indirectly. These especially include Drs. Gerald W. Timm and Sean Elliott, as well as, Dr. Badrinath Konety and Bhaskar Ravishankar. Dr. Timm's insightful suggestions as my adviser and his constant guidance and support in my ability to deliver were instrumental in developing the motivation and dedication I needed for the two years. His expertise in urological medical device innovation coupled with his entrepreneurial experience is unparalleled and was invaluable towards this research. Dr. Elliott's support for enabling the clinical studies that strengthened this research, and constant feedback on my work despite his busy schedule went a long way in shaping my research work.

I sincerely thank Dr. Badrinath Konety, who always listened to my research plans and offered to help advance the project and built a spirit of innovation, and research and development in the department through such efforts. I am also very grateful to my friend and lab colleague, Bhaskar Ravishankar. We built on our strengths and weaknesses and in the process taught each other all the time. Additionally, I would like to thank the administrative personnel, researchers, and nurses in the Dept. of Urology, including Elizabeth Mayock, Resha Tejpaul, and Kelly Ayd.

I am indebted to the Department of Electrical and Computer Engineering as well as the Department of Urology for providing a cohesive environment for my graduate studies and the resources necessary to fulfill all requirements for the program. The Department of Electrical and Computer Engineering was my first window into the world of technology and innovation outside India and soon Minneapolis, MN became a home away from home. The laboratories I have worked in, the students I have taught and studied with, the friendships and the connections I have built, my love for scientific curiosity and reasoning, and my restlessness to rid the world of conditions as degrading as urinary incontinence have shaped and molded me into my present self.

Dedication

This thesis is dedicated to my Dadu for teaching me that patience is an act of courage- the more we hear, the more we feel, the more we see, in return the more we learn. Learn to bring about change and challenge the status quo, learn to empathize, learn to build strong relationships and have the difficult conversations, learn to face adversity with humility, and learn to learn from one's mistakes.

This thesis is also dedicated in part to everyone who is suffering from cancer, fought and defeated cancer, succumbed to cancer, and their families and support systems, for having had the patience to fight through some bad days to sometimes earn the best days of their lives.

When a grandfather hallucinating in pain can remember his grandson's face as he walks up to his bed and he sits up to give him a hug with every healthy cell in his body fighting against a force so strong, just so that he could patiently love you as he did before- one realizes the importance of those lessons in patience being an act of courage.

There is almost no symptom more degrading or miserable than incontinence of urine; it inevitably brings at any stage after early childhood, shame, stink, soreness, and ostracism. It is hard to visit and love him.

– J.P. Blandy

(Quote from Tage Hald, and William E. Bradley. *The urinary bladder: neurology and dynamics*. Williams & Wilkins, 1982.)

Abstract

The American Medical System's AMS 800™ has been the gold standard for over 40 years with over 150,000 patients treated for Urinary Incontinence and is the leading treatment for male stress urinary incontinence (SUI) following prostate surgery. Type III SUI, or intrinsic sphincter deficiency, is the inability of the urethra to maintain closure pressure sufficient to keep the patient clinically dry at rest and during periods of heightened activity (~120 cmH_2O; coughs, sneezes, posture changes, and exercises). The current AMS 800™ is not personalized to a patient's needs and compromises with an in between pressure- as high (61-70 cmH_2O) as it can be without exceeding safety threshold levels. As such many men still leak when they are active. The market is hungry for a device that can adapt to the patient's level of activity, reducing pressure most of the day to protect the urethra and then briefly increasing the pressure when he is more active.

We are developing a novel implantable pump (henceforth called "add-on device") which will be an add-on to the AMS 800™ and it includes a solenoid coil-cum-plunger and a fluid reservoir within the pump body. The add-on device will be small, light-weight and battery powered, and maintain compatibility with the AMS 800™ device. The device idea is in its proof-of-concept stage. This add-on device can be a possible solution to reducing the risks including urethral atrophy (leading to return of incontinence) and erosion (leading to infection of the implant) resulting from the constant pressure.

Table of Contents

List of Tables

List of Graphs

List of Figures

Introduction

1.1. The Lower Urinary Tract System

The lower urinary tract system (LUTS), (Figure 1.1) consists of the bladder and urethra in females and additionally, a prostate in males [1]. Sexual function and pelvic anatomy bring about significant variability in male and female LUT anatomy. While the kidneys are responsible for changing the composition and amount of urine, the LUTS is solely responsible for periodic elimination of urine [2].

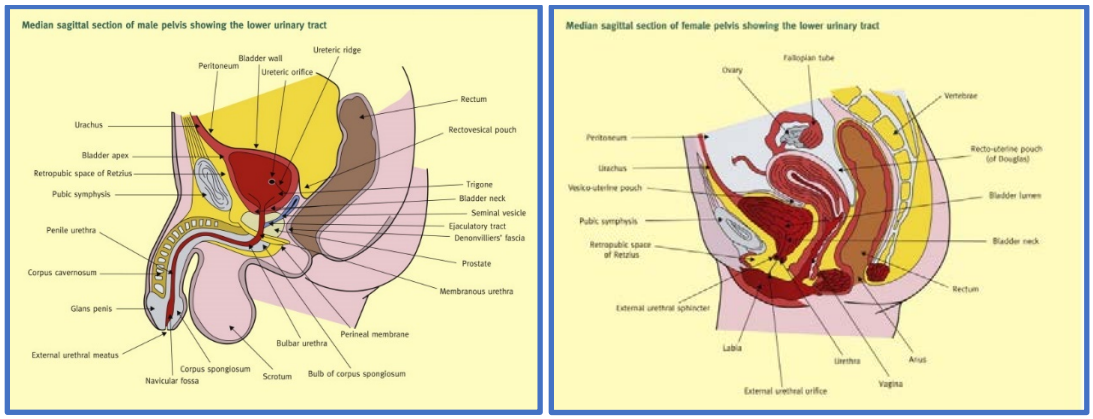

Figure 1.2. Median sagittal section of the male and female pelvis showing the Lower Urinary Tract [1]

In infants, the bladder lies in the abdomen but with growth the pelvic bone develops and the bladder positions itself within the pelvis. The LUTS is susceptible to various disorders including overactive bladder, urinary incontinence (topic of this thesis), and prostatic and bladder carcinoma. This section will cover the anatomy, physiology, and histology of the bladder and the urethra.

1.1.1. The Urinary Bladder

The urinary bladder as shown in Figure 1.2, is a hollow muscular organ capable of storing urine and expelling it when socially acceptable. In males, it is superior to the prostate gland and in females, it is inferior to the uterus.

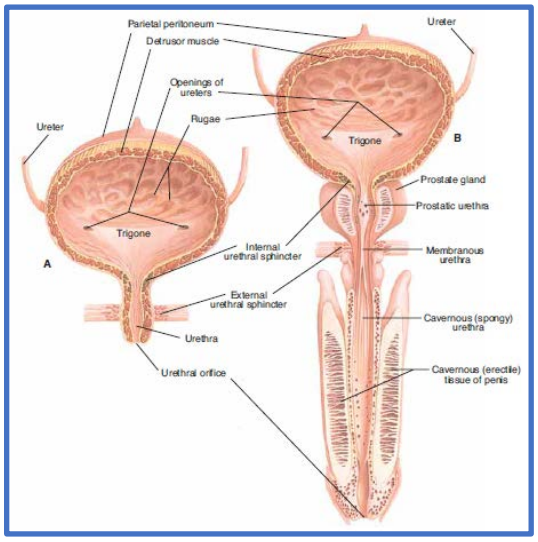

Figure 1.2. (A) Frontal section of the female urinary bladder and urethra, **(B)** Frontal section of the male urinary bladder and urethra along with the prostate [2]

The internal walls of the bladder are made up of several folds which allow the bladder to increase its capacity, for instance, at times when it is socially unacceptable to void one's bladder. The transitional epithelium appears wrinkled when the bladder is empty and expands as urine fills up the bladder. As seen in Figure 1.2, the trigone is a triangular area inferior to the apex of the bladder which does not have the expandable transitional epithelium, also referred to as rugae, and is the site where the two ureters and the urethra have their openings [2].

The musculature in the bladder that develops contractions within it are smooth detrusor muscles and as they accumulate around the urethral opening in the trigone, the muscles form the internal urinary sphincter which is an involuntary muscle. The urinary bladder has two principle functions [1]:

- Reservoir for storage of urine- An adult bladder can store 500 ml of urine with excellent compliance which implies that it can store large volumes with minimal changes in pressure. Higher pressures at high volumes would lead incontinence or damage to the kidneys.
- Generate sufficient pressure- Synchronized contractions of the detrusor muscle which initiates the voiding reflex called micturition (discussed in Section 1.1.3).

1.2. The Urethra

The urethra (Figure 1.3) stems from the trigone and trigonal urethral opening, as discussed earlier is surrounded by the internal urinary sphincter (also called the sphincter of the bladder). This research deals with the male urethra and the next few sections will deal with some important parts of the urethra that are essential in explaining urinary incontinence, it treatment and the risks from the treatment options.

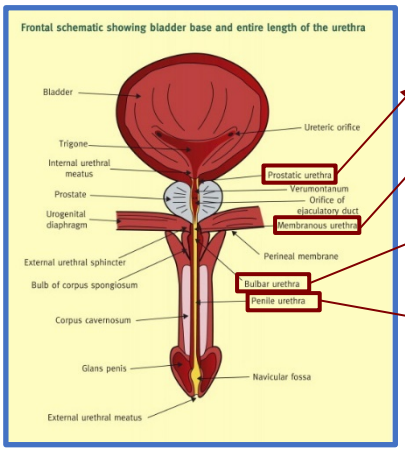

Figure 1.3. Frontal schematic showing bladder base and entire length of the urethra [1]

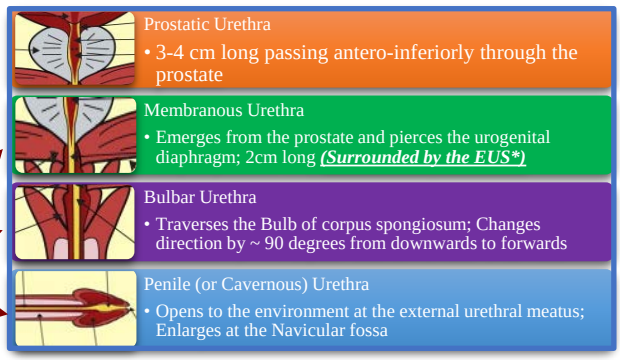

Figure 1.4. Anatomical sections of the male urethra including the smaller posterior urethra (prostatic and membranous urethra) and the longer anterior urethra (bulbar and penile urethra) [1] (*EUS: External Urethral Sphincter)

Clinicians must keep in mind that the urethra changes direction suddenly at the end of the bulb of corpus spongiosum and care should be taken while inserting catheters for cystometric and other urodynamic studies. As we proceed further, we will extensively cover the risks of implanting an artificial urinary sphincter (AUS) to treat stress urinary incontinence. Prior to that, one must understand the vasculature (blood supply) to the urethra- the internal pudendal arteries predominantly supply blood to the urethra and urethral and penile blood drainage is through the internal pudendal vein [1].

1.2.1. The Internal and External Sphincter

The internal sphincter at the bladder neck is formed by the smooth circular detrusor muscles and its physiology is better developed in males than females. The internal sphincter, also referred to as the "pre-prostatic" sphincter prevents retrograde emission of semen and contributes to urinary continence [1]. The external sphincter is secondary for continence [3].

The male external sphincter, also called the striated urethral sphincter is an integral component of the LUTS for preserving an individual's ability to micturate. This complex musculature that forms the pelvic floor is innervated by the sacral nerve roots from the spinal cord [3]. In the previous section, where we discussed the different sections of the urethra, the naming of the membranous (Figure 1.4) urethra is considered a misnomer, and this has led to several problems in defining the anatomy and physiology of the external sphincter [3], [4]. The membranous urethra extends from the apex of the prostate to the corpus spongiosum. Several anatomical papers have discussed the importance of reaching a consensus surrounding the accurate nomenclature and recommendations have been made to change it to "sphincteric urethra" [3], [5]. Henceforth, the membranous urethra will be referred to as the sphincteric urethra.

The striated urethral sphincter (s) as shown in Figure 1.5, is formed by the levator ani (la; Figure 1.5) musculature and in contact with the corpus spongiosum. Prominent contributions on the urethral sphincter came from researchers like Henle, Holl, and Kalischer in the 19th Century.

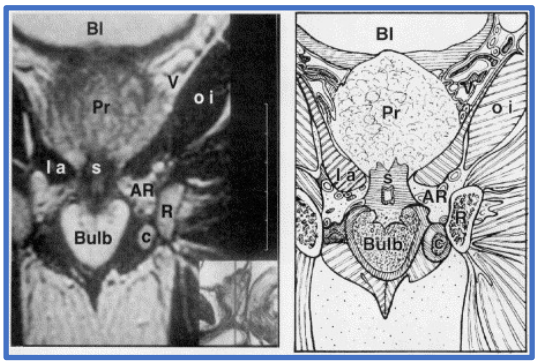

Figure 1.5. "Sphincteric urethra" might be more appropriate than "membranous urethra." Coronal view through bladder @I), prostate (Pr), striated urethral sphincter (s), bulb, veins (V), obturator internus (oi), levator ani (la), anterior recess (AR) of ischioanal fossa, ischopubic ramus (R), and corpus cavernosum (c). (Sagittal inset for orientation.) [4]

The internal sphincter with its smooth muscles and elastic tissues is the primary sphincter [3], and in the presence of bladder neck dysfunction, the internal sphincter is essential for urinary control. An interesting find by Ficazzola and Nitti [7] was that incontinence after either transurethral or radical prostatectomy (RP) was attributed more to internal sphincteric deficiency than the external sphincter. In cases where the internal sphincter around the bladder neck failed, preservation of the external sphincter gained paramount importance. We will deal with prostatectomy in more detail in a later section.

Henle was the first in discovering that the urethral sphincter was composed of smooth and skeletal muscles, and he named this sphincter as the *sphincter vesicae externus* (Figure 1.6, {8}) to distinguish it from the smoother *sphincter vesicae internus* (Figure 1.6, {6}) [6].

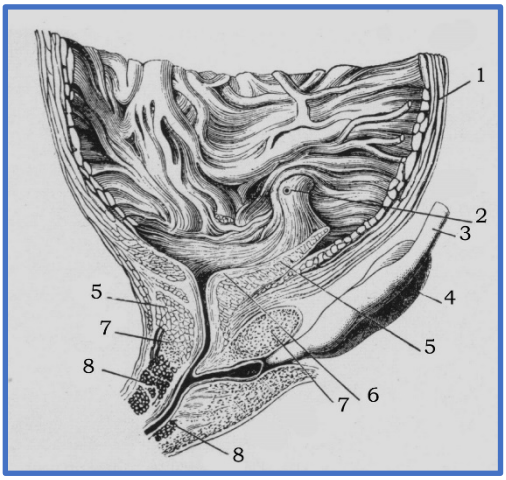

Figure 1.6. Median section of bladder and urethra according to Henle.*1*, bladder muscle wall. *2*, ureteral orifice. *3*, vas deferens. *4*, seminal vesicle. *5*, sphincter vesicae internus. *6*, trigone longitudinal muscle layer. *7*, prostate. *8*, sphincter vesicae externus. [6]

1.2.2. The Prostate

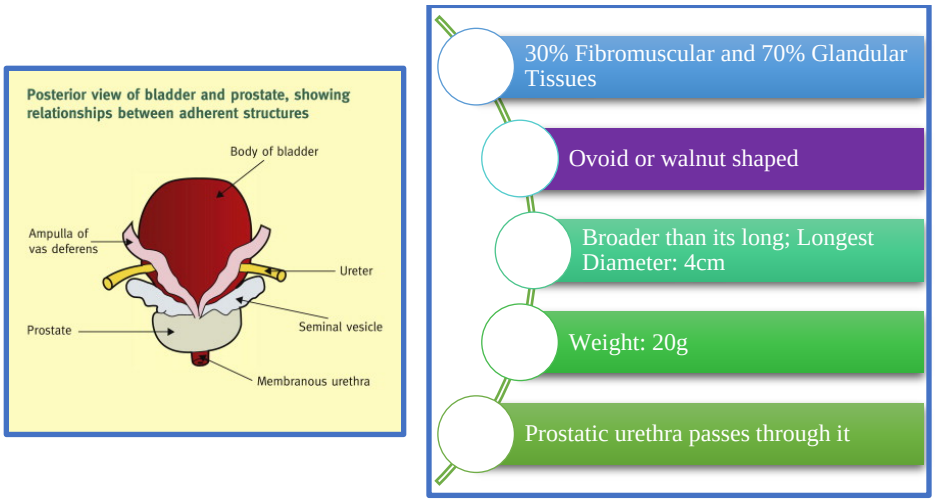

Figure. 1.7. Posterior view of the bladder and prostate, showing relationships between adherent structures and some physical characteristics of the prostate. [1]

Like controversies surrounding the accurate nomenclature of the "membranous urethra", several articles illustrate the controversies surrounding the anatomy of the prostate. However, for 25 years, John E. McNeal [8] presented his view of the prostate anatomy in terms of 4 anatomic zones [9].

The Peripheral Zone	70% glandular prostate Almost all carcinomas arise here Ducts are lateral and distal to urethra	**The Central Zone**	25% of the glandular prostate Lateral border fuses with proximal peripheral zone.	**The Preprostatic Zone**	The urethral segment Intimate relationship to a periurethral smooth muscle sphincter	**The Anterior Fibromuscular Stroma**	Entire anterior surface of prostate Non-glandular apron Inseparably fused to the glandular regions; shields the glands

Table 1.1. McNeal's 4 prostatic anatomical zones (regarding urinary continence Zone 3 plays a vital role). [8], [9]

To understand the four anatomic zones of the prostate, McNeal divided the prostate with three reference planes [8], which are as follows (Figure 1.8. (iv)):

- Sagittal plane: bisects the gland and reveals the urethral lumen in its full extent

- Coronal plane: shows both the ejaculatory ducts and the distal urethra longitudinally
- Oblique coronal plane: If the coronal plane is rotated by 35 degrees around the transverse axis that passes through the kinking in the urethra and follows the proximal urethra into the bladder.

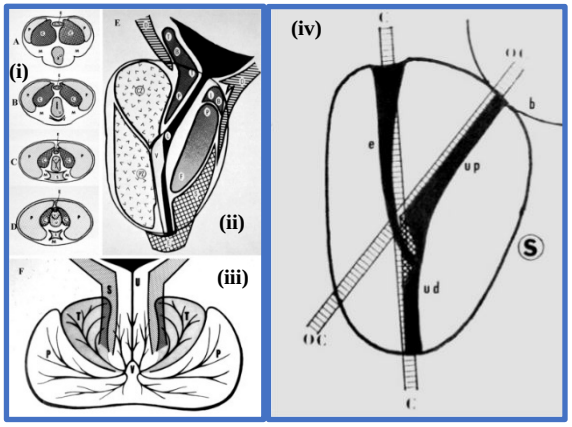

Figure 1.8. **(i)** Sections of the Central and Peripheral zones taken perpendicular to the urethra. **(ii)** Sections of the prostate as seen from a sagittal plane. **(iii)** Transition zone of prostate introduced in 1978 as the site for development of Benign Prostatic Hyperplasia. [9].
(iv) The sagittal (S), coronal (C), and oblique-coronal (OC) planes that highlight the ejaculatory ducts, the distal and the proximal urethra. [8]

Figure. 1.8. (iv) highlights the importance of maintaining extreme care during transurethral or radical prostatectomy to allow the bladder to preserve urinary control. A review by S. Selman [9] to understand the progression of McNeal's anatomical zones brought forth some interesting points regarding the preprostatic sphincter in the preprostatic zone (described in Table.1). McNeal's work published in 1972 [10], divided the prostatic urethra into two segments- the proximal and distal urethra (Figure 1.8. (ii);(iv)). The proximal urethra, also referred to as the preprostatic segment gave rise to the urethral glands and was surrounded by the cylindrical urethral sphincter, referred to as the "preprostatic sphincter" [9], [10]. This implies that sphincter, both internal and external includes the smooth sphincteric muscles around the bladder neck, the preprostatic sphincter in the proximal urethra, and the striated external sphincter muscles beginning at the caudal limits of the verumontanum.

1.2.3. Micturition- The Urination Reflex and its Neural Pathways

Having understood the anatomy and physiology of the sphincters and the prostate, understanding the voiding reflex or micturition will help us understand the different kinds of pressures applied on the bladder and the urethra.

This spinal cord reflex allows exertion of voluntary control [2] and the stimulus is the stretching of the detrusor muscle. As the bladder fills up and the folds (rugae) of the inner lining begin to stretch, the sacral section of the spinal cord receives a sensory input, which activates motor impulses via the parasympathetic nervous system to induce detrusor contractions [2]. The internal urethral sphincter involuntarily relaxes, now subjecting the entire bladder pressure on the external sphincter over which we have voluntary control. Once we relax the external urethral sphincter, urine flows out of the urethra and empties the bladder [2].

As discussed in Section 1.2.1, the internal sphincter is the primary sphincter and the external sphincter is the secondary sphincter. Voiding is situational and changes over time because of the state of the bladder [3], [11], [12], for instance situations like physical activity, auditory stimuli, fear and anxiety [3]. Yoshimura et al. found that micturition does not occur unless the urethral wall smooth muscles and the external sphincter contract. Micturition is controlled by the parasympathetic, sympathetic, and pundedal nerves (Figure. 1.9) [3], [11]. Studies have shown that the striated muscles of the external sphincter are 100% slow-twitch while the periurethral levator ani (Figure. 1.5) musculature is an amalgamation of slow and fast-twitch fibers [13]. This implies that the former passively assists in urethral closure once micturition is complete, while the latter is actively involved in maintaining musculature tone over prolonged periods to preserve continence, especially during events which cause an increase in intra-abdominal pressure [13]. From

my understanding, the levator ani musculature augments the urethral external sphincter's functionality in maintaining continence.

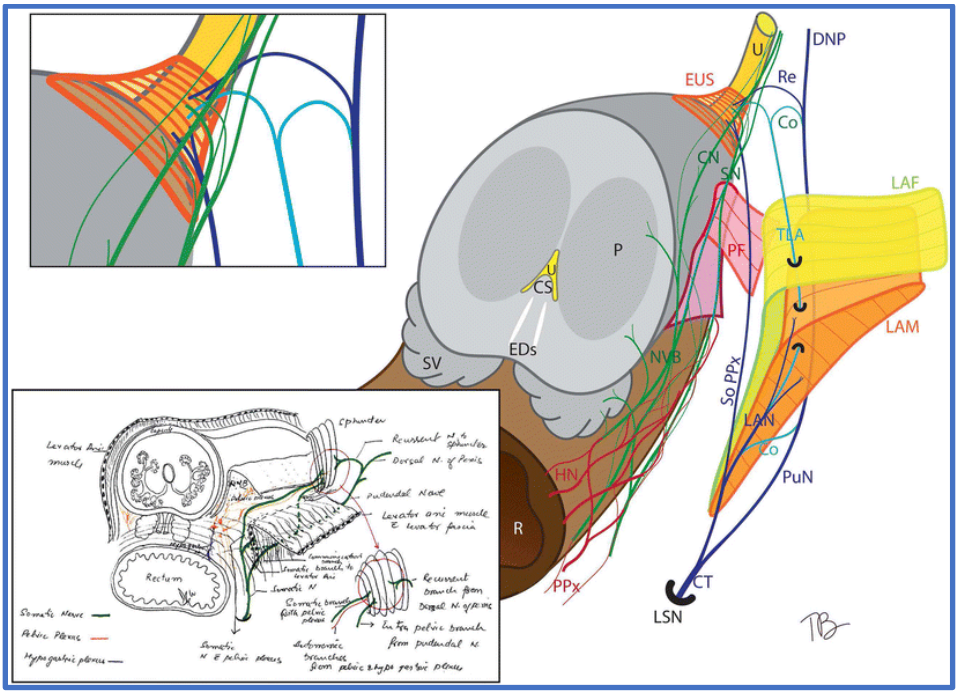

Figure 1.9. Integrated representation of the possible Urethral Sphincter (US) innervation pathways.
Somatic pathway in *dark blue*; neurovascular bundle in *green*; pelvic plexus in *red*; communications in *light blue*.
Co communicating branches, *CN* cavernous nerve, *CS* colliculus seminale, *CT* common trunk of the LAN and PuN, *DNP* dorsal nerve of the penis, *EDs* ejaculatory ducts, *EUS* external urethral sphincter, *HN* hypogastric nerve, *LAF* fascia of levator ani, *LAM* levator ani muscle, *LAN* levator ani nerve, *NVB* neurovascular bundle, *P* prostate, *PF* pelvic fascia, *PPx* pelvic plexus, *PuN* pudendal nerve, *Re* recurrent branches of the DNP, *SoPPx* somatic pelvic plexus, *SN* spongious nerves, *LSN* lesser sciatic notch, *SV*

The reason for introducing the innervation pathways of the external sphincter is to build our pre-requisite knowledge on the etiology of incontinence stemming from neural injury post radical or transurethral prostatectomy, pelvic surgery, spinal cord injury, or traumatic brain injury. From my understanding, there is significant complexity involving cross-communicating branches which brings in an element of neuroplasticity in the neuroanatomy of the external urethral sphincter [14].

1.2.4. Urodynamic Terminologies- Pressure Profiles [15]–[17]

Intravesical Pressure (P_{ves})
- The pressure within the bladder; [15], [16]
- The pressure recorded from a urodynamic catheter inside the bladder (Figure 1.12 (ii))

Abdominal Pressure (P_{abd})
- Pressure surrounding the bladder; [15], [16]
- Estimated from rectal, vaginal, extraperitoneal, or bowel stoma

Detrusor Pressure (P_{det})
- Component of intravsical pressure created by forces in the bladder wall (passive and active) ;
- $P_{det} = P_{ves} - P_{abd}$; [15], [16]

Cystometry
- Measurement of the pressure/ volume relationship of the bladder during filling and voiding. [15]

Maximum Cystometric Capacity
- Volume at which a patient has a strong desire to void. [17]

Effective Cystometric Capacity
- Maximum cycstometric capacity minus the residual urine. [17]

Bladder Compliance
- Change in bladder volume and change in P_{det}. [17]

Flow Rate
- Voluime of fluid expelled via urethra per unit time

Table 1.2. Urodynamic Terminologies used by Clinicians

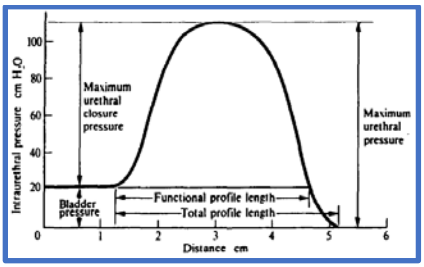

Figure 1.10. Schematic representation of urethral closure pressure profile [17]

"Urethral closure pressure is the intraluminal pressure along the length of the bladder with the bladder at rest. Maximum urethral pressure is the maximum pressure of the measured profile (Figure 1.10). Maximum urethral closure pressure (MUCP) is the difference between the maximum urethral pressure and bladder pressure" [17].

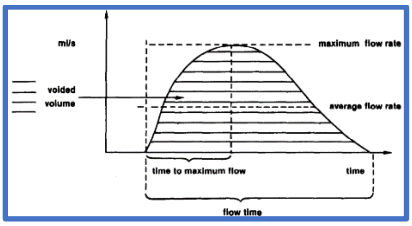

Figure 1.11. Diagram of continuous flow curve [17]

Continuous flow (Figure 1.11) as described in [17] is in terms of flow time, which is "the time over which measurable flow occurs" and the time elapsed to reach maximum flow rate (highest point in the 'bell' curve; Figure 1.11) is called maximum flow time. The

area under the curve gives the voided volume and the average flow rate is the voided volume divided by flow time [17].

Intermittent flow or continuous flow with substantial terminal dribbling (Figure 1.12. (i)) brings into picture the difference between voiding time and flow time. Unlike continuous where the flow time and voiding time are equal, under a scenario with an intermittent flow, the flow time is different from voiding time [17]. As highlighted in Section 1.1.3, voiding is subject to changes in environment (temperatures falling), auditory stimuli, physical activity, or fear and anxiety. The implication is that when flow and pressure measurements are taking in a clinic, the readings will have certain inaccuracy stemming from the mentioned changes and activities. This creates a challenge when the readings are being used to diagnose a disease condition.

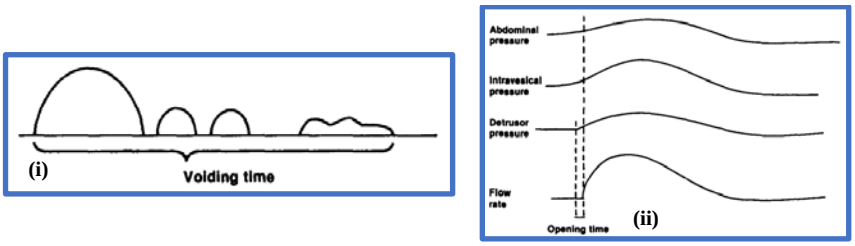

Figure 1.12. (i). Diagram of intermittent flow. **(ii)** Diagram of corresponding pressures and curves of flow. [17]

1.2.5. Urodynamics and Continence

Micturition when seen as a physical phenomenon can only occur when a gradient is established allowing urine to flow out. This means that urine flows from a point of high pressure to a point of low pressure. When the sphincters are observed as physical resistances or obstructions that resist urine flow out of the urethra, it means that the resistance must reduce to facilitate micturition. The smooth detrusor muscle is made of several contractile myofibrillar units [18] which begin the stretching of the bladder as it

fills up with urine. As the bladder stretches and engages several myofibrillar units, the muscles are under tension and gather significant force that sends out nerve impulses to the sacral spinal segments to produce a muscle contraction. The tensions stored in the contractile units is one aspect, the other is the velocity at which this tension is released and the detrusor muscle units come back to their original position and in doing so push out fluid from the bladder. Contraction velocity [18] has an inverse relationship with the force stored in the muscles. Instances where the muscle fibers are elongated and in tension, upon release, the contraction velocity increases and so does the flow rate. As we near the end of complete voiding, the contraction velocity reduces thereby reducing the flow rate. The detrusor muscles are mostly made of "slow-twitch" muscles (Section 1.2.3) but it's anatomy is like striated and cardiac muscles and three times slower [18], [19].

From an energy perspective, when the myofibrillar units are stretching as urine fills the bladder, sufficient potential energy is being built up and when the urethra opens, 90% of the energy is converted to kinetic energy [18] and the rest is lost as heat because of friction against the urethral walls. There are two types of muscle contractions- isotonic and isometric contractions. Isotonic contractions are those where the tension remains the same and the muscle length changes, while isometric are those where the muscle length does not change. The contraction of the detrusor muscle is initially isometric and as the bladder empties, it becomes more isotonic [18].

Hald and Bradley [18] elaborated on some of the factors that affect urinary continence and some of them are listed in Figure 1.13. The bladder factor includes increased stiffness, detrusor over activity, and lack of detrusor contractility. The urinary bladder is a visco-elastic and this important physical characteristic affects the detrusor reflex. Researchers in the late 1960s demonstrated transmission on intra-abdominal

pressure on bladder and urethra and also showed that pressure rise in urethra is higher owing to the possible existence of the striated sphincter reflex contraction [18]. The striated urethral sphincter has been known to maintain passive continence in addition to active continence. Since the load on the closed sphincter is low, it requires less force to prevent incontinence.

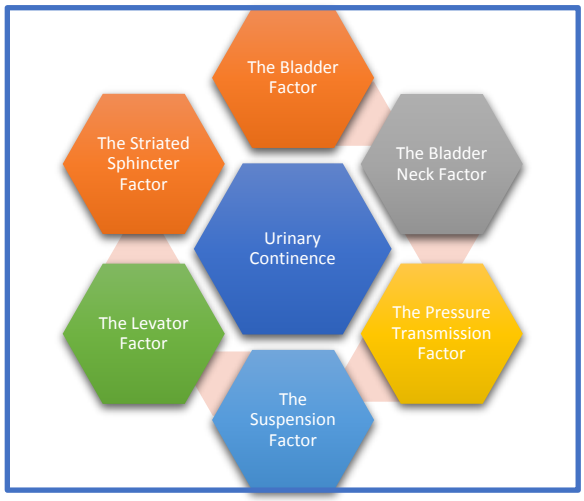

Figure 1.13. Factors affecting Urinary Continence [18]

2. Prostate Cancer: Epidemiology and Treatment

2.1. Global Incidence of Prostate Cancer

Prostate cancer affected 1.4 million men in 2013 leading to 293,000 deaths and rendered 4.8 million men to live with some form of disability [20]. Incidence was higher in developed countries because of lifestyle and a higher aging population. Younger countries like those in Asia, experienced the lowest incidence of prostate cancer. In 2013, prostate cancer was the leading cause of death in men in 24 countries. Prostate cancer is one of the most common cancers diagnosed in men. The number of incident cases increased four-fold in 2013 when compared with 1990 because of an aging and growing population. Overall, incidence of prostate cancer is rising in most countries while in some the numbers have stabilized. Figure 2.1 gives an insight into the incidence and mortality of prostate cancer in 2012. An interesting data point from the graph is that the mortality in less developed regions is higher than the more developed regions but the incidence rates are significantly higher in developed regions of the world. This ties into the availability of prostate cancer early detection programs in some countries.

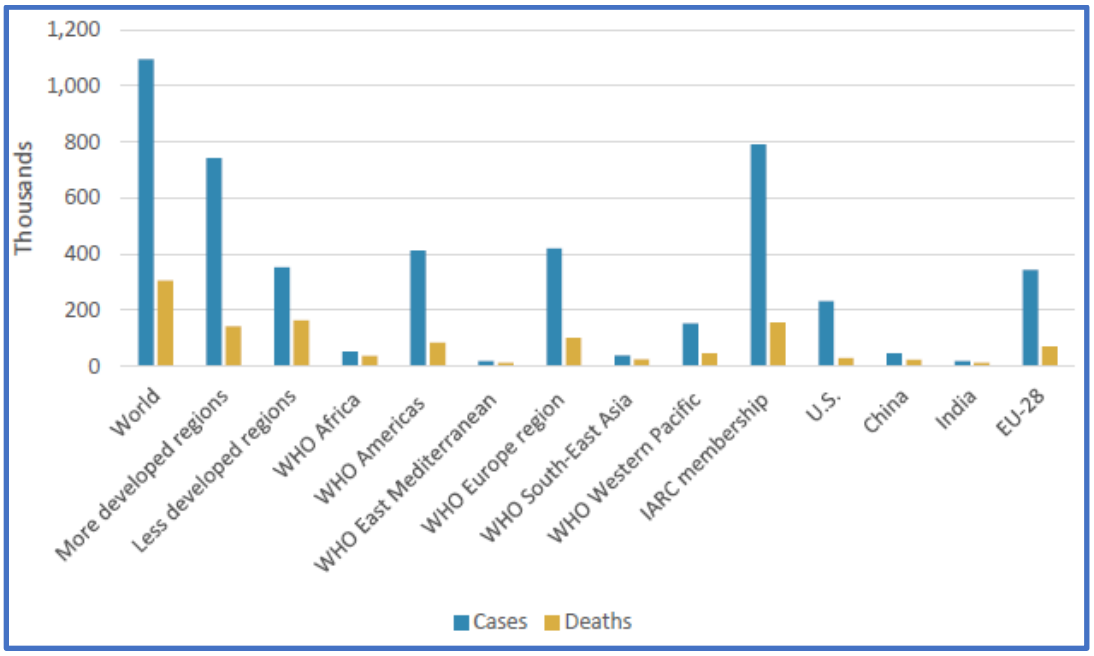

Figure 3.1. Prostate Cancer and mortality global, 2012 (Source: International Agency for Research on Cancer, GLOBOCAN), *[20]*

An estimated 307,000 men died in 2012 from prostate cancer making it the 5th leading cause of death in men. For the period of 2012-2020, trends in incidence rates suggest that the rise in prostate cancer in developing countries will be 1.6 times that in developed countries. The disease is expected to see 499,00 deaths by 2020 [20].

2.2. Prostate Cancer in the United States

"One in seven American men will have prostate cancer during his lifetime.[20]*"*

The American Cancer Society estimates that currently there 2.8 million men living with prostate cancer and 10.7% of new cancer cases are prostate cancer cases. Prostate cancer occurs in older men and the risk of developing it increases exponentially between 40-69 years of age.

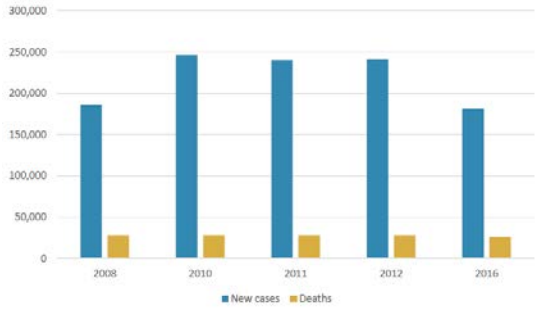

Figure 2.2. Prostate Cancer cases in the US, 2008-2016 [20].

2 million men living in the US live with prostate cancer and a whopping 17% will be diagnosed with this cancer. This cancer is rare before age 40 and two-thirds of men diagnosed with prostate cancer are aged 65 years or older.

2.3. Treatment for Prostate Cancer

Radical prostatectomy with some variations is the treatment option for Stage I-III prostate cancer. External beam radiation therapy and interstitial implantation of radioisotopes are used in treating this cancer in its Stage I and II. Radical prostatectomy involves the removal of the prostate gland, some surrounding tissues and a few lymph nodes [20]. There are different ways to perform this surgery:

- Robot-assisted surgery
- Incision in abdomen
- Incision between anus and scrotum
- Laparoscopic Prostatectomy
- Cryoablation

There are two types of radical prostatectomy (RP): retropubic and perineal prostatectomy. The former involves the removal of prostate and nearby lymph nodes through an incision in the abdominal wall, while the latter involves removal of prostate through an incision made in the perineum.

"Impotence and leakage of urine are some complications of surgery. [20]*"*

3. Radical Prostatectomy and Incontinence

Urinary incontinence is a major complication that affects several patients who undergo radical prostatectomy. Caregivers keep a track of micturition diaries, conduct pad tests, urodynamic studies and cystoscopy to understand the cause of incontinence in these patients. Post-prostatectomy urinary incontinence has been attributed to sphincter malfunction, detrusor abnormalities, and urinary retention with overflow [21]. Chao et al. [22] examined urodynamic record of 74 patients with urinary incontinence significantly affecting quality of life of patients post- radical prostatectomy. Of the 74 men, 42 had sphincter weakness alone, 29 had detrusor instability and/or decreased compliance combined with sphincter weakness and only 3 had just detrusor instability. The reason for an increased susceptibility to detrusor instability and sphincteric malfunction has been attributed alterations in bladder and bladder outlet anatomy [23]. Most patients post-RP strain their abdomen to void their bladder because of detrusor underactivity and this directly affects treatment options for stress urinary incontinence which will be discussed in detail in later sections.

Detrusor underactivity as defined by the International Continence Society is the "contraction of reduced strength and/or time resulting in prolonged bladder emptying and/or failure to achieve complete bladder emptying with a normal time span [23]." Maffezzini et al. collected data from 265 patients out of the 300 patients they were evaluating for post-RP complications and they found that at a median follow-up of 29 months, 262 patients were continent and 26 had stress incontinence with varying intensities who had to wear one to three pads per day, and 7 patients were incontinent

and had to wear 4 or more pads. However, 80% to 93% regained urinary continence after a variable period of 3-24 months [24]. Maffezzini's review of literature in Figure 3.1, compared the study with others in the 1991-2000 period, and found that the recovery of continence was in a short time span and almost 48.2% of the incontinent patients achieved complete urinary control. Different studies employed varied methods to collect the data but most had on an average 3-16 weeks to recover continence.

Investigator	Patients (n)	Continence (%)	Time (mo)	Assessment
Steiner *et al.*,[4] 1991	593	Complete 93 Stress incontinence 8 Artificial sphincter 0.3	3–24	Patient report, interview
Geary *et al.*,[5] 1995	458	Complete 80 Stress incontinence 14.7 Incontinence 5.3	3–12	Follow-up visits
Eastham *et al.*,[6] 1996	581	Complete 91–94 Stress incontinence 4–5 Incontinence 2–4	24	Patient interview, mailed questionnaire
Catalona *et al.*,[7] 1999	1325	Complete 92 Stress incontinence 7.9 Incontinence 0.1	<18	Patient report
Present study	300	Complete 88.8 Stress incontinence 8.8 Incontinence 2.3	48.2% immediate 4 wk (2–16)	Direct observation, telephone interview

Figure 4.1. Continence Rates and time to recovery in contemporary series of the past decade *[24]*

Sphincteric malfunction is usually observed as constant, dribbling, gravitational, or stress-induced incontinence. On the other hand, patients who show signs of urge incontinence have detrusor abnormalities. Sometimes, both sphincteric malfunction and detrusor abnormalities can exist in a patient [21]. Several review studies trying to understand the causes of post-RP incontinence have listed the SAME in Figure 3.2. Some etiologies mentioned in the figure are mutually dependent and occur at the same time. Detrusor instability includes low bladder compliance, involuntary detrusor contractions, and impaired or absent detrusor contractility [21].

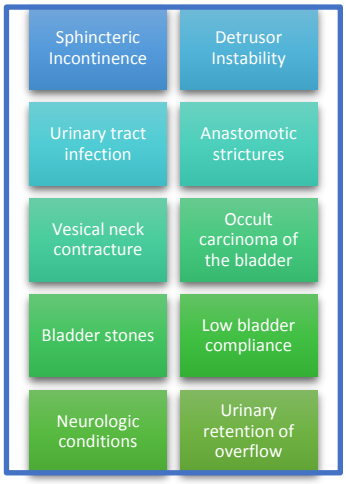

Figure 3.2. Etiology of Postprostatectomy Incontinence. [21], [23], [24]

Sphincteric incontinence can be recovered from within months post-RP, but there are patients who have this complication intermittently and lasts for months. Apart from inconveniencing the patient it further affects the psychology of a patient who has just been out of a cancer surgical treatment. Some patients with incontinence that shows signs of improving use absorbent pads, but for severe incontinence patients use condom catheters or undergo surgery. Pharmacological solutions, electrical stimulation, and biofeedback are some possible solutions for treatment of incontinence but significant clinical evidence does not exist [21]. Physicians recommend surgery to treat incontinence usually after a year has elapsed from prostatectomy, but if the incontinence incidents are severe and do not seem to improve, surgery is recommended earlier. Physicians have to weigh the cost of surgery against the possibility that a patient's conditions might improve suddenly and he will be continent henceforth. Sphincteric prostheses have been the mainstay of sphincteric incontinence and will continue to be and most physicians prefer using the sphincter prosthesis by American Medical Systems (AMS), Minnetonka, MN, USA.

4. Urinary Incontinence: Stress Urinary Incontinence

As defined by the International Continence Society (ICS), urinary incontinence is “a condition where involuntary loss of urine is a social or hygienic problem and is objectively demonstrable [17]”. Urinary incontinence may or may not be termed as a problem based on what is acceptable in one society and to one person may be unacceptable in another environment and to other persons [17]. For this reason, the words “social and hygienic” bring in a factor of variability in the above definition. Urinary Incontinence was and still is defined by symptoms, signs, physical conditions, etiology, age, occurrence, and anatomical factors [18]. Therefore, there exists a need to classify urinary incontinence per different criteria.

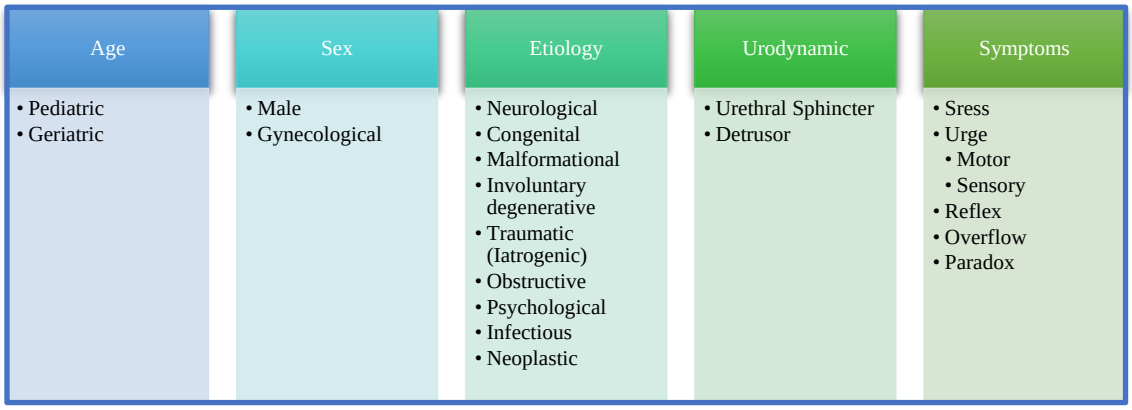

Figure 5.1. Classification of Urinary Incontinence *[18]*

This classification gives researchers the freedom to precisely describe large groups of patients with a similar clinical picture and identical urodynamic findings, although the etiology may be different [18].

Symptoms and Signs

With deeper understanding on urinary incontinence which could possibly be an episode with an extremely short time course, lasting a few seconds, or be prolonged, or continuous, researchers and clinicians need to develop an investigative protocol such that an incontinence episode is not missed [18]. Studies designed henceforth must consider both static hydrodynamic conditions in the lower urinary tract and situation of daily life, where the patient experiences incontinence. Emphasis has been given on the line of questioning where clinicians are curious about the time of first occurrence, and a previous history of urological, gynecological, nervous, rectal, and somatic diseases [18].

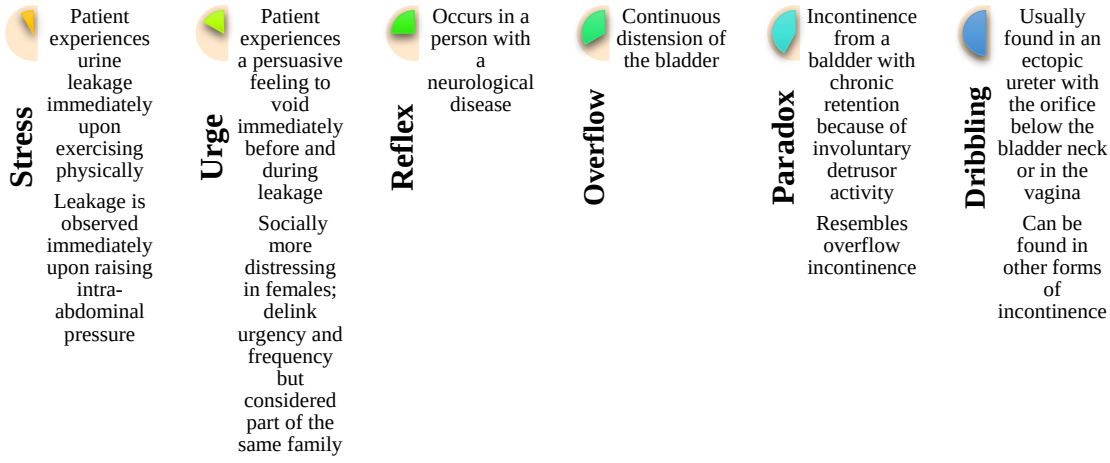

Figure 4.2. Distinction between various form of symptomatology related to leakage of urine [18]

4.1. Stress Urinary Incontinence (SUI)

Stress Urinary Incontinence (SUI) is the involuntary loss of urine during a physical movement like coughing, sneezing, exercising, laughing, or picking up heavy objects [25]. It occurs when the pelvic floor and urinary system's structures are stretched, damaged, or defective [26]. When the bladder pressure exceeds the urethral

pressure during incidents like coughing, sneezing or other strain activities which increases intra-abdominal and hence, bladder pressure [27]. There is a lack of accurate measurement systems for obtaining dynamic pressure profiles which makes it harder to diagnose incontinence.

Air-charged balloon on semi-rigid catheters are generally reliable and have reasonable response times to measure pressure during incidents of stress [27]. Maximum urethral closure pressures (MUCP; Section 1.2.4) are measured by subtracting the maximum bladder pressure from the maximum urethral pressure. These readings ate taken at rest and stress-inducing incidents like a cough. The maximum bladder pressure at rest and stress-induced incident is calculated usually 2cm inside the bladder. Continent subjects have a higher MUCP than incontinent patients when at rest but decreases significantly during cough/ strain maneuvers in incontinent patients [27].

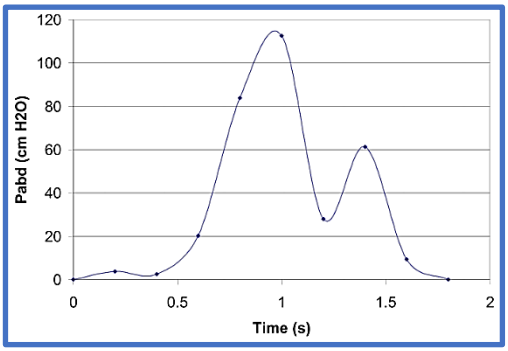

Figure 4.3. Pressure loads acquired from a 28-year old continent subject during a 1.8s cough event [28]

Spirka et al. (Figure 4.3) analyzed P_{ves} and P_{abd} in a 28-year-old continent patient during a 1.8s cough and finite element analysis was used to model a bladder [28]. In 1978, Bunne et al. studied the urethral closure pressure in stress-incontinent and continent patients and concluded that stress incontinence occurs because of low urethral pressure and defective pressure transmission from abdomen to urethra [29].

5. Stress Incontinence: Surgical Treatment

238,590 new cases of prostate cancer were estimated to arise in 2013 with an estimated 29,720 deaths with 1%-40% of patients suffering from urinary incontinence post-PR [30]. Literature suggests that 40% of patients with prostate cancer opt for radical prostatectomy. Post-PR, half of the patients seek treatment for incidences of incontinence, out of which 6%-9% elect surgery for treatment of incontinence [30].

There are conservative and surgical techniques to treat incontinence. The former includes pelvic exercises and lifestyle modifications, while the latter usually includes the very successful procedure of implanting an artificial urinary sphincter (AUS). There are other surgical procedures as well like the male slings for mild sphincteric deficiency, but for our study, we will consider the AUS implantation technique. For most patients, urinary incontinence and its severity is measured by the number of absorbent pads used, a bladder diary, uroflowmetry, and cystoscopy. But these studies are performed in a clinical environment and are not the same as measuring and evaluating an incident in real time.

Before the physician decides to proceed with the surgery, a thorough evaluation of the patient's history, onset, duration, description of the type and severity of incontinence, weights of absorbent pads and number of leakage incidents is necessary. Understanding the effects of incontinence on a patient's life is integral to treating this condition. Urodynamic studies confirm that 95% of patients with post-PR incontinence have stress urinary incontinence (SUI) [30].

5.1. Surgical Approach: Artificial Urinary Sphincter

The AUS has been the gold standard for the treatment for SUI post-PR and the device has undergone several design iterations over the past several decades. The latest device is the American Medical System's (AMS) AMS 800^{TM} which consists of a fluid-filled cuff around the urethra and the pressure is maintained by a pressure regulating balloon with a control pump that allows the patient to activate/ deactivate the device.

Understanding the implantation of the AUS was a major part of this thesis and with Dr. Sean Elliott's help, we could gain insight into the procedure of implantation and activation of the AMS 800^{TM}. The access to the bulbar urethra around which the cuff is wrapped is via a longitudinal midline perineal incision over the urethra. Several incisions through the bulbospongiosus muscle, the cuff is placed around the urethra, the control pump is placed in the scrotum, and the pressure regulating balloon is placed intra-abdominally or in an extraperitoneal prevesical space.

Subsequent sections will deal with the AUS design, components, complications and our novel design and its evolutionary journey. The AUS has many complications which will be elaborated upon and backed by literature studies. Overall, patients are very satisfied with the success of the device and its ability to maintain continence and physicians recommend the AMS 800^{TM} to all patients seeking a surgical approach, the journey of the device from an engineering standpoint has been historic and life-altering for several patients.

6. Prior Design and Clinical Work: Timm, Scott, Bradley

Urological devices stemmed from the idea of involuntary dretrusor contractions that made patients incontinent. This could be the result of an injury or a disease condition due to damage to the autonomic and neural pathways that control the micturition reflex (the filling and evacuation of the bladder) [31]. Timm et al. worked on electronic means of simulating a normal micturition reflex including evacuation, retention and volume sensing [31]. Electronic simulation requires coupling to the neural pathways and a method using electrodes (positioned on the dorsal and ventral surfaces) was used to simulate micturition. Mechanical and electrical ways of maintaining continence were being worked upon simultaneously and this required awareness of neural pathways and which nerves sensed volume and stimulated the bladder to void [31], [32].

In the same work, Timm et al., developed an inflatable cuff around the urethra which could provide continence. They were trying to demonstrate techniques for urinary incontinence using electrical and mechanical techniques. The set up and the components in their environment have been illustrated in Figure 6.1. Urethral clamps and stimulators were designed to maintain continence. In the hydraulic type as seen in

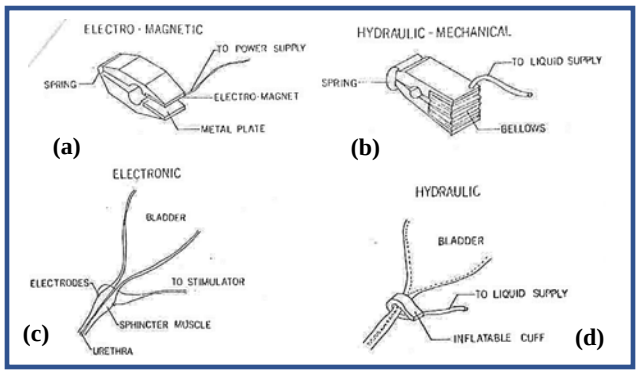

Figure 6.1. Urethral clamps and stimulators to maintain urinary incontinence. (a) Clamp is opened and closed with an electromagnet. **(b)** Hydraulic mechanical clamp using inflatable balloon to open and close. **(c)** Electrical stimulation of external sphincter used to stimulate imparted pudendal nerve input. **(d)** Cuff placed around the urethra has inflatable inner balloon to

Figure 6.1, we can see the use of a reservoir attached to a cuff that maintained constant occlusive force on the urethra. The same concept is used in the AMS 800^{TM}.

In 1970, Timm et al. [33] designed a deformable cuff attached to a modified hydraulic system shown in Figure 6.1, which intermittently occluded a collapsible tubular structure like the urethra. The cuff, shown in Figure 6.2 inflates inwardly because of nylon sutures in its backing and this was the idea considered for the AMS's current narrow-back cuff. An intravesical pressure equal to or greater than cuff pressure is required for urinary leakage and therefore the cuff should maintain higher pressures for maintaining continence. Figure 6.2 is a diagrammatic representation of the deformable cuff when unpressurized and pressurized.

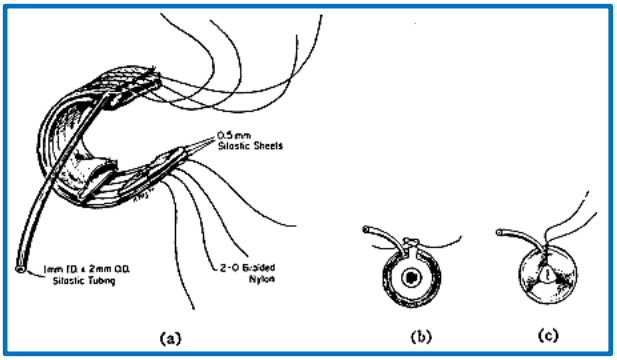

Figure 6.2. Diagrammatic views of deformable cuff. (a) Inner balloon attached to reinforced backing. (b) Cuff in position but unpressurized. (c) Pressurized cuff occluding the encircled vessel. [33]

The work also highlights advances made in designing reservoirs and pumps that could maintain constant pressure in the cuff, and these are illustrated in Figure 6.3. The cuff was made of silicone rubber and one made of dacron-reinforced silicon rubber provided maximum pliability. The stainless-steel bellows system (Figure 6.3(a)) was considered the best in maintaining constant pressure at the time.

Development in any medical device is inspired from prior short-comings and this has led to iterative design changes in urinary incontinence devices. In 1971, Timm described a device was comprised of an inflatable cuff (similar to the one in [33]) to

occlude the urethra and an internally implanted but externally controlled hydraulic system that can maintain pressure and periodically remove volume from the cuff [34].

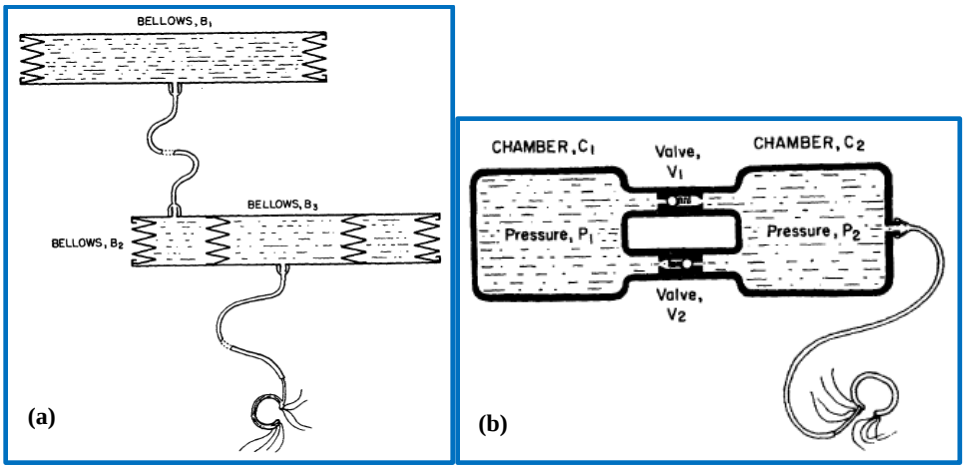

Figure 6.3. (a) Stainless- steel bellows system for maintaining constant pressure in cuff. **(b)** Alternative hydraulic pressure system with cuff utilizing two-check valves and pliable chambers to permit activation of the cuff from outside. [33]

The experimental arrangement for determining cuff pressure to prevent urine leakage is shown in Figure 6.4. The setup allowed continuous intravesical and cuff pressure measurements.

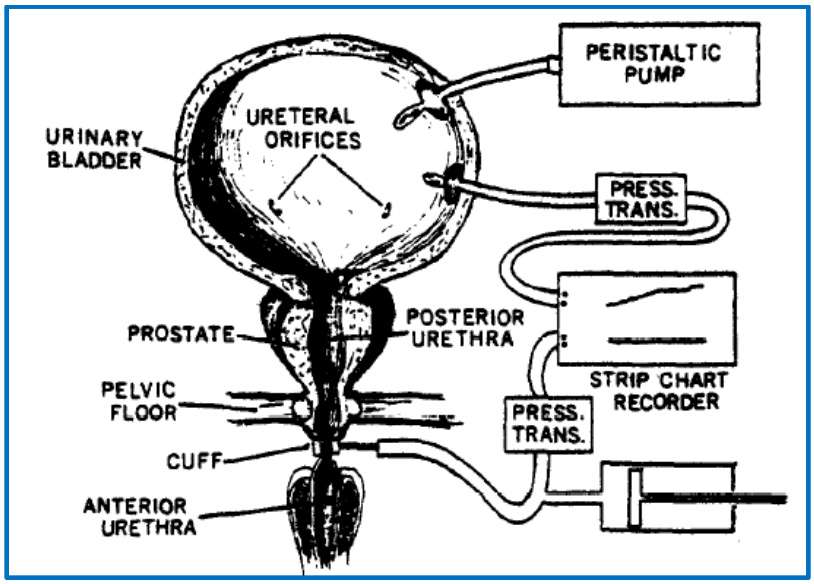

Figure 6.4. Illustration of placement of cuff and experimental set up for determining cuff pressures required to prevent urine leakage from the bladder. [34]

The device used the bellows system from [33] to maintain constant pressure on the cuff and each component was connected using silastic tubing. Clinical studies in dogs with this device showed that there was no tissue impairment from the cuff around the urethra. Cuff pressures lower than 80 cmH_2O and 40 cmH_2O in male and female dogs, respectively, did not show any signs of tissue impairment. However, going above these pressure values led to penis engorgement in males and tissue necrosis in females [34]. The study considered potential sources of complications that could limit the application of the device but were not observed in the animal studies. These included development of strictures, intolerable pain, tissue necrosis, and stress urinary incontinence at momentary high levels of bladder pressure [34].

Control over lower urinary tract functions are lost during neurological diseases and spinal disorders, and Timm et al. developed implantable prosthetic devices for restoring bladder function using electrical dretrusor stimulation with occlusion and volume sensing capabilities [35]. Several biological problems needed to be solved before proceeding to an engineering design and these included- excitation-contraction coupling of smooth muscle cells, drestrusor contractile sequence, pain with stimulation, loss of muscle contractility, and candidate selection [35]. The system designed to restore the micturition reflex is shown in Figure 6.5 and it requires a combination of three techniques- urethral occlusion to maintain continence, volume sensing for determining appropriate evacuation time, and electronic stimulation to induce dretrusor contraction [35].

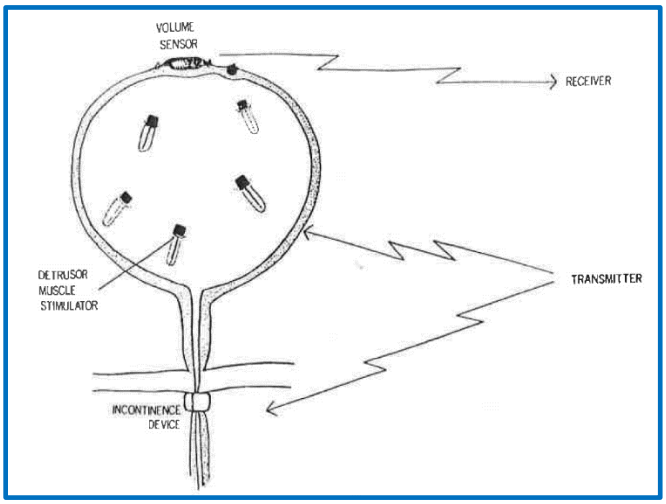

Figure 6.5. Total system for restoring the micturition reflex. [35]

Simultaneously, in 1973, a mechanical device was implanted in patients for the treatment of urinary incontinence. Preliminary results using this device (Figure 6.6) showed successful restoration of continence in all five patients. The prosthetic device consists of 4 parts: an inflatable cuff, two pumps, and a reservoir. The pumps are each used to deflate and inflate the cuff, respectively. This prosthetic sphincter was activated 44,000 times which is equivalent to activating the device 6 time/ day, 365 days per years for full 20 years [36]. At this point, the surgical techniques still had to evolve [36], [37].

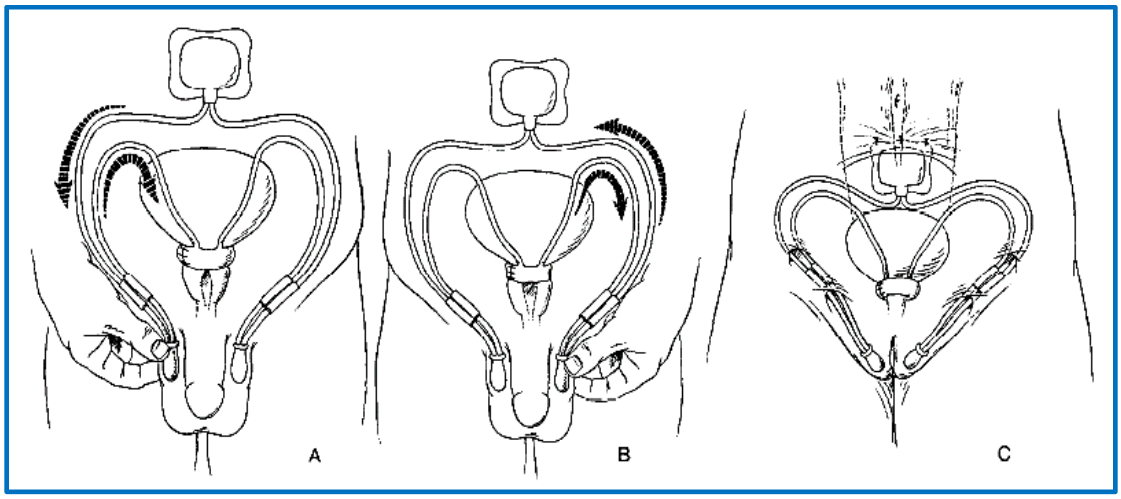

Figure 6.6. Four parts of prosthetic urinary sphincter: reservoir, inflatable cuff, and two pumps. **(A)** Squeezing pump on right transports fluid from reservoir into cuff, and **(B)** squeezing pump on left deflates cuff into "open" position. **(C)** Implantation with bulbs placed in labia of female or in scrotum of male. [36]

We need to understand each component of this device that went on to be named the AS 721 as shown in a later section where we will discuss the evolution of the current device. The inflatable cuff was made from silicone rubber and come in varying sizes. The average size of the cuff is 2 cm wide and 8 cm long [38]. At this point, research into developing a universal cuff was ongoing. The reservoir was made from two sheets of thick silicone rubber formed into a sphere. The tear-drop shaped pumps were activated by palpitating them through the skin [38]. The components are shown in Figure 6.7.

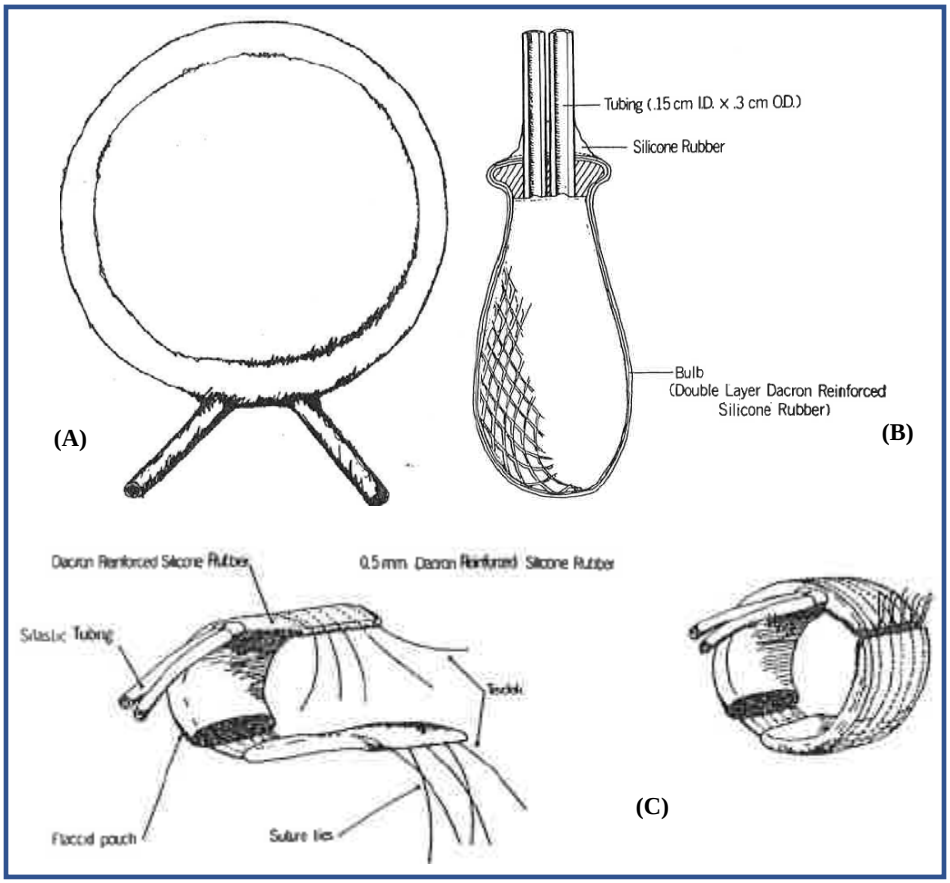

Figure 6.7. (A) Reservoir acts as fluid storage chamber between cuff fillings. **(B)** Hollow pump-bulbs are easy to compress and refill automatically when released. **(C)** Urethral occlusive cuff is formed by tying a flaccid rectangular pouch into an annular ring around the urethra. [38]

Like the design as part of this thesis work (discussed later), Timm et al., developed an electromechanical bellows system (Figure 6.8) to deflate the cuff on patient command. These ideas were developed way back in 1976 and involved a certain amount of fluid to be injected to raise pressure to 70 cmH_2O. This electromechanical device was coupled with radio frequency and removing this signal allowed the cuff to fill back up again, after voiding [38].

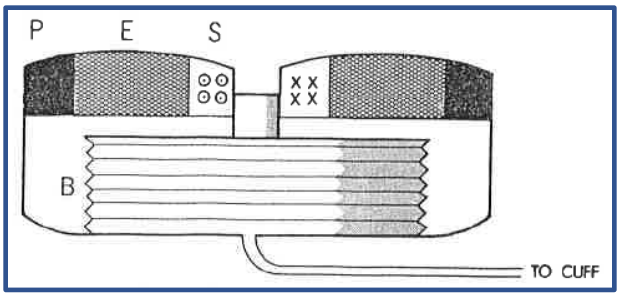

Figure 6.8. Solenoidally controlled bellows for cuff pressure regulation. [38]

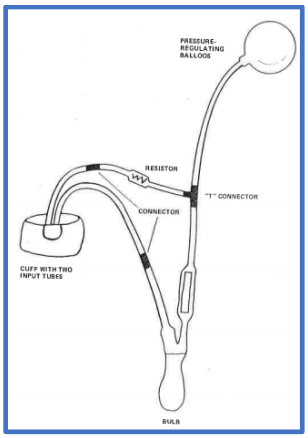

Figure 6.9. The delay-fill sphincter used only one bulb and the cuff repressurizes within 2 minutes after pumping of the pump bulb. [39]

In 1977, Burton et al. laid down the design criteria for an artificial urinary sphincter and there are listed as follows [39]:

- Device should be totally implantable
- Must be biocompatible
- Pressure occluding urethra should be enough to prevent leakage but not impair urethral viability
- Device should have automatic pressure-release
- Device should allow intermittent removal of occlusion so that urine flow is not impeded
- Operation of device should be easily understood by patient

- Pressure regulating features should be inherent and not dependent upon the way the device is used
- A failed device should leave a patient in his preimplant, incontinent condition
- Must achieve long-term success for control of incontinence

At this point, patient selection criteria were also established which are listed as follows [39]:

- Complete emptying of bladder with less than 10 mL of residual volume
- Adequate flow rate
- No infection
- Adequate intravesical volume
- No uncontrolled hyperreflexia of dretrusor muscle
- Adequate manual and mental dexterity to manipulate pump bulbs
- No response to conservative measures
- Incontinence for than 1 year in the case of pelvic trauma and selected cases of neurogenic bladder

The AMS 800^{TM} was inspired from the AS 742 (Figure 6.9) which was a delay-fill sphincter that incorporated a balloon which applied constant pressure on the urethral cuff. The cuff is deflated by removing by the fluid and then takes 2 minutes to fill back up again [39].

7. AMS 800™: Design, Components, Mechanism

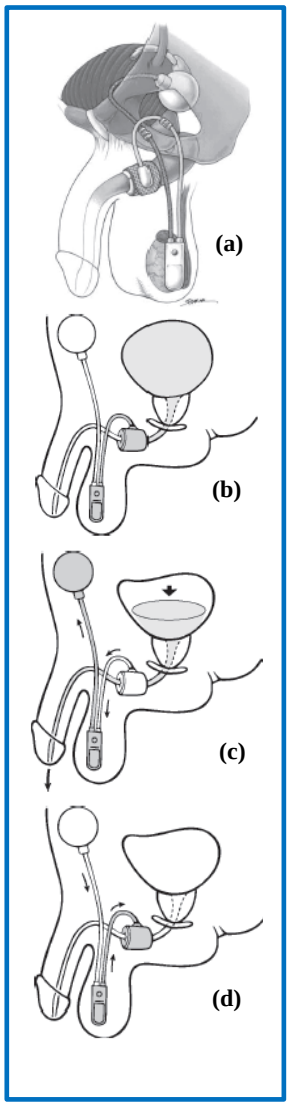

Figure 7.1. (a) The AMS 800™ Urinary Control System, **(b)** Closed cuff, **(c)** Pumping opens cuff, **(d)** Re-pressurizes automatically [40].

The AMS 800™ [Figure 7.1(a)] is used in cases of severe incontinence due to intrinsic sphincteric deficiency [40]. The device mimics the natural sphincter by performing the opening and closing of the urethra. The device has three components: the pressure regulating balloon, the control pump and the urethral cuff (Figure 7.2). As seen in Figure 7.1 (b), the cuff is filled with fluid and this is preventing urine from flowing out, which it would because of the loss in sphincteric activity. To void, the patient squeezes on the control pump in the scrotum, which draws out the fluid from the cuff and moves it to the pressure regulating balloon. The urine passes through the urethra and gradually the cuff fills back up automatically within 11 minutes.

Sterile fluid free of particulate matter must be used to fill all the components because the presence of a foreign matter in a system with incompressible fluid can cause mechanical failure of the device and prosthetic dysfunction. The operating room manual recommends using normal saline water for filling the prosthesis. Usually, the perineal or trans-scrotal approach is used for bulbous urethra cuff placement and the patient is placed in a lithotomy position or supine position respectively. The cuff is sometimes also placed more proximal to the bladder

at the bladder neck. Besides the components mentioned in Figure 7.2, the AMS 800™ Urinary Control System also includes an accessory kit with connectors, a quick-assembly tool, and an optional inert package and deactivation package.

Occlusive Cuff	Pressure Regulating Balloon	Pump
Closes the urethra by applying pressure	Determines amount of pressure applied by the cuff	Implanted in the soft tissue of the scrotum
Made of Silicone elastomer	Implanted in the prevesical space	1.2cm wide and 3.3cm long
Available in 13 sizes: 3.5cm to 11cm	Available in 6 ranges: 41-50, 51-60, 61-70, 71-80, 81-90, 91-100 (cmH_2O)	Upper (hard) part contains fluid resistors
Placed at Bulbous Urthra/ Bladder Neck		Lower (soft) part is squeezed by patient at time of voiding
		Deactivation Button: Stops fluid from being transferred between components

Figure 7.2. The major components of the AMS 800™ [40]

7.1. Bulbar Urethral Placement: Perineal approach

Just the surgical technique takes around 30 minutes and the patient preparation takes longer than the surgery itself. As part of understanding the working of the device, several procedures were observed and the technique usually followed is as follows (Figure 7.3):

- A midline perineal incision is made and the bulbocavernosus muscle is dissected from the bulbous urethra. [Figure 7.3 (a)]

Source: Boston Scientific

- Place a cuff-sizer around the urethra such that it fits snugly around the urethra but doesn't constrict the urethra. [Figure 7.3 (b)]
- Select the appropriate cuff size that corresponds to the length seen from the previous step.
- Prepare the cuff for implantation (Figure 7.4) such that the pillow cushion side faces the urethra and the mesh towards the outside.
- Rotate the cuff, so the tube adapter on it is lateral to the urethral midline and position the tubing to avoid contact with the cuff.
- Select the appropriate sized regulating balloon and make a suprapubic incision to reach the prevesical space and create a space for the balloon. [Figure 7.3 (c), (d); Figure 7.5]
- Like the blunt dissection made to access the prevesical space for the regulating balloon, make another such for the scrotum and place the control pump in the scrotal pouch with the deactivation button facing the outward so that it is palpable. [Figure 7.3 (e); Figure 7.6]
- Make all the connections with appropriate tubing and cycle the device to test the connections.
- The device system must be left in the deactivated mode for four-six weeks after implantation.

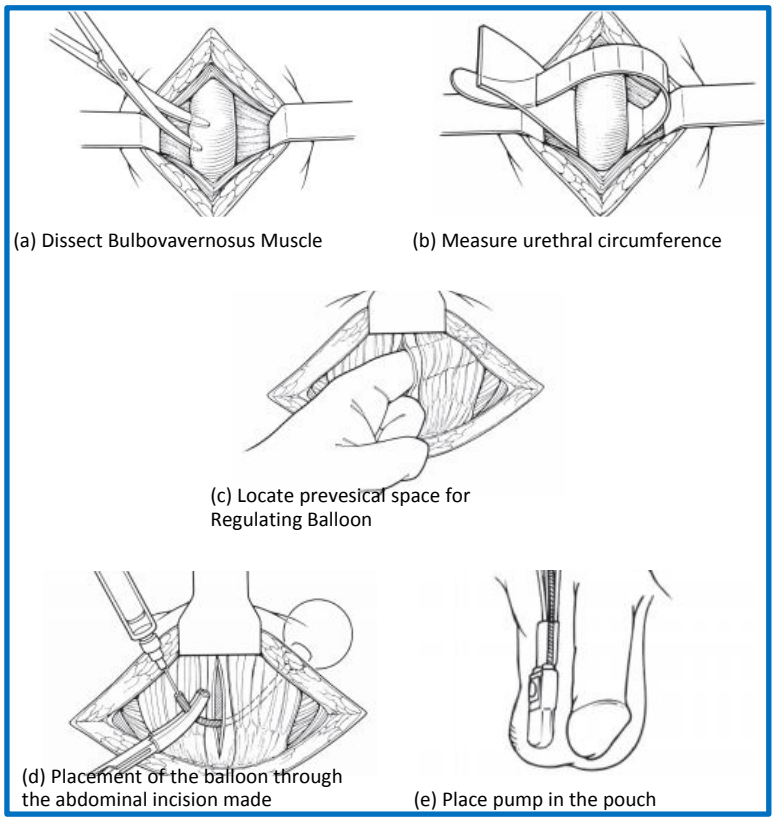

Figure 7.3. Bulbous Urethral Cuff Placement- Perineal approach [40]

The AMS Suture-Tie connectors are used to connect the tubing. AMS Quick Connect Sutureless Window connectors are also available which should not be used in revision procedures involving previously implanted tubing. It takes a few minutes for the cuff to refill and close off the urethra.

Figure 7.4. Preparing the Cuff (a) Fill Cuff; **(b)** Roll end of cuff [40]

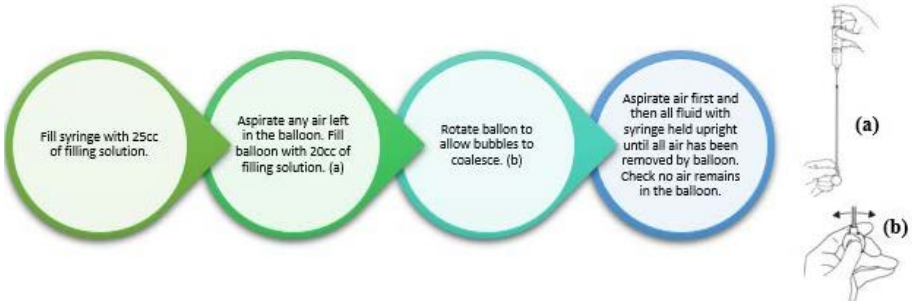

Figure 7.5. Preparing the Regulating Balloon (a) Fill Balloon; **(b)** Rotate balloon [40]

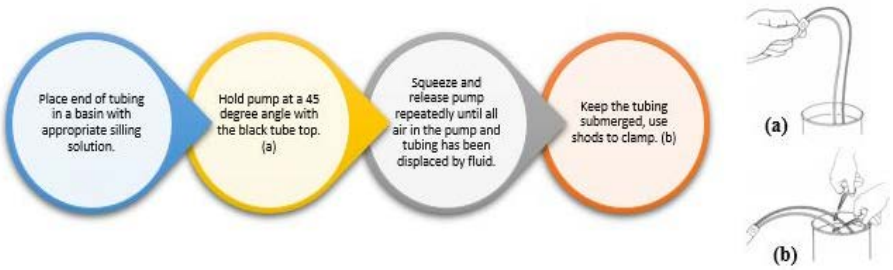

Figure 7.5. Preparing the Pump (a) Place Tubing into filling solution; **(b)** Clamp tubing with ends in filling solution [40].

7.2. Evolution of the AMS 800™

The artificial urinary sphincter came into existence in 1974 and it evolved over time to get to the current gold standard for treatment of post-PR- the AMS 800™ or AS 800 [41]. AS 721, AS 761, AS 742, AS 791, AS 792 (Figure 7.7) were the previous designs that the current device had to go through before becoming the best option for alleviating urinary incontinence. The AS 721 consisted of a hydraulic cuff around the urethra, the fluid was contained in a reservoir placed behind the rectus muscle, two pumps for opening and closing the cuff each [41]. This led to the development of AS 761 because of pressure regulation difficulties. The pressure regulating balloon was introduced here but the device ran into roadblocks. The AS 742 was the first and closest to the current device back in the days and involved the use of a pressure regulating balloon which filled the cuff passively in 3-5 minutes, thereby allowing the patient to void the bladder. AS 791 and AS 792 were refinements to this design and the former was designed for bulbous urethra while the latter was bladder neck. The AS 800 included the refinements from AS 791

AND 792 and reduced their disadvantages by introducing a deactivation button on the control pump and housing the valves, resistors and pump in one unit [41].

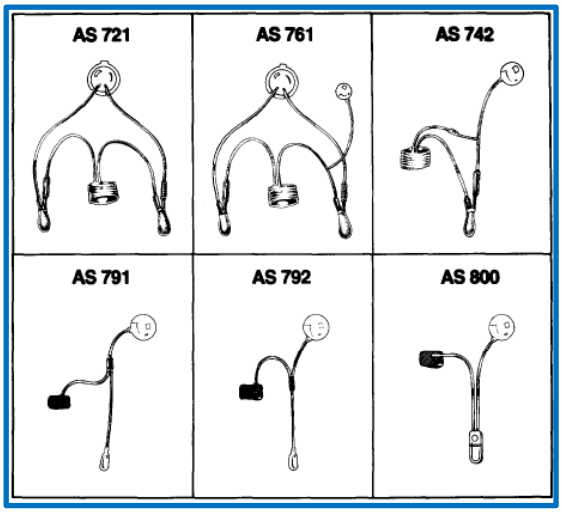

Figure 7.7. The evolution of the AMS artificial urinary sphincter [41].

The paper by Tage [41] discusses the success of these different AMS artificial sphincters and at the time that this paper was published (1986), there was only one AS 721/761 operational out of the 19 that were implanted in patients. The graph in Figure 7.8 gives us an idea about progression of the device and their overall success as implants in patients.

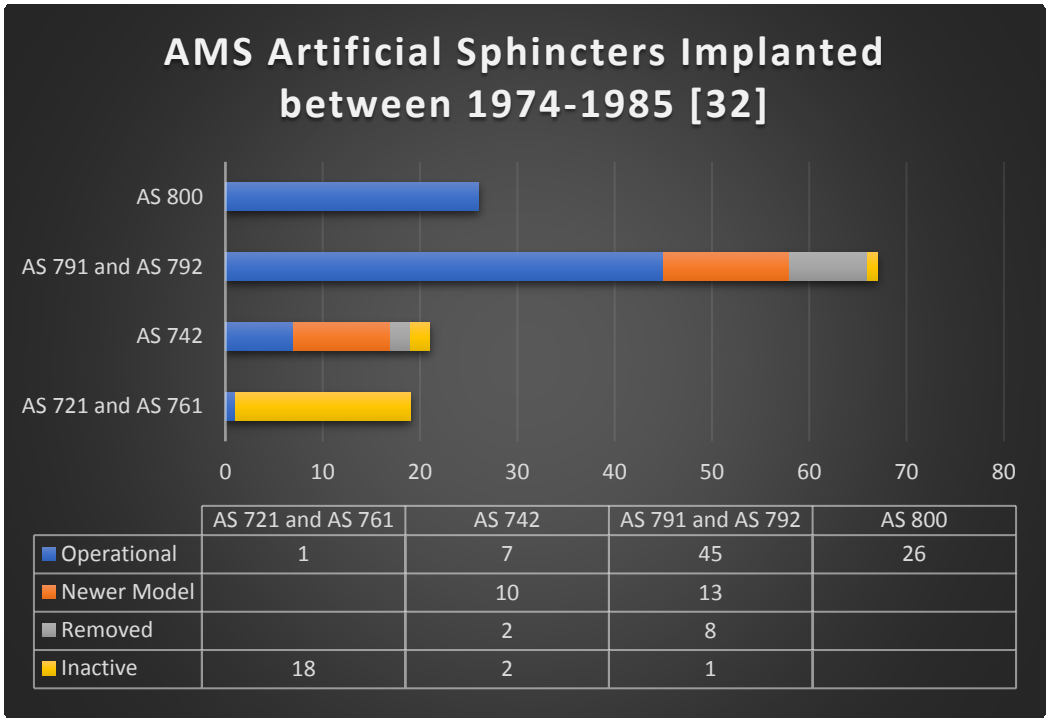

	AS 721 and AS 761	AS 742	AS 791 and AS 792	AS 800
Operational	1	7	45	26
Newer Model		10	13	
Removed		2	8	
Inactive	18	2	1	

Figure 7.8. AMS Artificial sphincter models used and their status as of 1986 *[41]*

From this 1986 data, Hald found that the overall success rate of the AMS sphincters was 77%. He also concluded that patients with detrusor instability stemming from prostatectomy can be treated with such implants but those with detrusor hyperreflexia having a neurogenic etiology disqualifies patients as a candidate for artificial sphincters [41].

7.3. Other AUS-like Devices

7.3.1. FlowSecure™ (Sphinx Medical, UK)

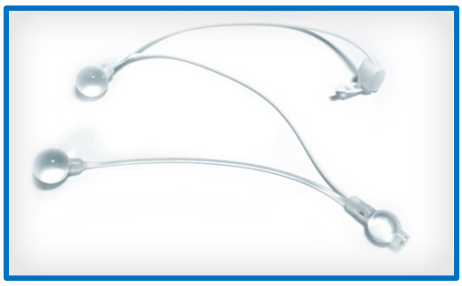

Figure 7.9. FlowSecure™ device [43].

The device has four components as shown in Figure 7.9: a regulating balloon, a stress release balloon, a urethral cuff, and control pump. The device is implanted as a single unit which eliminates mechanical failures due to tubing and provides in-situ pressure management. We will discuss the complications of the AMS 800™ in later sections but it is important to highlight that the FlowSecure™ did not exceed 40 cmH_2O, thus minimizing urethral erosion and atrophy [42]. Several publications have reported a high mechanical failure from pump perforation and infection as well [42], [43], [44].

7.3.2. Zephyr ZSI 375™ (Mayor Group, France)

Created in 2005 and commercially available in 2009, this single-unit silicone device comprises of two components (Figure 7.10): a cuff and a pump control unit [42], [44], [45]. The control pump is used to activate the

device and also behaves as a pressure regulating tank which pumps normal saline water using a piston actuation mechanism. The ZSI 375^{TM} has a reduced cost, lesser number of components, and opportunity to adjust cuff pressure and size [42]. This device has not been widely implanted and data seems to be disappointing.

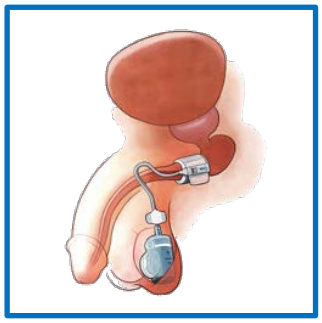

Figure 7.10. Zephyr ZSI 375^{TM} device [45].

7.3.3. Silimed periurethral constrictor device (Silimed, Brazil)

Figure 7.11. Silimed periurethral constrictor device [46].

Created in the 1990s and popularized in 2000, this device (Figure 7.11) was intended for pediatric patients with deficient sphincter activity [42], [44], [46]. The cuff is linked to a self-sealing valve and pressure is applied on the cuff by injecting sterile saline. This device is inexpensive and patients do not have to operate a pump manually. The single unit design also makes the pump easier to use but constant cuff pressure can cause higher erosion and tissue ischemia. Mechanical failure attributed to frequent injection of saline is another drawback of this device.

Device	More compact than the AMS 800®	Improved control of pressure during stress	Improved detection of the administered pressure	Adjustable	Key remaining questions
FlowSecure™	No	Yes	No	Yes	Pump perforation at pressurisation
Periurethral Constrictor	Yes	No	Yes	Yes	Controversial results on continence
Tape Mechanical Occlusive Device	Yes	No	No	No but simplicity of use with its on/off button	?
ZSI 375	Yes	No	No	Yes	No multicentre prospective controlled study
Versatile Automated Device	Yes	Yes	Yes	Yes	?
Electromechanical Device	?	Yes	Yes	No	?

Figure 7.12. Innovative characteristics of AUS compared with the current AMS 800^{TM} [47].

8. AMS 800™ Complications: Literature Survey

The previous section dealt with the evolution of the AMS artificial sphincters and each of their success rates. The AMS 800 has become a gold standard to treat urinary incontinence, especially stress urinary incontinence post-prostatectomy. The 1986 publication authored by Tage Hald, talks about the complications observed in patients post-AUS implantation. Susceptibility to infections and possibility of urethral erosion were listed as major complications that usually led to termination of the sphincter treatment, sometimes permanently [41].

Physicians in the 1974-1985 period removed the entire device in the case of an infection and implanted a new one. In cases where the infection had led to erosion of the urethra because of high pressure (scarring of the urethra, arterial hypotension) it was difficult to implant a new AUS [41]. Within these patients who had an erosion because of infection, some received a new AUS which failed permanently due to urethral erosion. These problems including urethral atrophy, tissue ischemia, and urethral erosion continue to affect the success rates of implants and in turn, the patient satisfaction levels. Urinary tract infection is also a very real problem. Researchers have also tried to find a suitable location to place the artificial sphincter and some consider the region behind the central perineal tendon as a good location [41].

Per Crivellaro et al., SUI is a complication post-RP and different techniques of RP had different incidence rates. For instance, 4- 31% of patients undergoing robotic prostatectomy or 7-40% undergoing open RP have chances of contracting SUI [47]. This extensive review of SUI post-RP included every publication with the keywords

incontinence, radical, prostatectomy, and treatment. From this search, they found that AUS (Figure 8.1) had a high number of patients with sufficient follow-up data and continence rates ranging from 20-89% [47]. The overall complication rate for an AUS was 19.4% [47] and was the highest among other similar devices because of the high number of patients available. However, the AUS is the best option for severe incontinence.

A similar review by James et al. [48] concluded through their analysis of several publications on the device that the AMS 800^{TM} had very successful outcomes and patient satisfaction was very high. However, with significant follow-up data available, researchers could determine that the device was plagued by several complications including infection (0.5%-10.6%) and erosion (2.9-12%) [48]. Infection from any prosthetic device is a major complication and in the case of the AUS, it involves removal of the device [48]. The AUS is now surface treated with antibiotics to reduce infections.

The method used for analyzing publications on the complications of the AMS 800^{TM} is based on the idea that every device has a certain gestation period before it is accepted and made popular by physicians. We analyzed all the literature beginning from 1990 to 2016 (Appendix A) and the device was used in patients in mid-1983. This gives us a gestation period of about 5 years which is acceptable for any device since it will undergo design changes and iterations based on physician feedback and patient satisfaction.

Author, year	Device	Prosp. study	Patients	% Severe incont	% Dry	% Improved	24 h PT pre	24 h PT post	Validated iQuol	Erosion %	Infection %	Malf/displ %	Trans UR %	P-O pain
Mottet 1998[2]	AMS 800	Yes	103	100	89	7	—	—	—	6	6	10	—	—
Perez 1992[3]	AMS 800	No	75	100	52	33	—	—	—	5.3	0	35	—	—
Litwwiller 1996[4]	AMS 800	No	50	90	20	55	—	—	—	—	—	—	—	—
Montague 2001[5,a]	AMS 800	No	113	82	32	64	—	—	—	0	0	12	—	—
Haab 1997[6]	AMS 800	No	68	7,5	80	20	—	—	iQ, UDI	7.4	0	44	—	—
Gomes 2000[7]	AMS 800	No	30	—	70	—	—	—	Aua qol	3.3	3,3	6,6	—	—
Lai 2007[8]	AMS 800	No	218	62	69	9	—	—	—	6	5,5	6	—	—
Gousse 2001[9]	AMS 800	No	131	25	59	15	—	—	—	4	1,4	—	—	—
Staerman 2012[10]	ZSI 375 device	No	36	—	73	—	—	—	—	2.7	8,3	0	—	—
Schiavini 2010[11,b]	Periurethral constrictor	No	30	100	73	—	—	—	—	13	10	0	6.6	—
Introini 2012[12]	Periurethral constrictor	Yes	66	—	79	15	—	—	—	3	3	0	—	—

Figure 8.1. Continence and Complication rates across publications for AMS 800^{TM} and similar devices *[47]*.

Reference	No. patients	Mean follow up (months)	Continence outcomes	% Infection	% Erosion	% Revision/removal	% Atrophy	% Mechanical failure	% Patient satisfaction	AUS durability %/year
Elliott and Barrett[2]	184†	68.4	92‡	0.5	6.5	16.8	1.6	7.6		75/5
Lai *et al.*[4]	218	36.5	69 (0–1 PPD)	5.5	6.0	27.1	9.6	6		75/5
Litwiller *et al.*[8]	65	23.4	20 (0 PPD) 55 (few drops)	6	3.1	18	9		90	
Raj *et al.*[9]	554	68	90 (0–1 PPD)	1.74§	5.2	19.1	11.4	8.3		75/5
Kim *et al.*[10]	124	81.6	82 (0–1 PPD)	7	10	9.5 (removal)		29		
Venn *et al.*[11]	70¶	132	92 (undefined)	28.5 infection/erosion	28.5 infection/erosion	64		28.5		66/10
Haab *et al.*[12]	68	86.4	80 (0–1 PPD)		2.9	25	8.8		80	
Montague *et al.*[13]	113	73	40 (0 PPD) 64 (0–1 PPD)			12			73	
Gousse *et al.*[14]	71	91	59 (0–1 PPD)	1.4	4	29		25	77	
Trigo Rocha *et al.*[15]	40	30	90 (0–1 PPD)	2.5	5	20	5	5		
O'Connor *et al.*[16]	29	60	83 (0–1 PPD)	3.4	10	14/14	6.8			
Clemens *et al.*[17]	66	26.6	34 (0 PPD) 80 (0–2 PPD)	10.6	12	36.4		9		

†Includes only patients implanted with narrow back cuff. ‡Defined as properly functioning AUS. §Combined rate for primary and secondary (n = 118) procedures. ¶Includes 31 patients with cuff placed at bladder neck.

Figure 8.2. Comparative outcomes of AUS implantations in contemporary cases [48]

8.1. Data Analysis

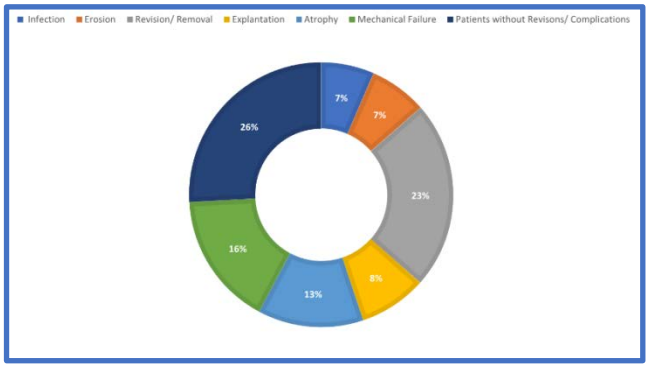

Figure 8.3. Average Complication chart in 100 patients receiving an AMS 800^{TM} implant (derived from Figure 7.4)

The results from the data analysis of several publications on the AMS 800^{TM} implant is used to understand the market for urinary incontinence post-RP. The data from 1987-2017

Figure 8.4. Comparative Study of Outcomes of AMS 800^{TM} Implantations from 1987-2017 (Numbers have been rounded to nearest whole numbers) (Refer Table 8.1)

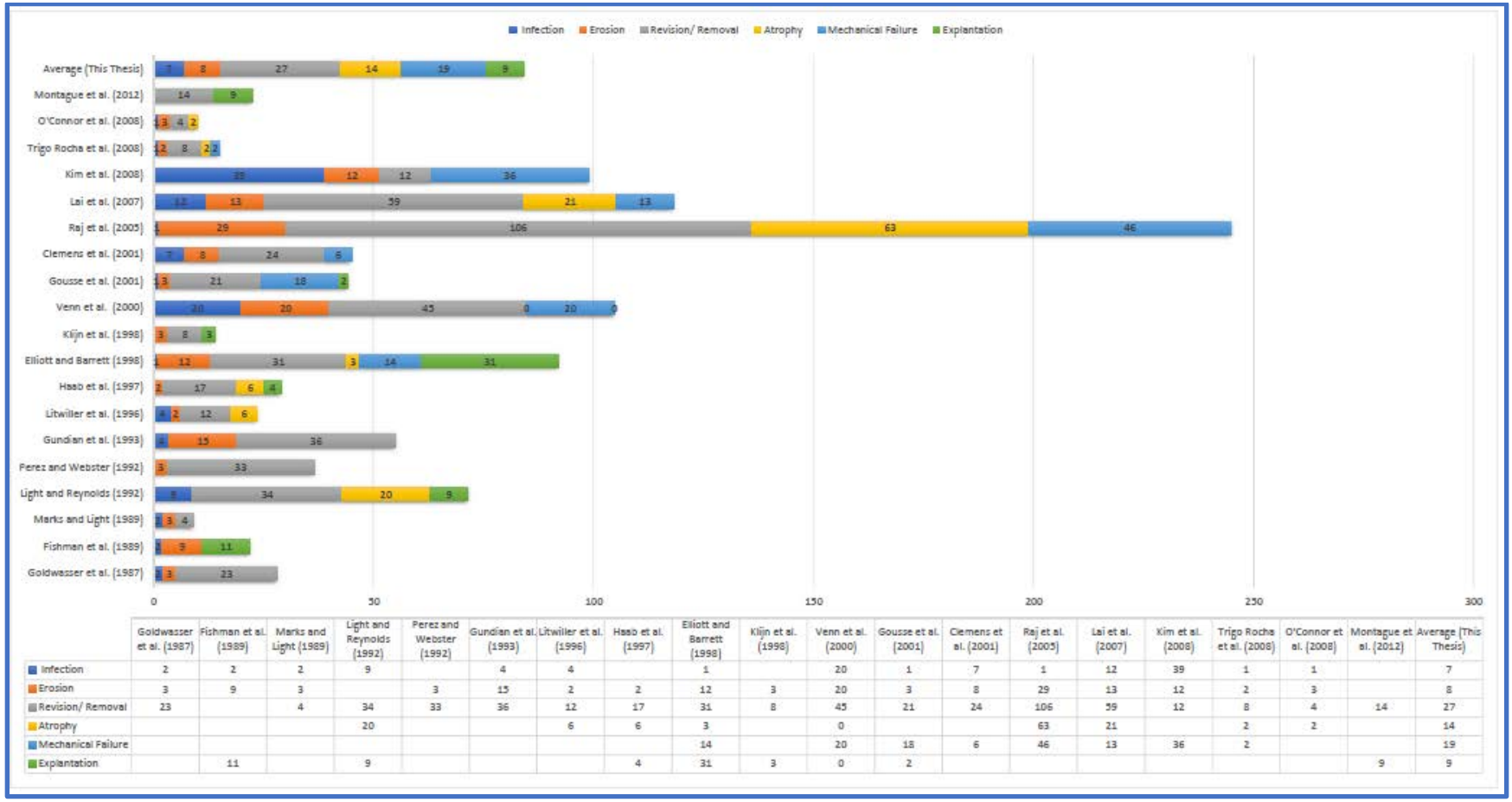

	Goldwasser et al. (1987)	Fishman et al. (1989)	Marks and Light (1989)	Light and Reynolds (1992)	Perez and Webster (1992)	Gundian et al. (1993)	Litwiller et al. (1996)	Haab et al. (1997)	Elliott and Barrett (1998)	Klijn et al. (1998)	Venn et al. (2000)	Gousse et al. (2001)	Clemens et al. (2001)	Raj et al. (2005)	Lai et al. (2007)	Kim et al. (2008)	Trigo Rocha et al. (2008)	O'Connor et al. (2008)	Montague et al. (2012)	Average (This Thesis)
Infection	2	2	2	9		4	4		1		20	1	7	1	12	39	1	1		7
Erosion	3	9	3		3	15	2	2	12	3	20	3	8	29	13	12	2	3		8
Revision/ Removal	23		4	34	33	36	12	17	31	8	45	21	24	106	59	12	8	4	14	27
Atrophy				20			6	6	3		0			63	21		2	2		14
Mechanical Failure									14		20	18	6	46	13	36	2			19
Explantation		11		9				4	31	3	0	2							9	9

was tabulated in percentages and then brought down to whole numbers based on the total number of patients. Complications including erosion, atrophy, surgical revision, explantation, and mechanical failure were tabulated against each reference and then plotted onto a stacked bar chart shown in Figure 8.4. As shown in Table 8.1, the total number of complications in each category across all publications was determined. Calculation of the mean of all complications against an average number of patients in all the publications helped determine the average percentage of patients suffering from each complication and designed the pie chart as shown in Figure 8.3. 74% of all patients with an implanted AUS experienced some form of complication and had to go back for a revision or a follow-up. This data does not reflect the follow-up time in each study since several references in Appendix A highlight the 5-year and 10-year durability outcomes of the device. The numbers used in the data analysis here is more of a cumulative value including patients who undergo secondary or tertiary revisions, or patients who are implanted with a tandem-cuff, or patients with multiple incidences of erosion, atrophy, mechanical failure or infections.

Consider Singla et al. [30] and the statistics this publication provided with respect to the number of patients suffering from SUI and those undergoing surgery. The assumptions we make are:

- Number of new cases in a year (2013) is considered instead of total number of patients with prostate cancer over a certain number of years.
- Build a yearly market assessment for SUI and those undergoing surgery

- For patients undergoing surgery, we assume they are all implanted with the AMS 800™ only.
- Cumulative number of patients undergoing

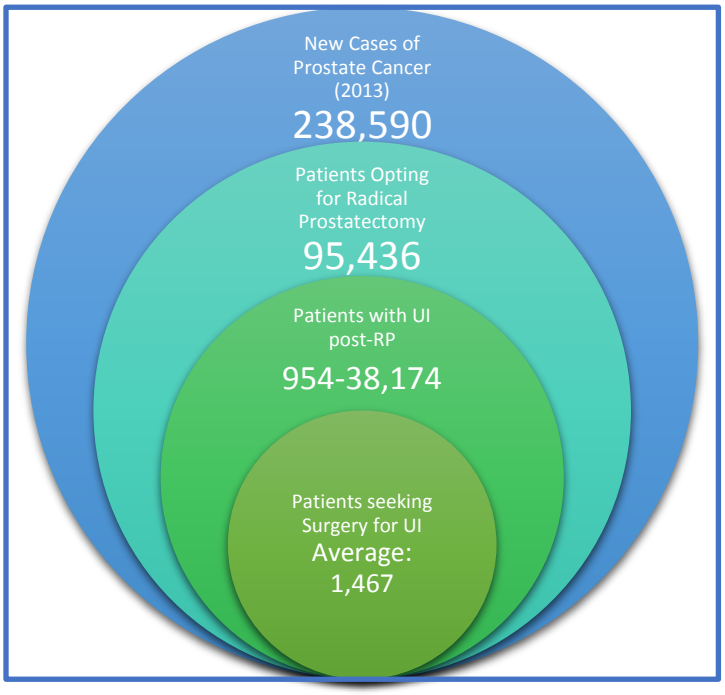

Figure 8.5. Number of AUS cases in a year (2013 taken as example) [30]

Based on data from [30], we have on average 1,476 cases of AMS 800™ implantations. Brown et al. [49] in 1998 found that the average Medicare and non-Medicare cost for an AUS implant was $15,400 and $20,300, respectively. If one accounts for inflation between 1998 and 2013 (compare with Figure 8.5), the average Medicare cost would be $30,000 in 2013. The average reoperation rate was 22.4% which brought the average Medicare cost to $18,850 [49] and accounting for inflation this would be $32,000 in 2013. This gives us a $44.3 million market in 2013 alone and this considers only the new prostate cancer cases that came up in 2013.

$$Total\ Target\ Market = Average\ Medicare\ Cost \times Patients\ seeking\ surgery\ for\ UI$$

$$= \$30{,}000 \times 1467\ people = \$44{,}010{,}000 = \$\,44\ million$$

With 1,467 patients undergoing surgical intervention to treat SUI post-RP, 74% (Figure 8.3) of these come back with some complications. However, from publications underscore the effectiveness of this device and estimate continence rates at 20% to 89% [47]. Though this number seems to be very high when compared to the overall complication rate of 19.4% published in [47], it gives innovators like us the motivation to make an even better attempt at reducing these complications and improving the quality of life. The reason for a high complication rate, as mentioned earlier, is because we have assumed every case as a new case and have not considered a mean follow-up time as in many studies. This helps us determine the higher side of the market. If all the 74% of the patients came back for a surgical revision, the revision rate would be very high, which reiterates our assumption of not considering the follow-up time. Most patients at some point with the AMS 800^{TM} will come back to his physician with a complication irrespective of the number of days they have had the device. Some, which as shown in Figure 8.3 is 26%, will have an improvement in their continence, will be satisfied with using 0-1 pads per day, and will be complication free.

Table 8.1. Comparative Study of Outcomes of AMS 800™ Implantations from 1987-2017 (Numbers have been rounded to nearest whole numbers) (Refer Figure 8.4)

References	Infection	Erosion	Revision/ Removal	Explantation	Atrophy	Mechanical Failure	Number of Patients
Goldwasser et al. (1987)	2	3	23				109
Fishman et al. (1989)	2	9		11			148
Marks and Light (1989)	2	3	4				37
Light and Reynolds (1992)	9		34	9	20		126
Perez and Webster (1992)		3	33				75
Gundian et al. (1993)	4	15	36				117
Litwiller et al. (1996)	4	2	12		6		65
Haab et al. (1997)		2	17	4	6		68
Elliott and Barrett (1998)	1	12	31	31	3	14	184
Klijn et al. (1998)		3	8	3			27
Venn et al. (2000)	20	20	45	0	0	20	70
Gousse et al. (2001)	1	3	21	2		18	71
Clemens et al. (2001)	7	8	24			6	66
Raj et al. (2005)	1	29	106		63	46	554
Lai et al. (2007)	12	13	59		21	13	218
Kim et al. (2008)	39	12	12			36	124
Trigo Rocha et al. (2008)	1	2	8		2	2	40
O'Connor et al. (2008)	1	3	4		2		29
Montague et al. (2012)			14	9			113
Total (References Only)	113	150	490	69	123	155	2359
Average (This Thesis)	7	8	27	9	14	19	118

8.2. Surgical Methods for reducing Incidence of Complications

From the extensive literature survey, the fact that the AUS has been a very successful device and the surgical procedure followed provides excellent patient satisfaction. Certain complications make patients undergo revisions or reimplantations and the most common reason for revisions was urethral atrophy. Such complications reintroduce incontinence in a patient and a pelvic X-ray and cycling of the device can show that the diameter of the pressure regulating balloon has reduced and there is excess fluid in the cuff [48].

In cases of atrophy, physicians usually opt for cuff-downsizing and place the new cuff in the same location as before. American Medical Systems makes cuffs with the lowest being 3.5 cm. In cases where the smallest cuff has already been used or is not tight enough, physicians perform a tandem-cuff procedure or a transcorporal cuff-placement. In a review by Hudak and Morey [50], 67 patients with the 3.5 cm cuff were studied to understand the effectiveness of the cuff-size compared to others and its impact during primary and revision surgeries. 45 patients underwent primary and revision AUS surgery without any difference in the methodology, and 8 patients underwent transcorporal cuff placement. The study found the patients with the 3.5 cm cuff had a higher chance of erectile dysfunction and urethral erosion compared to those with a 4.0 cm cuff [50].

Papers on comparative outcomes of different treatments for prostate cancer consider prostatectomy as a contributor to urethral atrophy, decreased penile length due to collagenation, and decreased vascular supply leading to ischemia. Radiation

therapy has also been considered to cause small vessel obliterative endarteritis, increasing the risk of atrophy further. There has been a shift in the way the cuff is measured and physicians pay special attention to the way they use the measuring tape provided in the device package (Figure 8.6). Hudak and Morey observed that a loose AUS cuff can cause significant incontinence requiring revision surgery.

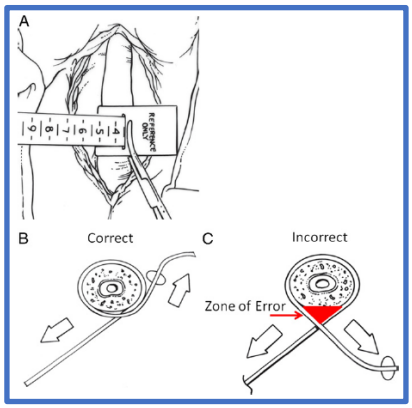

Figure 8.6. Push-pull measurement technique for urethral cuff sizing prior to cuff selection. [50]

Tandem cuff placement was developed in 1997 in patients who suffered from UI despite a single-cuff placement and was usually attributed to insufficient urethral coaptation. A second cuff was placed a few centimeters away the existing cuff using a Y-connector. Studies found that the erosion rates for tandem-cuffs and single-cuffs were comparable, even though one would think that the tandem-cuffs would increase erosion. The success rate of tandem-cuff placement procedures was 95% [48]. Urethral atrophy occurs when blood supply is limited to the urethra and periurethral-tissues [51]. A lack of urethral compression or coaptation is observed in cystoscopy even though an activated AUS is present around the urethra and requires a tandem cuff placement, a reduced cuff-size, higher pressure regulating balloon, or a transcorporal cuff.

A transcorporal approach in AUS revision cases uses incisions in the tunica albuginea of the corpora cavernosum which avoids a perineal incision in the corpus spongiosum [48]. Guralnick et al. [52] studied the effects of a transcorporal cuff

placement in patients with limited urethral coaptation and increased incontinence despite the presence of an AUS and 84% of the patients in the study responded positively to the procedure. The study did not find any case of erosion or infection but the patients do run the risk of developing erectile dysfunction. Figure 8.7 shows a comparison between a standard AUS placement dissection usually performed in a primary surgery and the transcorporal placement performed in a revision surgery [52]. In another study by Aaronson et al. [53], 18 patients underwent standard AUS surgery and 8 underwent transcorporal procedures, and it the data from their study was very interesting and is presented in Figure 8.8.

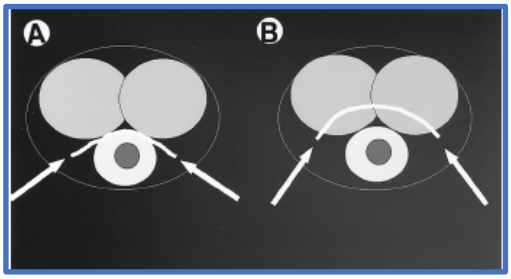

Figure 8.7. Difference in dissection depth. **(A)** for standard artificial urinary sphincter cuff placement dissection plane (arrows and curved line) **(B)** for transcorporal cuff placement [52]

Variable	ST Group	TC Group
Socially continent	11 (61)	7 (89)
Malfunction	1 (6)	0 (0)
Hematoma	0 (0)	0 (0)
Postoperative retention	4 (22)	1 (13)
Infection	4 (22)	1 (13)
Urethral atrophy	1 (6)	0 (0)
Erosion	2 (11)	1 (13)
Removal	5 (28)	1 (13)

Figure 8.8. Continence and complications after AUS placement [53].

The tandem cuff procedure is less popular when compared with the transcorporal approach and with the introduction of the 3.5 cm cuff, it has become less popular [48]. When cuff-downsizing alone is taken as a measure to mitigate AUS complications, Saffarian et al. [54] found that in 17 patients with in whom the larger cuffs were replaced by a 4cm cuff, patient satisfaction was 80% after cuff-downsizing. Cuff-downsizing also plays into the perfect urethral location for cuff placement and there are several papers on cuff locations which is beyond the scope of this thesis.

9. Concept Generation: Lets Sketch

9.1. The Idea and the Motivation

The device would be an accessory to the AMS 800^{TM} for treating stress urinary incontinence (henceforth our device is called the add-on device). The idea originated from a simple problem that was observed in patients with the existing AUS, where patients had leakage during exercise, coughing and sneezing. When viewed as a technical problem, it was found that the current device applied a pressure that was much lower than the pressure applied on the bladder when a person exercises, coughs or, sneezes. In addition to the excess pressure, the several complications that plague the existing device were motivating factors to come up with a device. The major advantage of this device modification would be that it permits the occlusion pressure to be set at a much lower average value, thereby improving tissue perfusion, reducing ischemia and preventing urethral atrophy and erosion. The innovation would develop a way in which a nominal pressure can be applied through the cuff onto the urethra at rest but the pressure can increase rapidly in response to the patient activating a switch when he gets a feeling of possible stress on the bladder (e.g., during exercise, coughing or sneezing).

The research team appreciates the simplicity of the current device and it is safe to say that the device has worked for so long because of its simple mechanism and biocompatibility. In our study and brainstorming sessions, ***we found that having the existing Pressure Regulating Balloon (PRB), control pump and the AMS 800 cuff as part of the design will help reduce research time and in the long run- time***

to market. Our concept would implant the 41-50 cmH_2O pressure regulating balloon (the lowest pressure balloon that AMS has) because this would help maintain a constant fixed pressure on the cuff when the patient is sedentary/ inactive. The novel implantable pump in turn would bring pressure up to 120 cmH_2O when incidents of stress occur.

The questions that we needed to ask ourselves were:

- Within what time-frame would the pump have to actuate?
- Since coughs and sneezes are difficult to detect, how would we anticipate such incidents?
- What kind of actuation mechanism will be the best for a quick response?
- Can a patient control it wirelessly?
- As an implantable, what kind of battery storage are we looking at?
- Why retain the AMS 800™ components? Can we get rid of them completely?
- What is maximum pressure during a stress-inducing incident?
- How much volume would be required to raise pressure from an optimal value to the maximum pressure during a stress-inducing incident?

As we dive deeper into answering some of these questions and find solutions to a problem that has existed for very long, as engineers it is essential to interact with the medical community and find out if there is a need for a device like this and if they would be willing to accept changes to the existing device. From a medical standpoint, we found out that this was an urgent need and could significantly improve quality of life for patients suffering from incontinence.

Our discussions with Dr. Sean Elliott in the Department of Urology at the University of Minnesota helped shape, solidify and pivot our idea time and again. When asked about the importance of an adaptive AUS, he had the following to say and that was our cue to begin working. Working with the creator of the device- Dr. Gerald Timm, there was constant feedback on ways we could tweak our prototype and present it as a viable option to treat the condition.

The current AMS 800™ is not personalized to the patient's needs. Most men only need 20 cmH_2O of urethral compression to remain dry when they are sedentary, yet need 120 cmH_2O when active. The current device compromises with an in between pressure- as high as it can be without exceeding a safe threshold. The market is hungry for a device that can adapt to a patient's level of activity.

Sean Elliott, MD, MS

9.2. Evolution of Pump Designs

We kept two things in mind: quick response time and implantability of the device. In our search for ideas to have a quick-action pump, we looked at several toys that had a water pump in-build into them. Most were comparable to simple piston pumps that needed considerable manual effort to actuate. I have always been fascinated by toys made from trash and we decided to search for pump ideas from do-it-yourself (DIY) manuals. I got my pump design ideas from three designs from Arvind Gupta's "Toys from Trash" webpage [55] and a combination of these pumps into a single unit would be perfect for our application. For every pump design, we had to weigh them against the actuation mechanism and many had to be filtered out

for requiring significant effort to actuate. This would go totally against our requirement for a quick-action pump. Arvind Gupta's Air-Water Pump design [55], [56] caught my eye. The design as I drew it in my journal is shown in Figure 9.1. and I called this a Bellow pump.

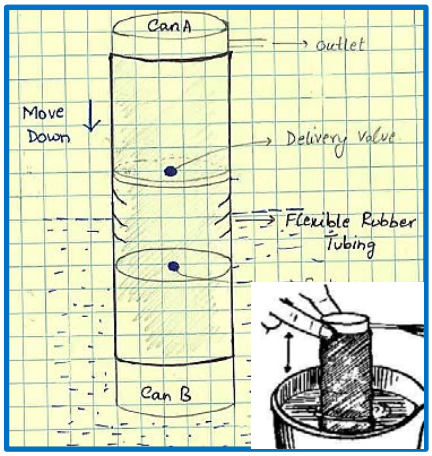

Figure 9.1. The Bellows pump as taken from Arvind Gupta's Air-Water Pump [46], [47]. Sketched on 7/8/2015.

Arvind Gupta in collaboration with Suresh Vaidyarajan published a DIY book titled "Pumps from the Dump" [56] and this was a treasure trove of various kinds of materials one could use to make a variety of pumps. A design titled the Diaphragm Pump [56], seemed a viable idea. It used a jam lid and balloon to pump water from a reservoir by manually pushing on the balloon diaphragm. I decided to try this out on a Coca-Cola bottle cap and the size of the cap was just enough to be an implantable. I used the specifications of a Coca-Cola bottle cap to design my diaphragm pump using the same idea as in the book with a few minor tweaks. Figure 9.2 illustrates the design, components and operating principle and Figure 9.3 depicts this design with a rubber balloon diaphragm.

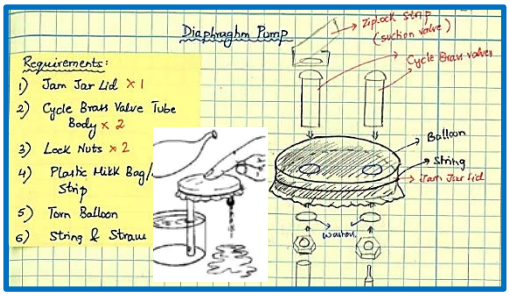

Figure 9.2. The Diaphragm pump and its operating principle as taken from [47]. Sketched on 7/8/2015.

Figure 9.3. Design in Figure 9.2 realized using a balloon diaphragm and MinuteMaid® bottle cap.

The design of the diaphragm pump was a platform for more work. Actuating the designs was a major part of designing an implantable pump and we looked at several existing micropumps and motors that could work effectively for our application. Th disadvantage of purchasing a micropump or micromotor was the cost of such a device. But the idea of an electromechanical actuation was very interesting and we considered actuating the diaphragm using permanent magnets. The idea came from a setup that produced a damped motion of two magnets along a shaft with the opposite poles facing each other. This idea on a large scale was used to create a cordless bungee-jumping setup where the participant wore a magnetic suit that was oppositely polarized to the magnets on the ground and the magnetic repulsive force allowed cordless damped vertical motion of the participant. Illustrations depicting the setup with some initial sketches of this "cordless bungee-jumping" idea incorporated in our implantable pump are shown in Figure 9.4.

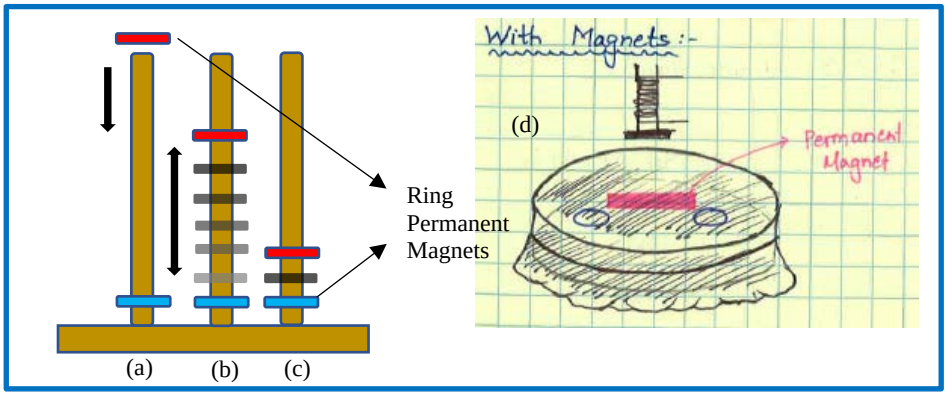

Figure 9.4. (a) Inserting a ring magnet into the shaft with opposite pole facing the second ring magnet; (b) Vertical motion because of magnetic repulsive forces; (c) Time dependent damping of the magnet's motion; (d) Sketch of the diaphragm pump in Figure 8.3 with a magnet and a solenoid.

The motion of two oppositely polarized magnets gave birth to idea of using solenoids. But, we wanted to completely rule out the idea of using two magnets as shown in the setup in Figure 8.4 to actuate the diaphragm. The advantage of just using permanent magnets is power conservation but the disadvantage is the constant motion of the magnet before it settles will cause occlusive cuff pressure fluctuation when used in the actual device. One of the designs made using this magnetic actuation mechanism was a combination of a piston-diaphragm pump as shown in Figure 9.5.

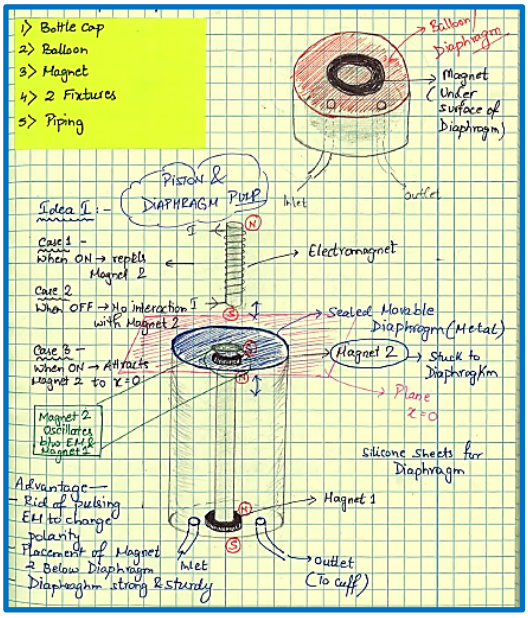

Figure 9.5. The Diaphragm-Piston pump actuated by permanent magnets and an electromagnetic coil. Sketched on 7/29/2015.

The working principle for this magnetic piston diaphragm pump was the simple application of the law that like poles of a magnet repel each other and unlike poles attract. It also uses the rule that the change in direction of current through a coil alters the magnetic poles on an electromagnetic coil. This pump design needed two magnets, one electromagnet and a rigid diaphragm that moved vertically along a shaft. With 3D-printing gaining traction and its advantages in rapid prototyping, I printed a few designs using the Medical Devices Center's 3D printing facility. One of the designs I printed along with its dimensions is shown in Figure 9.6 and the volume calculations for this pump are also shown.

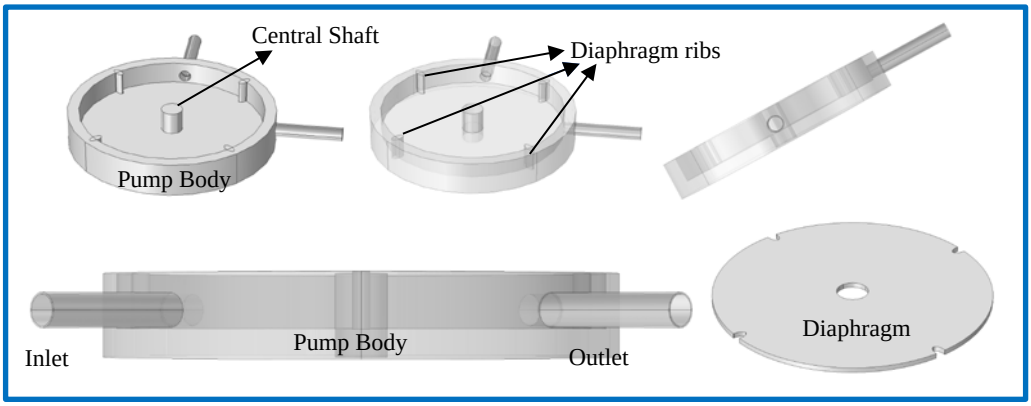

Figure 9.6. Diaphragm Piston pump design 3D printed at the Medical Devices Center. The inner diameter (ID) of the pump body is 27.71mm and the outer diameter (OD) is 31.13 mm. These dimensions are comparable to a Coca-Cola bottle cap. The overall height is 11.5 mm. The 4 diaphragm ribs around the periphery of the pump body as 9.4 mm high. The diameter of the shaft is 2.16 mm. The diaphragm is 27.68 mm in diameter. The pump body was closed off with a sealed ring (not shown in figure) with a diameter of 31.13 mm and thickness of 2.765 mm. The inlet and outlet both had a 10-mm long extrusion from the pump body and was 1 mm (0.8 mm) [OD (ID)].

$$Volume\ of\ liquid\ within\ the\ pump\ body = Volume\ of\ Inner\ cylinder - Volume\ of\ Cental\ Shaft$$

$$= \pi r_1^2 h - \pi r_2^2 h = 5.91cc - 0.77cc = 5.14cc$$
$$r_1 = Inner\ radius\ of\ pump\ body = 13.855\ mm;$$
$$r_2 = Radius\ of\ Cental\ shaft = 1.58\ mm$$
$$h = 9.8\ mm$$

The design in Figure 9.6 was unsuccessful because of the following:

- The rigid diaphragm and the uneven inner surfaces of the pump body (obtained from FDM (Fused Deposition Modeling) 3D Printing contributed to immense friction.
- The sealing was not sufficient to keep the liquid within the pump body.
- An attempt at magnetic actuation failed because the magnetic forces were unable to overcome the frictional forced.

The next design was inspired from the keyboards that we use to type theses like the one you are reading. Old keyboards had a mechanical scissor switch action like the one shown in Figure 9.7 (a) and the scissor design allowed the keys to return

to their original position after use so that they could be used again. Current QWERTY keyboards (especially those used with PCs or Desktops) are usually equipped with different audible and tactile switches which create the distinct sounds and sensations of typing. A very common one is the rubber dome [Figure 9.7 (b), (c)] which has a hard center that is pushed down upon by a plunger below the key and this hard center presses against the key matrix which eventually types the word one needs. Such keyboards have good tactile responses and are resistant to spills and corrosion [57].

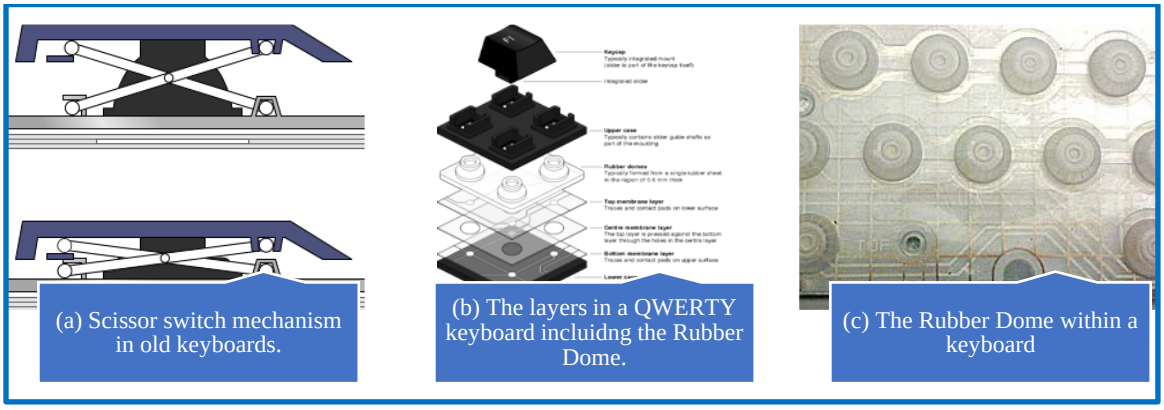

Figure 9.7. Keyboard switching mechanisms: The Scissor Switch and the Rubber Dome *[57]–[59]*.

The design inspired from the keyboard's rubber domes is shown in Figure 9.8 and the volume calculations can be found alongside the design. Two designs using the rubber domes allowed flexibility from a volumetric perspective. Volume calculations were necessary for the designs because we were also trying to determine the volume of fluid it takes to raise pressure from 20 cmH_2O to 120 cmH_2O. A clinical study to determine this volume in the existing device was conducted and will be elaborated upon in a later section.

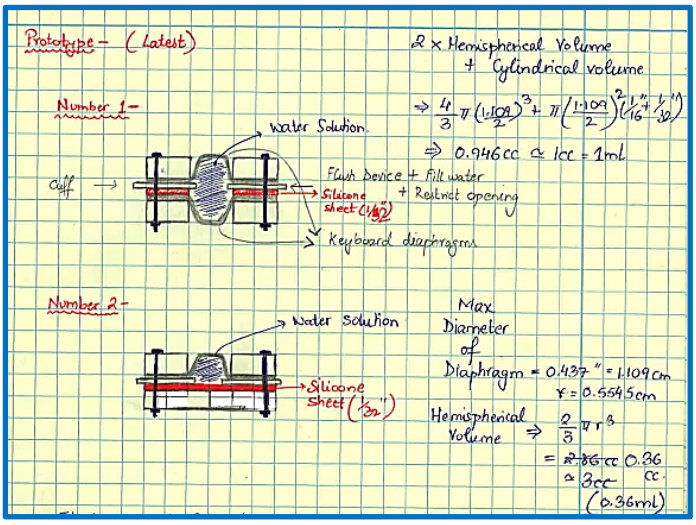

Figure 9.8. The Rubber Dome pump. Sketched on 8/30/2016.

The design was made with the idea that the device can be implanted subcutaneously and the patient simply must activate the pump by applying pressure on the rubber domes. The other advantage was that the pump could be filled with volumes up to 1mL, which as it turns out is enough to raise the pressure from 20 cmH_2O to 120 cmH_2O (through the clinical study discussed later). The failure of this pump was due to reduced magnetic actuation that resulted in ineffective application of force on the fluid within the pump.

Going back to the board and trying out other ideas such as the ones shown in Appendix D gave me ideas on the actuation mechanism which must be instantaneous, applies uniform compression, and occurs within sufficiently sealed conditions. The sealing of pump bodies was the single largest contributing factor for the failure of some of these designs. As we proceed further we will discuss other major tweaks in the design like completely doing away with the permanent magnets, testing different diaphragm materials, and a variety of sealant adhesives.

9.2.1. Development of the Current Designs

After the designs shown in Section 9.2 and Appendix D, we tried to design pumps that applied uniform pressure on the liquid inside it and the best option was designing a system like a syringe. The diaphragm would be rigid and lined by a well-lubricated O-ring that traversed the height of the pump body in a frictionless manner. The diaphragm, to maintain its alignment at all time was made to pass through 3 or 4 shafts. A variation to the design was making the inner lining of holes on the diaphragm through which the shafts passed smooth and properly sealed such that the O-ring could be done away with. These designs are shown in Figure 9.9 (a)-(c). Figure 9.9 (d) uses the idea that a flexible diaphragm can be tightened between two pieces designed like a cap-screw and this would naturally allow excellent sealing.

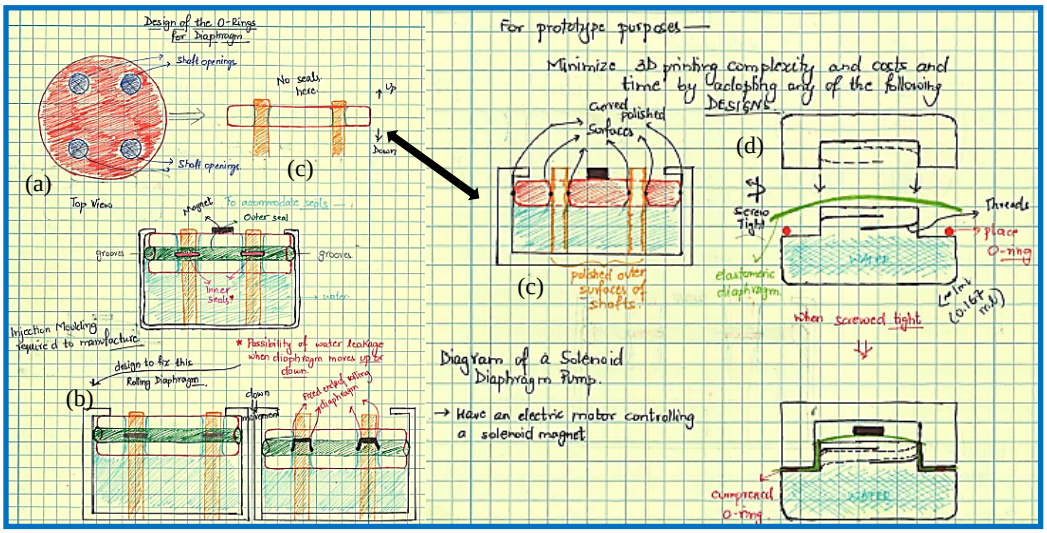

Figure 9.9. (a) Holes for the pump shafts in a rigid diaphragm (shown in navy blue color); (b) O-Ring incorporated design with O-ring seals around the diaphragm (shown in green) and rolling diaphragm seals around the shafts within the diaphragm holes (shown in red); (c) Similar pump design without O-rings and frictionless surfaces inside the pump for smooth diaphragm movement; (d) A cap-screw design with an elastomeric diaphragm sandwiched between the two parts that evenly stretches out over the pump opening as the cap is tightened. (The magnets are shown in Black)

The designs from a prototyping perspective were hard to implement because of the complexity and the interaction of the O-ring seals with the diaphragm. If 3-D printed, they would have to be made with a printer that has very high resolution for a smooth finish. This could be achieved by injection molding but this endeavor would have been very expensive. Additionally, the actuation mechanism with magnets had to be tested and that had not been given sufficient attention. We filtered our ideas and brought down the designs to the 4 shown in Figure 9.10. Each of these designs had a rigid diaphragm and for sealing to not cause failure in the design, we decided to put in a miniature life-saver tube or the silicone-made AMS 800™ cuff or pressure regulating balloon. These 4 designs with minor tweaks made on the fly have been the basis of our current device. The designs were built in Onshape (Cambridge, MA, USA)- a cloud based CAD software and then 3-D printed for bench testing. The Onshape models are shown in Appendix E.

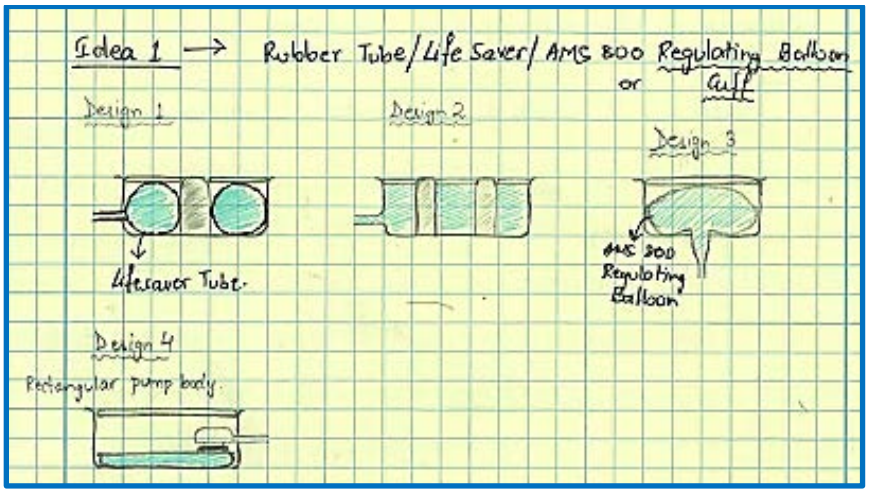

Figure 9.10. **(a)** Pump with a life-saver shaped tube for fluid; **(b)** The usual rigid diaphragm idea as shown in Figure 8.9 (c); **(c)** Pump with AMS 800™ pressure regulating balloon; **(d)** A rectangular pump with AMS 800™ cuff.

9.3. Designs Incorporated with Electromagnet

9.3.1. Solenoids: Design and Fabrication

The idea for the solenoid stems from our initial design depicted in Figure 9.4 and 9.5. We looked at making our own coils and miniaturize these solenoids for our application to make them implantable. Our immediate guess was incorporating electromagnetic transducers from hearing aids, despite these coils producing very small displacements. Stieger et al., studied the variations of air gap, distance between the coil and permanent magnet, diameter of the coil, and uniform pressure distribution on a low power milliwatt EM micro speaker using PDMS membranes [60]. Figure 9.11 gives a schematic of the arrangement of the coil (CO) and the permanent magnet (PM).

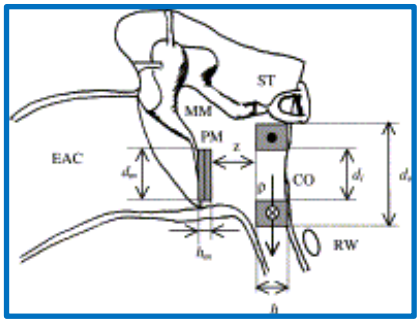

Figure 9.11. Schematic drawing of the proposed electromagnetic transducer for a middle ear hearing aid. A permanent magnet (PM) is mounted on the manubrium mallei (MM). A coil (CO) is placed between the stapes (ST) and the round window (RW) on the wall of the middle ear cavity (EAC= external auditory canal) [60].

$$d_0 = Outer\ diamter\ of\ CO$$

$$d_i = Inner\ diamter\ of\ CO$$

$$h = Height\ of\ N-turns\ of\ the\ CO$$

$$d_m = Diamter\ of\ PM$$

$$h_m = Height\ of\ PM$$

$$q^2 = \frac{(d_0 - d_i)\eta h}{2N}\ ;\ L = N\pi\frac{d_o + d_i}{2}\ ;\ j = \frac{IN}{(d_o - d_i)\frac{h}{2}}$$

Cross-section of Wire | Total Length of Wire | Current Density

Equation 8.1 [51]

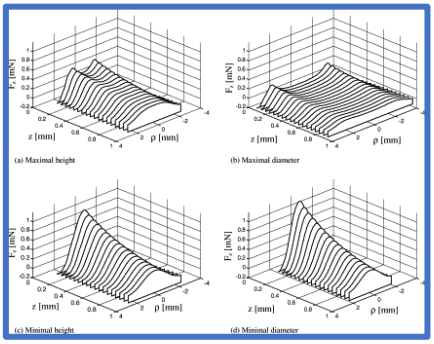

Figure 9.12. Results of Force simulations for four different coil geometries [51].

The simulation results of different coil configurations (Figure 9.12) showed that a minimal diameter, minimal height, and zero-airgap (denoted by the x-axis) in a CO gives the maximum force between a PM and a CO. This result will be useful in our design when we work on designing our own coils for our application and it works completely in our favor since it implies that the device size will be smaller. Stieger et al, used a reference coil to compare the results and this coil was made up of isolated Cu wire with a diameter of 40μm, length of 1.75m, 166 turns and a filling factor (η) or space required between wires of 0.35 [60]. The current density produced from the reference coil was 4.46 A/mm^2.

Gradually, we moved from the idea of designing our own solenoid coil to acquiring mini-solenoids from the market directly. This was done for time and monetary constraints. During this search, we found industrial solenoid valves (Figure 9.13) that worked on the principle that a ferromagnetic plunger surrounded by a coil will undergo displacement when current passes through the coil [61]. Such a valve was called the direct-acting solenoid valve and the law they follow is famously known as the Biot-Savart Law. The advantages of using an electromagnetic actuator are:

- Fast response
- Simple control law- based on flow of current
- Low manufacturing time and costs

Several references highlight the importance of the material of the ferromagnetic plunger for greater magnetic fields.

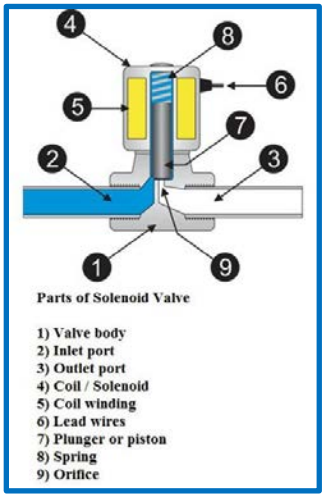

Figure 9.13. A direct-acting solenoid valve with a ferromagnetic plunger [61].

Using this concept of the solenoid valve, we designed the following (Figure 9.14) using the AMS 800^{TM} cuff and pressure regulating balloon.

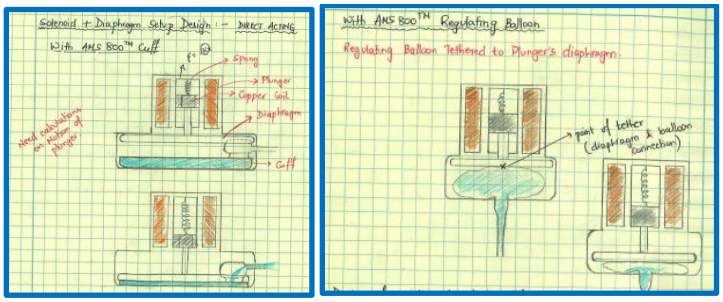

Figure 9.14. Pump using a solenoid actuating valve and AMS 800^{TM} components.

We were convinced with the efficacy of the solenoid actuators from Song and Lee's publication on solenoid actuated miniaturized segment robots [62]. The ferromagnetic plunger in the solenoids were made of a permanent magnetic core and the robots were actuated by alternate in-phase and out-of-phase actuation that caused linear and rotatory motions. The design of the solenoid used by Song and Lee is shown in Figure 9.15. The solenoid they fabricated has 1250 turns with an outer diameter of 15 mm, length of 20 mm and an inner diameter of 5 mm. They had a constant input current of 0.6 A, which as we will see in later sections, is very high for an implantable device that needs to have a good power saving mechanism. Nonetheless, the results from the fabricated solenoid both experimental as well as theoretical showed that the pushing force increased with the increase in number of turns.

Solenoid valves operate on a digital principle which means that the coil is activated by an electrical current and deactivated without any current. Solenoid valves can also be of the latching type which has a permanent magnet built in that holds the plunger in a working position without an electrical energy consumption. We considered a latching solenoid (Solenoid Push Pulse 5V, Delta Electronics; Appendix F) [63] for our prototype but the solenoid drew a very high initial current for activation which was beyond the scope of the power supply we had and therefore, had to look at other options.

For our prototype, we used the Mini 5V Push-Pull Solenoid from Adafruit Industries LLC (Figure 8.15; Appendix G) [64]. The solenoid has a 3-mm plunger stroke and at a rated voltage of 5V and rated current of 1.1A, the solenoid weighs 12.6g. The solenoid is 12mm by 11mm by 26mm. The technical specifications are mentioned in Appendix G.

Figure 9.15. Mini 5V Push-Pull Solenoid from Adafruit Industries LLC (Appendix G) [63]

9.3.2. Designs with the Adafruit Solenoid

When it was time to consider 3D printing, we tried a variety of designs on Onshape and this section gives a sneak peek into the designs printed with the Stratasys Fortus

250mc provided to the MIND Lab by the Department of Urology. The design variability was dependent on the following:

- type of diaphragm used
- the position of the magnet
- the quality of sealing
- ease of force application on the diaphragm
- fluid volume within the pump.

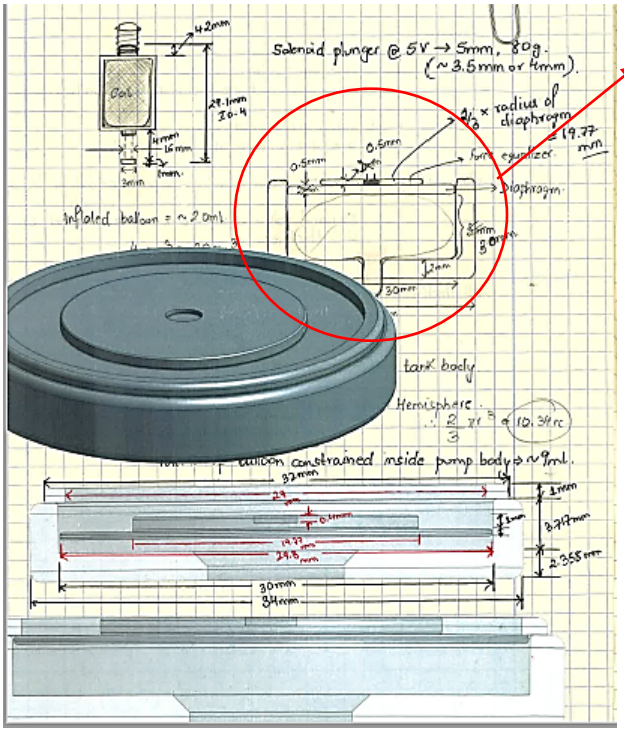

Figure 9.16. Mini 5V Push-Pull Solenoid with the pump design using the pressure regulating balloon to hold the fluid. (Sketched on 5/22/2017)

Inflated AMS 800™ Balloon:

~20 cc

$$20 = \frac{4}{3}\pi r^3 \Rightarrow r = 1.7\ cm$$

Assuming balloon is rectangular inside the pump and the stroke length of the Adafruit solenoid is 3 mm, the volume of fluid within the balloon will be close to hemispherical:

$$Volume = \frac{1}{2} \times \frac{4}{3}\pi r^3$$

$$= 10.34cc$$

The design in Figure 9.17 was the first design we printed and it failed because of incorrect dimensions with respect to the pressure regulating balloon. The other mode of failure was that the solenoid did not have a strong base or foundation to sit on, and upon actuation, the solenoid wobbled. The same problem was observed when we used a surgical nitrile glove as a diaphragm instead of a 3D printed rigid diaphragm. To create an effective seal, we used a Loctite Silicone adhesive. The models in Figure 9.18 were some attempts made at perfecting the design and comparing the effectiveness of a pump with an in-built fluid chamber using the pressure regulating balloon versus a pump with a nitrile glove diaphragm. The model with the pressure regulating balloon also failed because of a tear in the balloon with constant inflating and deflating cycles. The nitrile diaphragm gave a good result but without a strong support for the solenoid, the device was wobbly and the force from the solenoid actuation did not apply uniform pressure. The sketches for a solenoid support area over the pump body are shown in Figure 9.19.

Figure 9.17. Oshape design and 3D printe model of a pump with rigid diaphram to be used with the pressure regulating balloon.

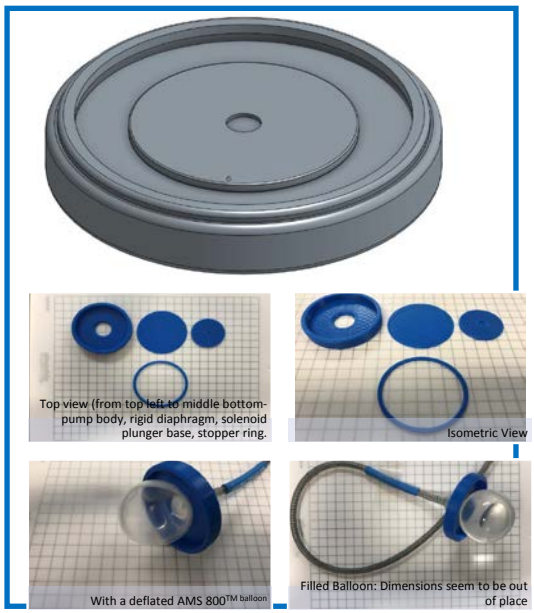

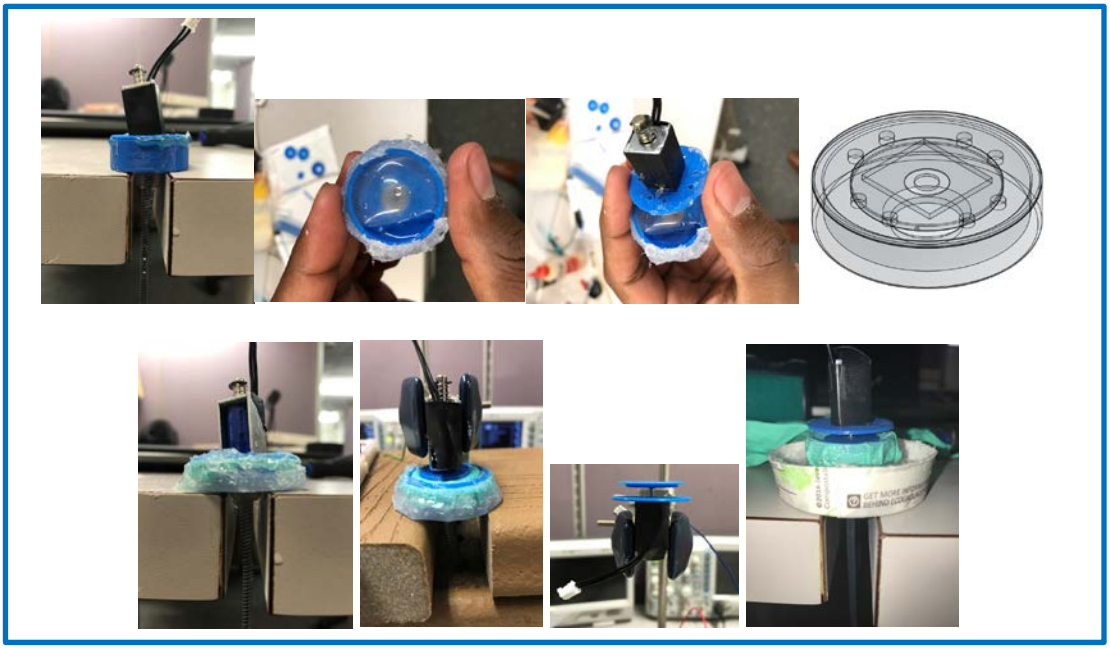

Figure 9.18. Top Row- 30 mm diameter pump design with in-built solenoid support, pressure regulating balloon. The balloon tore with repeated inflation and deflation during testing. **Bottom Row-** 34 mm diameter pump with a nitrile glove diaphragm and without an in-built solenoid support.

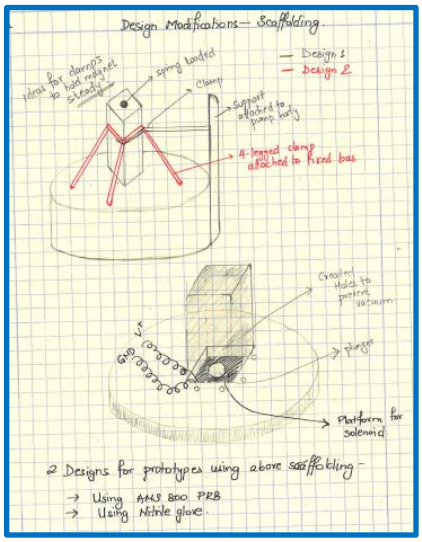

Figure 9.19. Scaffolding for the Mini 5V Push-Pull Solenoid with the pump. (Sketched on 6/5/2017).

An aspect of the pump design that we had not considered until now was the volume required to raise cuff pressure from 20 cmH_2O to 120 cmH_2O and this leads us into the designs that we obtained after the IRB approved clinical studies that conclusively showed that we need 0.31-0.62 mL of fluid to reach the desired pressure. The Onshape designs and the 3D printed models have been shown in Figure 9.20.

Figure 9.21 shows designs using a lid configuration like the idea presented in Figure 9.9 (d), where the pump has two components- a pump body with grooves into which a lid with a solenoid scaffolding is inserted and while doing so, a nitrile diaphragm

is sandwiched between the two parts before it is sealed. This allows better sealing and effective translation of actuation force to diaphragm displacement. The design also took into consideration volume measurements from the clinical study.

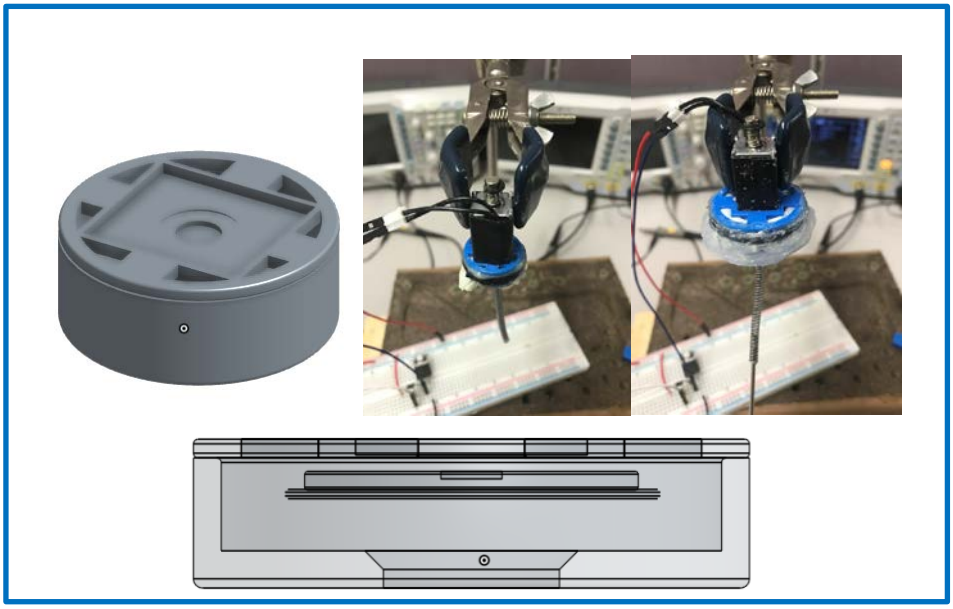

Figure 9.20. Pump designs with in-built solenoid scaffolding and nitrile diaphragms.

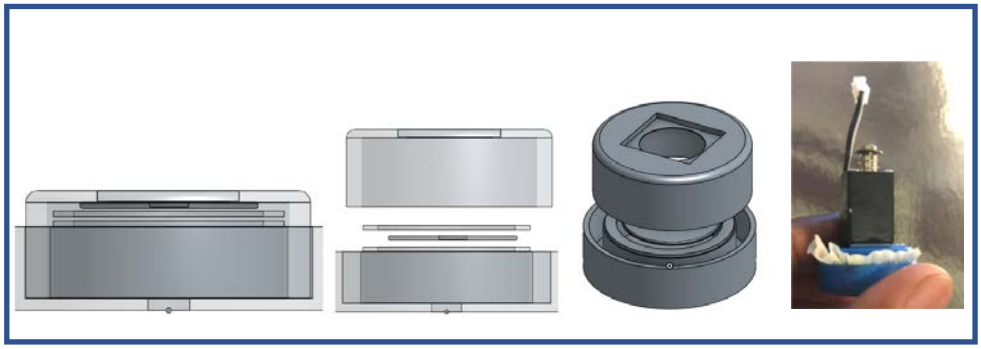

Figure 9.21. The lid design inspired from Figure 8.9 (d)

9.4. Characterization of the AMS 800^{TM} Cuff: Pressure vs. Volume

9.4.1. Pressure vs. Volume: Inside Cuff Only

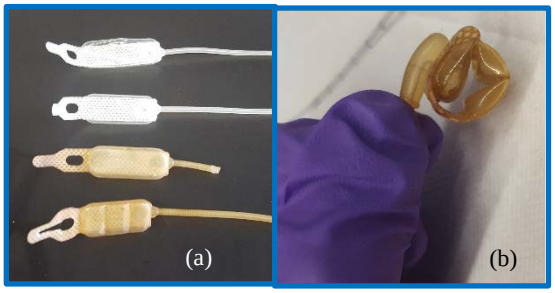

Figure 9.22. (a) AMS 800^{TM} Occlusive Cuffs: 3.5cm, 4cm, 5 cm, 5.5 cm. **(b)** A 4cm cuff at a pressure of 20 cmH_2O.

Figure 9.22 (b) shows the uneven pressure distribution of the cuff with the narrow back design. The kinks cause uneven pressure profiles around the urethra. Mahdi et al., conducted a 360^{o} pressure profile around the urethrato understand the ways in which it varies [65]. Their sensing catheter with a series of sensors were used to measure the profiles around the urethra using a protractor rotatory system. The Goby^{TM} portable urodynamics system setup is shown in Figure 9.23 along with the corresponding data obtained from the sensor in relation to the angle as the cuff wraps around the urethra. The results were at different values of cuff pressure.

We used the same setup as Mahdi et al., and got the following graphs for pressure in cuffs of different sizes. The graphs were then fitted along a mathematical curve using Microsoft Excel mathematical1y

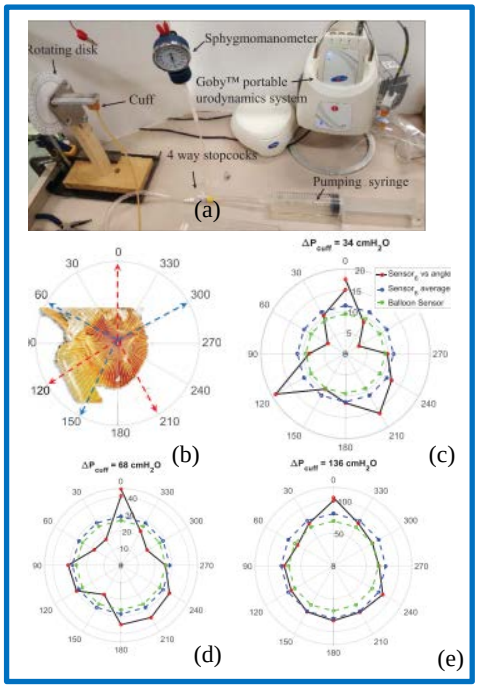

Figure 9.23. (a) Goby^{TM} portable urodynamics system setup; **(b)** Cuff's cross section after inflation. The blue arrows show high pressure locations and the red ones point to the angle with low pressure; **(c)** sensor response to ΔP = 34 cmH_2O at different angles and comparing the average value with air-charged balloon sensor; **(d)** sensor response to ΔP = 68cm H2O at different angles; **(e)** sensor response to ΔP = 136cm H2O at different angles. [65]

gives us the volume required for different cuff sizes to reach 120 cmH_2O when used outside the body. The equations were solved using Wolfram Alpha. The volume ranged between 0.6 – 0.7 mL.

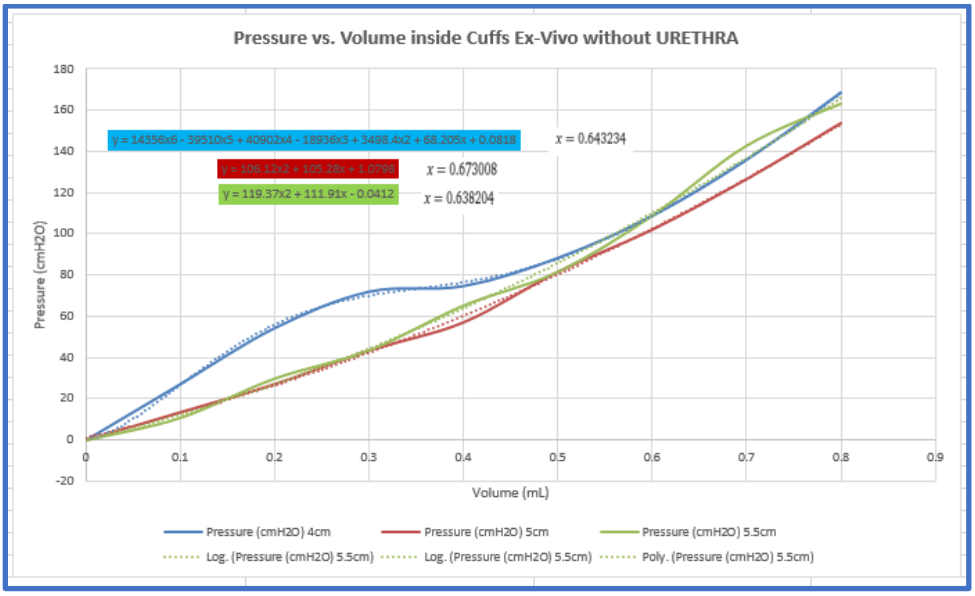

Graph 9.1. Pressure vs. Volume in Cuff only: Volume required to raise cuff pressure to120 cmH_2O in different cuff sizes. Polynomial Curve Fitting also shown. Volume determined using Wolfram Alpha.

9.4.2. Pressure vs. Volume: Around Ovine Urethra

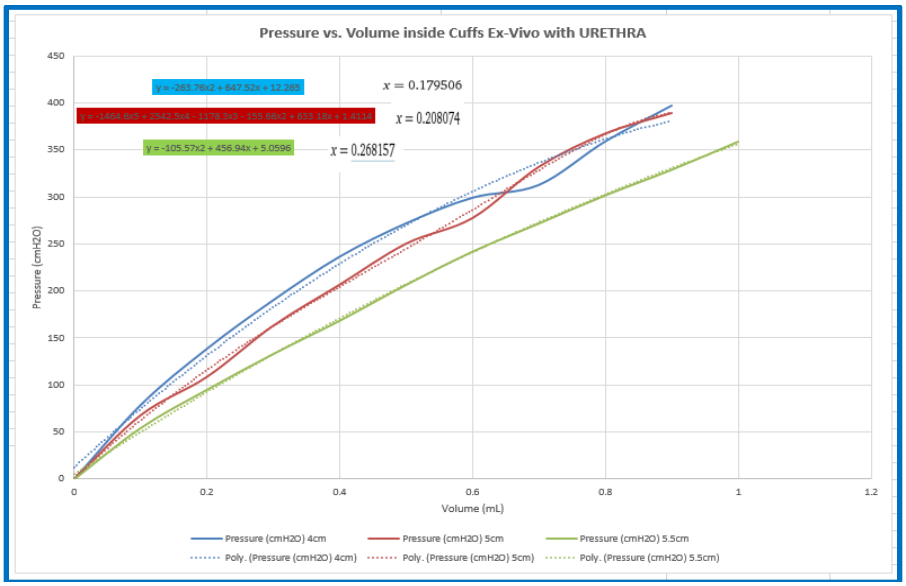

Graph 9.2. Pressure vs. Volume in cuff when around Ovine urethra. Volume determined using Wolfram Alpha.

9.4.3. Clinical Study: Pressure-Volume Measurements on the AMS 800™ Cuff

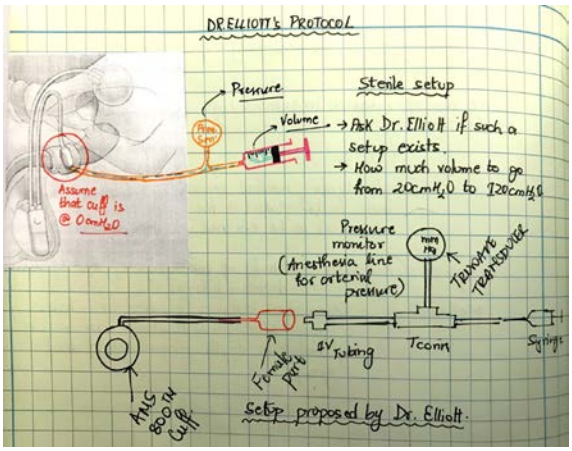

Figure 9.24. Sketch of the setup for the clinical study.

The University of Minnesota Institutional Review Board approved this clinical study on 5/30/2017. We collected pressure and volume data while an AUS was being implanted. One patient underwent a revision surgery and was implanted with a tandem cuff of 4 cm and 5 cm sizes, while the other two patients were implanted with a 4 cm and 4.5 cm cuff, respectively. The setup as shown in Figure 9.24 uses an Edward LifeSciences TruWave pressure transducer (Appendix H) which is connected to a pressure measuring system [66]. The transducer has a three-way stop cock with an inlet for flushing the system with saline, another inlet for providing saline at intervals of 0.1cc, and an outlet that goes to the cuff. The readings from patient 1 do not seem comparable to patient 2 and 3 and we consider this as errors which would have crept in because it was the first time. The procedure was refined for patients 2 and 3.

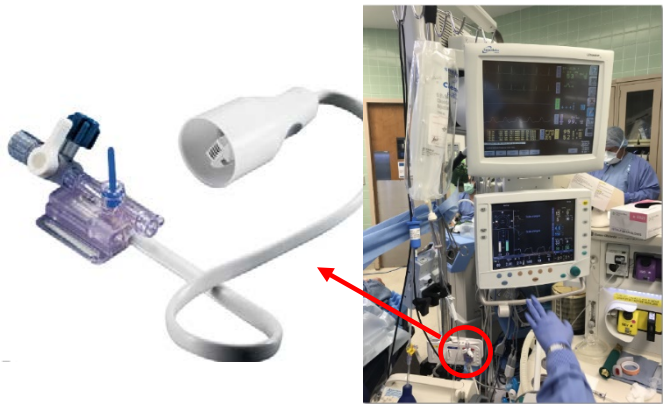

Figure 9.25. The Edward LifeSciences TruWave Pressure Transducer as used in the University of Minnesota hospital OR setup while operating on Patient 2. The TruWave Pressure transducer is traditionally used as an anesthesia line for arterial pressure, but in this case, will be used for a simple pressure-volume measurement. [57]

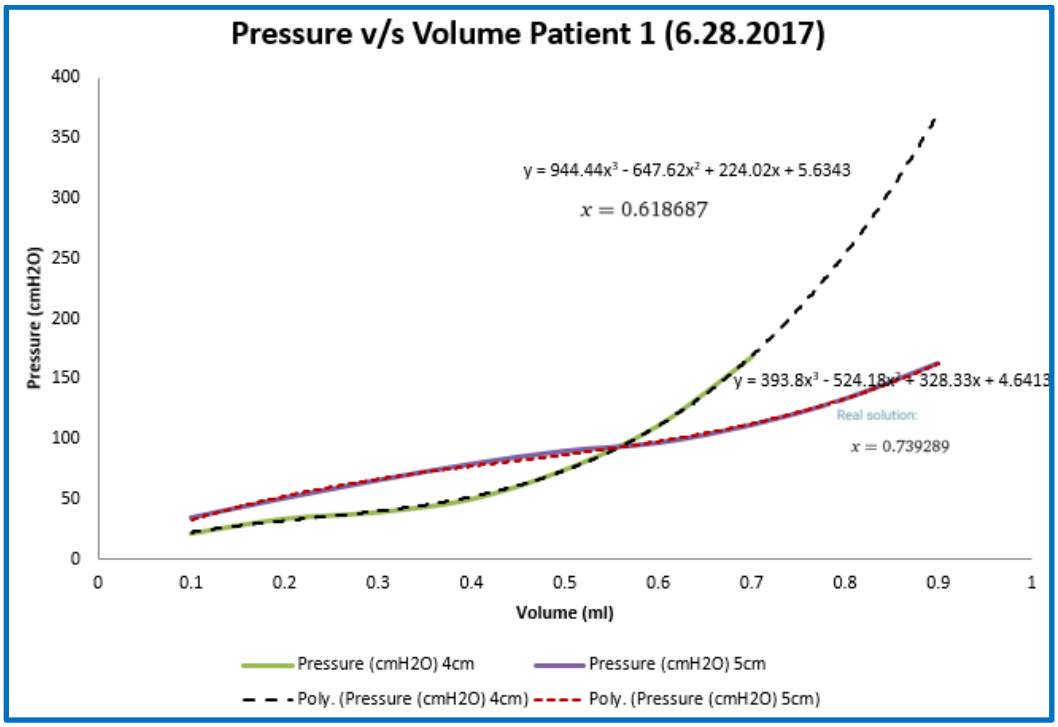

Graph 9.3. Pressure vs. Volume in 4 and 5 cm cuff in Patient 1.

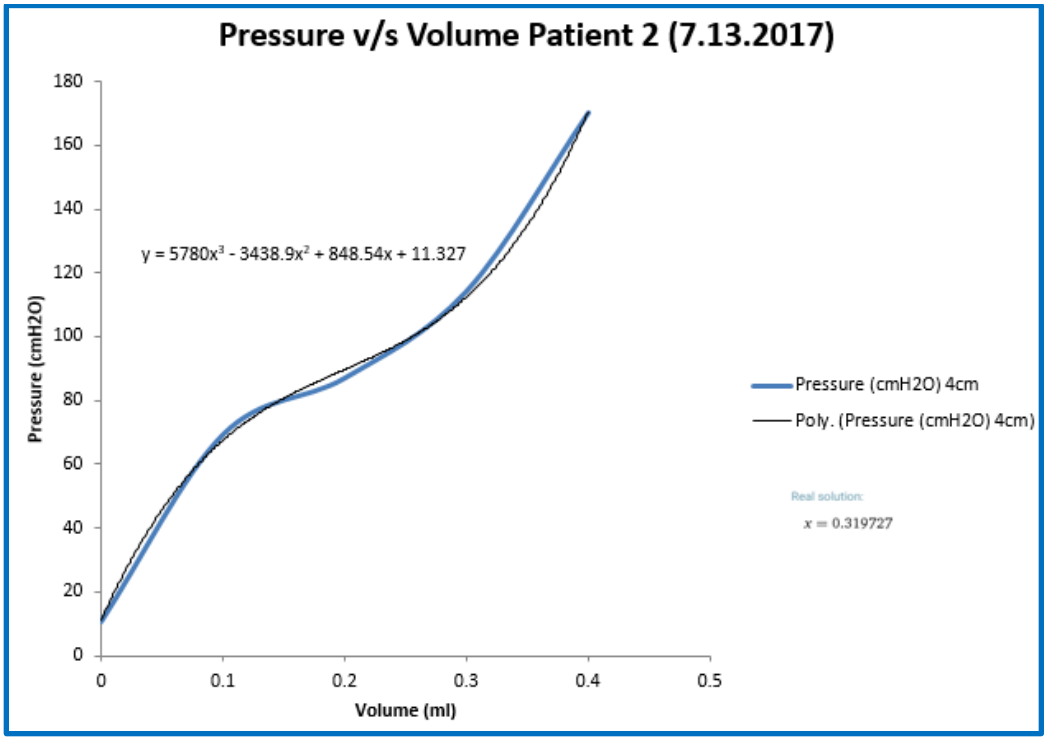

Graph 9.4. Pressure vs. Volume in 4 cm cuff in Patient 2.

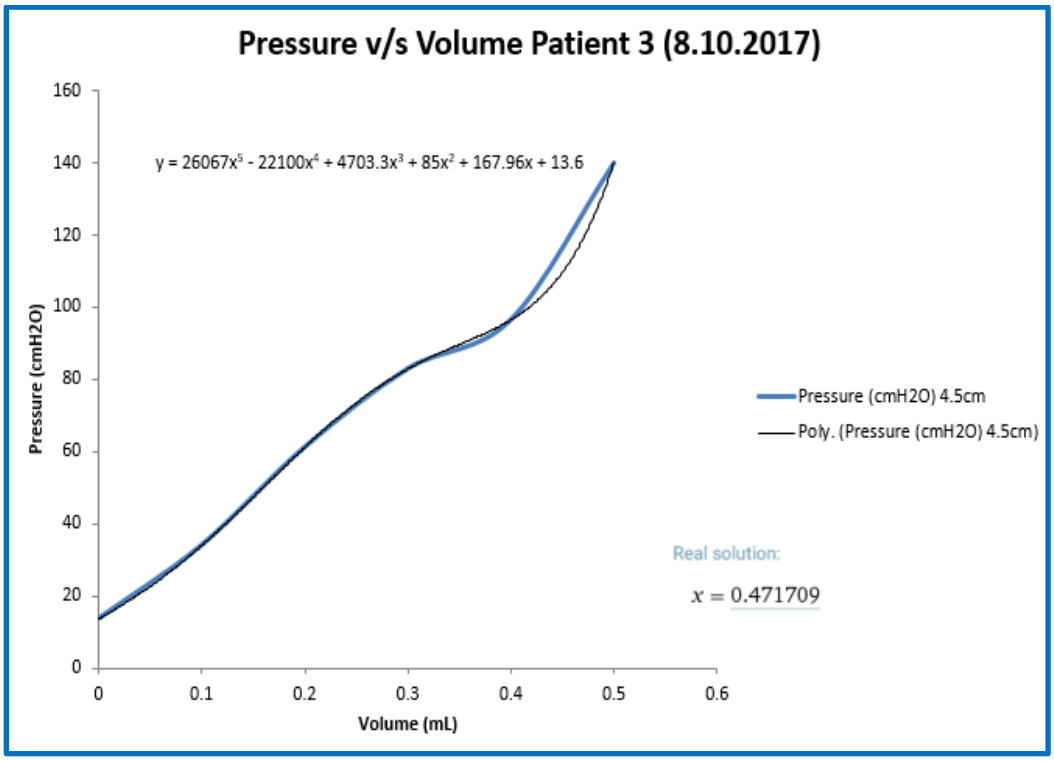

Graph 9.5. Pressure vs. Volume in a 4.5 cm cuff in Patient 3.

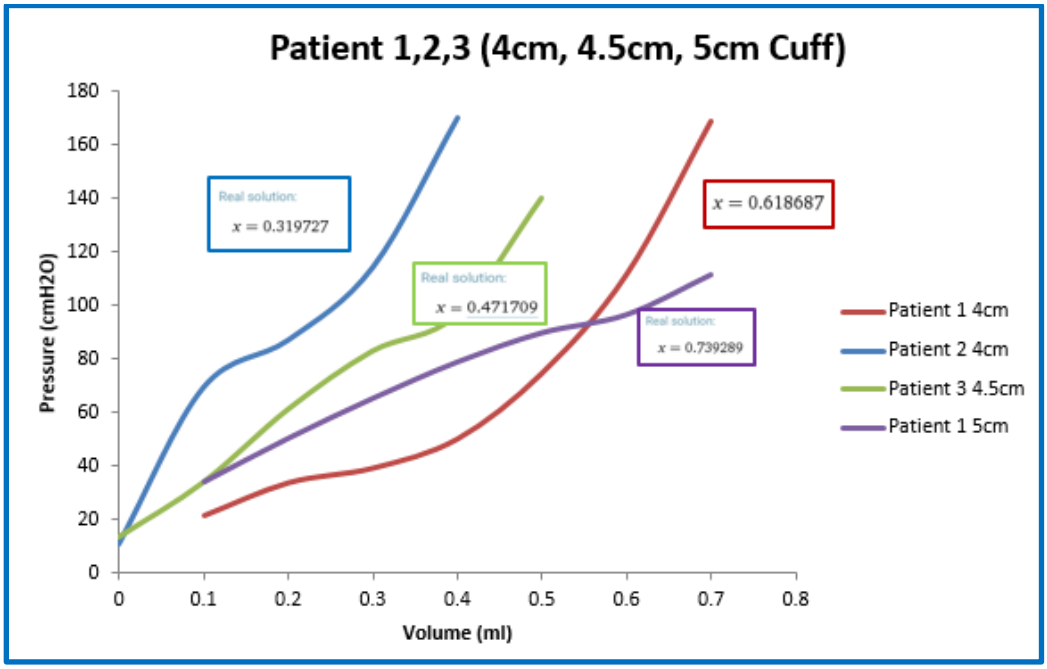

Graph 9.6. Pressure vs. Volume Comparison in all 3 patients. Volumes at which pressure reaches 120 cmH_2O are mentioned in colored boxes.

9.4.4. Conclusions from Ex-Vivo and Clinical Data

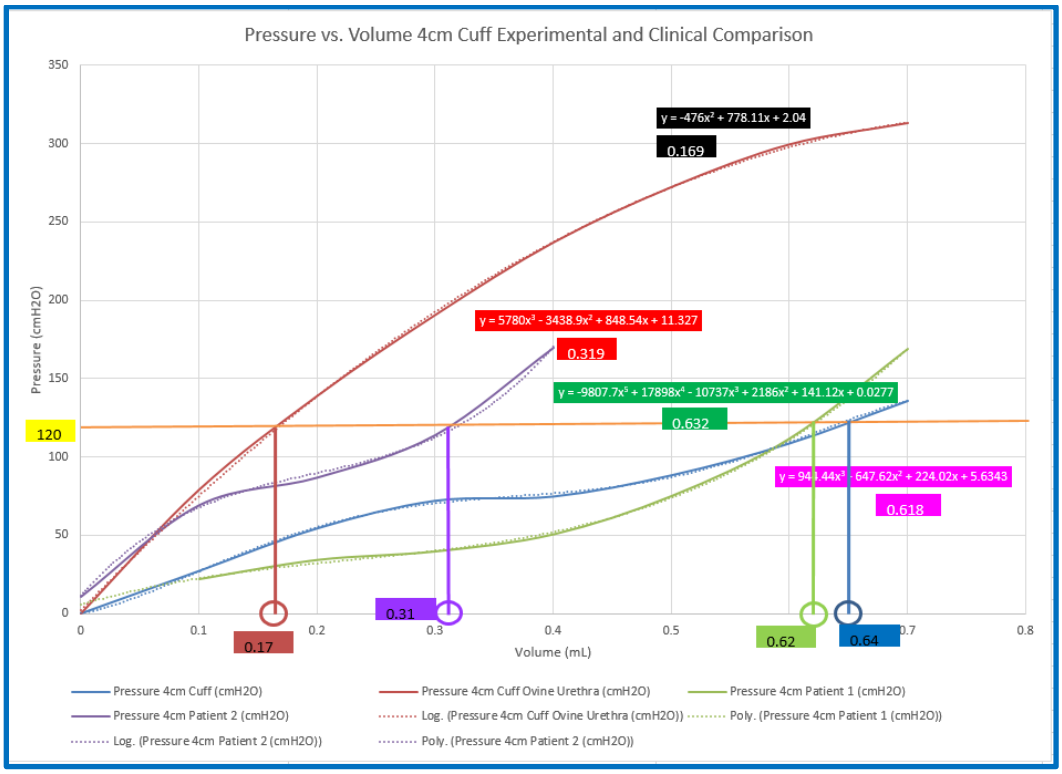

Graph 9.7. Pressure vs. Volume in a 4cm cuff- ex-vivo, around ovine urethra and Patients 1 and 2.

All equations to determine mathematically the volume needed to raise pressure in the cuff to 120 cmH_2O were calculated using Wolfram Alpha. When used ex-vivo without an ovine urethra, the volume needed was within 0.6-0.7 mL (Graph 9.1). When the cuff was placed around the ovine urethra (Figure 9.26), volume needed was between 0.15-0.27 mL (Graph 9.2). The reason for such low volume is because of the presence of fat around the urethra which applied pressure on the cuff as it was being filled with fluid (Figure 9.26). In the ex-vivo and ovine urethra studies the size of the cuffs were 4 cm, 5 cm, and 5.5 cm. When the studies were done on patients, the urethra is separated from the corpus spongiosum and the cuff is wrapped around it after being sized. In patients, the volume required to reach

120 cmH_2O was in the range of 0.32-0.75 mL (Graph 9.3-9.6). Since the 4 cm cuff was used in majority of the cases so far, a comparison of the said cuff ex vivo, around the ovine urethra and the patients gave a volume within the range of 0.17-0.64 mL (Graph 9.7). As intuition would tell us, the cuff volume when ex-vivo would be higher than around the urethra because the urethra applies a back pressure on the cuff as it inflates.

Figure 9.26. Pressure vs. Volume measurements around an ovine urethra using the Goby™ portable urodynamics system setup

10. Other AUSs from the Literature

During the designing process, an honest survey of publications is essential to make the new designs unique and novel. Ruthmann et al. in 2009 published their idea for the first ever tele-automatic sphincter prosthesis called the modified German Artificial Sphincter System (GASS) or GASS II, which worked at low voltages [67]. Their idea was to design a sphincter prosthesis that could work for fecal or urinary incontinence as well as in the GI tract. Their design allowed the device to operate between -10 V to +20 V and the pump flow rate was 2.23 mL/min [67]. They present a high-performance piezoelectric pump that is housed with the fluid reservoir in an isolation casing (Figure 10.1).

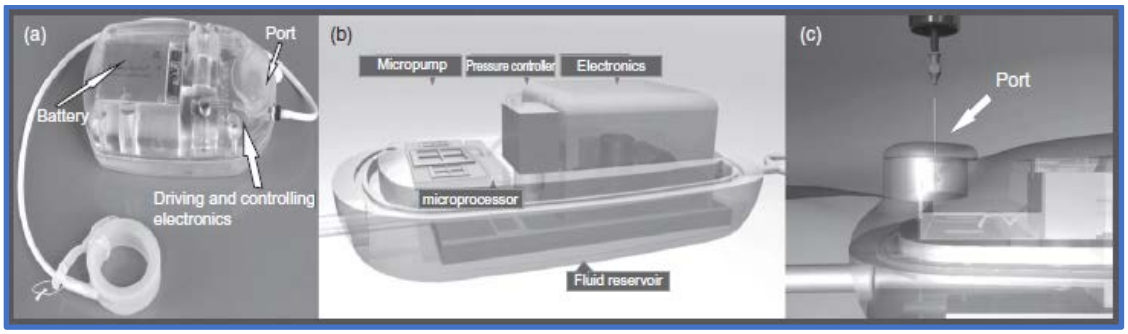

Figure 10.1. (a) Modified prosthesis GASS II; **(b)** Design with all mechanical and electrical components; **(c)** filling through the port *[67]*.

The cuff seen in Figure 10.1(a) is called the Soft-Analband from Agency for Medical Innovations (AMI GmbH, Austria) and is much different from the AMS 800^{TM} discussed in previous sections. The isolation unit measures 8.3 x 4.5 x 2.7 cm and holds the piezo-pump, regulator, microprocessor, telemetry transmitter and receiver coils, and rechargeable batteries [67]. From an energy stand-point, the batteries could be used for 6 days in the case of urinary incontinence at a rating of 84mAh/ day with inflation

and deflation cycles. The battery had a capacity of 570 mAh and 1000 charging cycles. This would be a major drawback for an implantable device.

In 2010, Lamraoui et al., published a design for a novel, automated AUS which exerted constant pressure circumferentially around the urethra and the occlusive pressure could be controlled with an accuracy of 1 cmH_2O. Their motive behind coming up with a novel device was the high risk of injuries due to constant urethral compression. The device had an electromechanically driven pressure system, wireless communication, adaptive pressure regulation mechanism through accelerometer sensing, safety system to prevent urinary retention, and control of micturition (Figure 10.2). The pressure system applied a maximum of 120 cmH_2O in a 4cm cuff at a volume of 0.5-0.7 mL. The electromechanical pressure system is based on a rolling diaphragm attached to an electric motor that generates an occlusive pressure of 500 to 800 cmH_2O [68]. For this device, the power requirement was 100µW and the entire device had a volume of about $60cm^3$ [68]. The researchers were considering using a transcutaneous wireless charging mechanism for effective power delivery and reduced hospital visits for reimplantations.

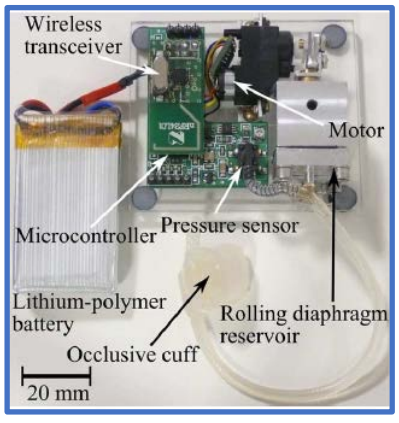

Figure 10.2. Lamraoui et al's Automated AUS (AAUS) [68].

In 2014, Ramesh et al., came up with a design from a materials perspective and introduced the idea of using an ionic electro active polymer (EAP) [69]. The challenge with any cuff is that it should not restrict blood flow through the urethra and the EAP cuff had to take this into consideration.

EAP bends upon voltage biasing and some of the most common materials used are Ionic Polymer Metallic Composite (IPMC), Ionic Polymer Gels (IPG), Carbon nanotubes, and conductive polymers. The EAP will circumscribe the urethra and to get a material that requires minimum power, researchers had to find one that required minimum voltage but produce maximum displacement.

Hached et al., developed a novel AUS in 2014 which could be operated wirelessly and helped control the sphincter rapidly [70]. The implant does away with the AMS 800^{TM} control pump so that it can be implanted in women as well. The hydraulic circuit is the most important part in any smart AUS, and here Hached et al., replace the manual control pump with a micropump and microvalves. They use the pressure regulating balloon and study its characteristics during inflation cycles to understand its behavior. Considered as a Mooney-Rivlin material, the silicone material of the pressure regulating balloon evolves in four distinct phases during inflation. They compared their work with Ruthmann's and Lamraoui's which is shown in Figure 10.3.

Research group	Flow/ pumping time	Voltage	Power consumption	
			Pumping	Holding
Lamraoui et al. [12]	500 to 800 cmH_2O/s	Not indicated	500 mW	0 W
Ruthmann et al. [13]	2.23 ml/min	30 Vpp	120 mW	10 mW
This work	15 ml/min – 40 to 60 cmH_2O/s	5 V	≤65 mW	0 mW

Figure 10.3. Comparision of Ruthmann's, Lamraoui's and Hached's work [70].

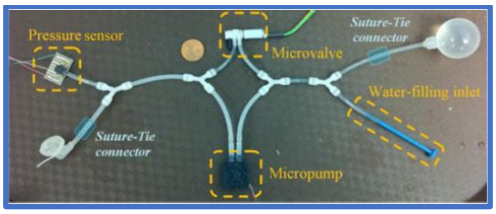

Figure 10.4. Hached et al.'s wireless AUS and it components [70].

The system shown in Figure 10.4 is powered by a 3V battery and uses the 61-70 cmH_2O pressure regulating balloon. The Li-ion battery used will be able to power the device for 41 days at 3.7V with a power rating of 540 mAh that can be recharged 500 times [70]. The components shown in Figure 8.4 are encased in cases ranging from 50 x 35 x 20 mm to 50 x 50 x 20 mm. The

smaller case configuration was because of a smaller micropump that was used which had a flow-rate of 3 mL/min. Both the prototypes are shown in Figure 10.5.

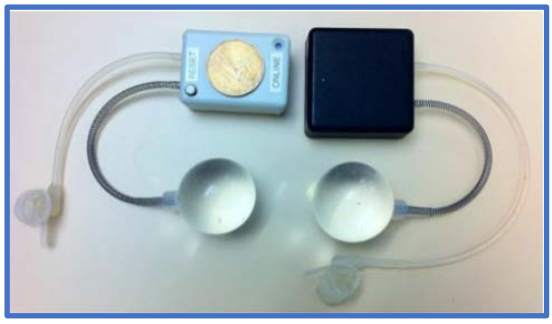

Figure 10.5. Hached's prototypes with different sizes of casing. Size differences were attributed to pump sizes used. [71].

Hached et. al published another design in 2015 and is similar to the black-box design shown in Figure 10.5 [71]. The new prototype by the authors consists of an electromechanical hydraulic system, a control unit for hydraulic micro actuators, and wireless communication. The hydraulic circuit consists of a centrifugal micropump coupled to a latched solenoid between the pressure regulating balloon and the cuff [71].

Hached et al. compared their device extensively with Rathmann's and Lamraoui's (Appendix B) and some of the positive points of their prototype were that it was adaptive to pressure changes, low stand-by power consumption, low pumping power and high a pump flow rate for a faster response time. Power consumption when the pumping occurred was 367 mW [71] . Some of the challenges in the prototype were that the implant used non-implantable batteries and the device experienced heat dissipation and the heat requires a path to escape the casing. Overall, all these researchers realize that the UI market is underserved and underdeveloped.

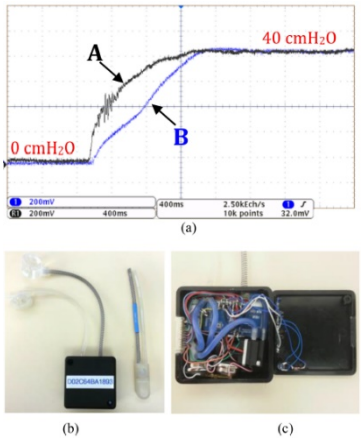

Figure 10.6. Proposed eAUS prototype and pressure control curves. **(a)** Cuff pressure control with proposed voltage control method. **(A)** Pressure curve for cuff surrounding 6-mm diameter plastic rod simulating presence of the urethra. **(B)** Pressure curve for an empty cuff. **(b)** eAUS prototype compared with classic AMS manual pump. **(c)** Display of eAUS internal construction. [71]

The most recent development in the eAUS has been the endourethral AUS from 2016 by Mazzocchi et al [72]. The advantage of an endourethral device is that the procedure is minimally invasive and involves the placement of the AUS in the urethral lumen. Catheters are the simplest example for endourethral devices, but the idea of having an endourethral AUS is not new. Femsoft system by Rochester Medical Corp., USA and the InFlow by Vesiflo, Redmond, USA are some of the commercially available endourethral systems, used especially in women. These devices are battery powered and operated wirelessly by a remote placed close to the device. The wireless coupling activates a pump inside the endourethral device that opens a valve allowing the bladder to be emptied. A unisex endourethral device is not available and that creates a challenge for a device in this category.

Mazzocchi et al., designed a remote-magnetically controlled endourethral AUS (Figure 10.7) and the device disappeared in the body in a quick, less painful procedure, allows easy urination, and maintains continence during abdominal contractions or physical activity [72].

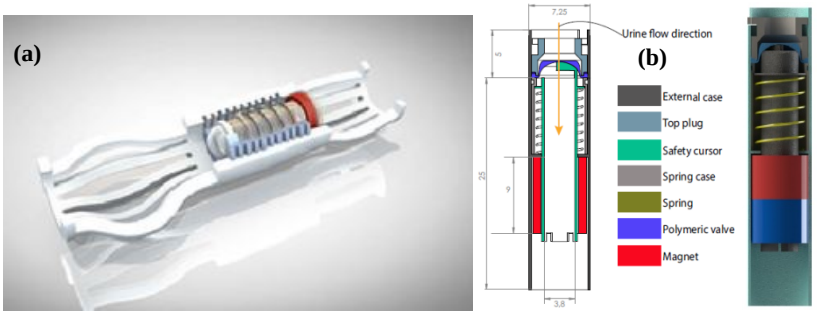

Figure 10.7. Concept design of the endourethral AUS (a) the device with its components, **(b)** the main components namely the safety cursor, spring, valve, and the internal magnet. [72].

The device is triggered by an external magnet which is aligned with the device's internal magnet and the magnetic coupling allows the operation of the device.

11. Actuation Circuit: Powering the Solenoid

11.1. Some Basic Concepts

$$Inductivity\ of\ Coil\ (L) = \frac{\mu_o \mu_r N^2 A}{S_L}$$

L: Inductivity
μ_o: Relative permeability
μ_r: Permeability of Core
A: Coil Surface Area
N: Number of Windings
S_L: Coil Length
I: Current flowing through coil

$$Generated\ Mechanical\ Force\ (F) \propto Strength\ of\ Magnetic\ Field\ (B)$$
$$B = \mu_o \mu_r NI$$

$$Current\ change\ in\ a\ coil\ occurs\ after\ voltage\ change\ with\ a\ 90°\ phase\ shift:$$
$$\frac{dI}{dT} = \frac{V}{L}$$

Current can be reduced after activation as a power saving technique and reduction in loss of power as heat. An electromagnetic coil behaves as an energy storage device and becomes a constant current source when the current is switched off. Switching off current abruptly results in voltage increase [73].

Applying DC voltage to a coil with Inductance L and Internal resistance R_i, the time dependent current equation showing discharge of the coil:

$$I(t) = \left(1 - e^{-t/\tau}\right) \times \frac{V}{R_i}\ ;\ \tau = \frac{L}{R_i}$$

Equivalent circuit of an actuator coil is [73]:

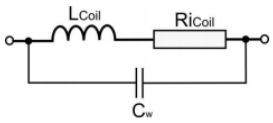

Switching characteristics of the coil:

- Inductance of the coil changes with closing of magnetic circuit.
- Current change in magnetic circuit is proportional to the applied voltage.
- The coil is an energy storage, as discussed earlier, and this releases energy during switch OFF.

The switching characteristics give us cues that will help conserve power, speed-up actuation, and protect the circuit. A faster activation would require a sudden burst of current and brief voltage which can help overcome the static mechanical friction from the rest position. The voltage and current can be reduced and keep the magnetic circuit closed once the solenoid has been actuated to hold it at a certain position. While opening the actuator circuit, the coil tries to maintain a constant flow of current and this translated to stored energy which requires a free-wheeling diode to protect the circuit from over-voltage. A free-wheeling diode does this by delaying the switch-off process and extend the time until idle state is reached [73].

The coil also heats up and the coil resistance will change with change in temperature. An EM actuator is mostly made of Copper wire and this produces an ohmic internal resistance. The temperature coefficient α_{Cu} is 0.00393 per kelvin, which implies that a per degree increase in temperature will change the resistance by 0.4%. At the same operating voltage, the result is a lower current and longer activation time as resistance changes due to temperature. We performed a simulation on our foundational circuit to actuate the solenoid and found a variation

in actuation characteristics with increase in temperature when the device is ex-vivo and in the body at 37°C.

11.2. Power Reduction Methodologies

Power reduction in an EM actuator can be done in two ways:

- Coil Winding Material and Air-Gap in the Coil

  We learnt from Stieger et al., that a minimal diameter, minimal height coil, and with zero air-gap will generate the maximum force [60]. Though, this thesis does not dive deep into designing a coil from scratch- to increase the efficiency of the implantable device, we need to look at designing our own coils. Kartmann et al., have a detailed coil design (Figure 11.1) that they designed for a disposable dispensing valve for microliter operations [74]. However, our design should consider the fact that it should push almost 1mL of fluid in the pump and it should do this at a reduced current with a faster actuation time.

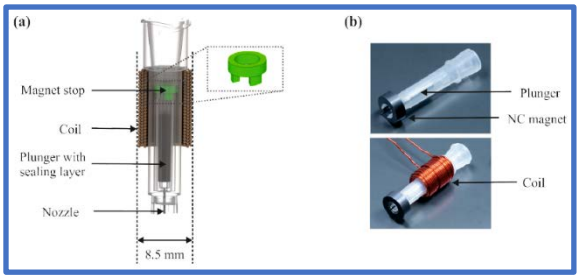

Figure 11.1. Kartmann's coil design **(a)** CAD model of the one-part valve body with an insert molded polyimide nozzle. The plunger with a 1 mm thick silicone layer is inserted and the valve is closed with a stopper (**green**); **(b)** Photographs of the first samples of the injection molded, disposable, non-contact dispensing valve with and without coil. [74].

Our device as shown in Figure 8.9 has three forces- force between the plunger and the coil ($F_{plunger}$), force applied on the diaphragm ($F_{diaphragm}$) and pressure force of the AMS 800^{TM} pressure regulating balloon ($F_{balloon}$). As common sense would dictate $F_{diaphragm} + F_{balloon} < F_{plunger}$. Kartmann et al.'s device used a NdFeB magnet as a plunger with an outer dimeter of 2 mm

and length of 10 mm. The maximum force in their device was 50 mN, but our device would need greater forces for moving almost a milliliter of fluid. They compared the coil designs and although it is not scaled for our device, it gives us a good picture about designing a coil that better suits our application (Figure 11.2).

Dimensions	Prior functional model [5]	Miniaturized design
Coil outer diameter	16.5 mm	8.5 mm
Coil inner diameter	9 mm	5.5 mm
Coil length	8.5. mm	12 mm
Number of windings	105	72
Required peak current	8 A	5 A
Overall valve length	27.1 mm	29.35 mm

Figure 11.2. Comparison of the dimensions of the prior functional model [5] and the miniaturized design of the disposable, electromagnetic dispensing valve [74].

Using the concepts from section 11.1 and Kartmann et al's work, we did our own calculations for a possible coil that suits out application. The Mini 5V Push-Pull Solenoid from Adafruit Industries LLC (Figure 9.15; Appendix G) [64] has a rated voltage of 5V and 1.1A. The force rating on it is 80g which is 0.78N. The number of turns in the coil were not mentioned on the data sheet and we worked our way backwards to calculate *N*.

We make some assumptions for our calculations:

- Diameter of our solenoid are the same as the length of the frame: 12mm
- The material of the coil is assumed as Copper (μ_{Cu}: 1.256e-6 H/m)
- Assume an air-gap (g) between 0.5 to 1 mm

Some other given values were the height of the coil- 20mm, internal resistance of 4.5Ω. The inductance (L) of the coil calculated by conducting a simple experiment using the concept that in an inductor current lags voltage by 90°, was 29.1mH (Section 10.3.1).

$$Magnetomotive\ Force\ F_m = N\ \times I = H.L; H: Magnetic\ Field\ Strength$$

$$N\ \times 1.1A = H\ \times 29.1mH\ \Rightarrow \frac{N}{H} = \ 26.45\frac{mH}{A}\ \Rightarrow H = \frac{N}{0.02645\frac{H}{A}}$$

$$Flux\ Density\ B = \ \mu_{Cu} \times H = \ \mu_{Cu}\frac{N}{26.45\frac{mH}{A}}$$

$$Cross\ sectional\ Area, a = \ \pi(6^2) = 113.04\ mm^2$$

$$F = \frac{(NI)^2\mu_o a}{(2g^2)} \Rightarrow 0.78\ N = \frac{N^2 \times\ 1.1^2 \times (4\pi \times 10^{-7}) \times 0.00011304\ m^2}{4 \times (g)^2}$$

$$\Rightarrow N^2 = 4540 \Rightarrow N = 67\ turns\ for\ g: 0.5\ mm$$

$$\Rightarrow N^2 = 18161 \Rightarrow N = 135\ turns\ for\ g: 1\ mm$$

For any further calculations, we will consider N= 120 turns for the Mini 5V Push-Pull Solenoid.

- Intelligent control through circuitry

EM actuators ideally should have a zero air-gap for low power requirement. The holding current required to hold the solenoid at a position is 40-50% of the activation current. Most papers stress on reducing the voltage and current using pulse width modulation (PWM) techniques. A simple PWM circuit sets a lower average current and has a time-controlled switch-off. The circuit suggested for the Mini 5V Push-Pull Solenoid employs this technique at a lower level and is

shown in Figure 11.3. The free-wheeling diode is extremely essential to protect the coil and the circuit from a sudden current surge. The current control circuit shown in Figure 11.3 is considered a better circuit design.

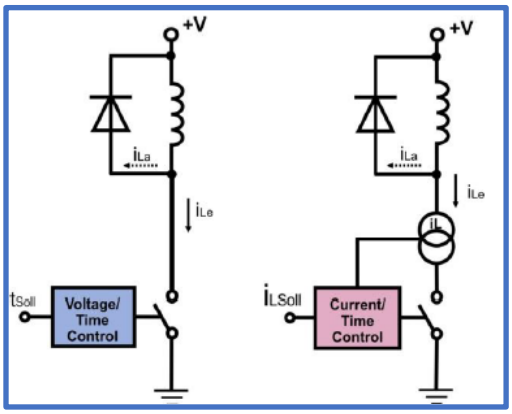

Figure 11.3. Comparison of PWM with and without current control [73].

Figure 11.4 is a practical implementation of the current controlled PWM using an IC named iC-GE (Appendix J) for coils of 10mH to 10H and current ranging from 100mA to 1A [73].

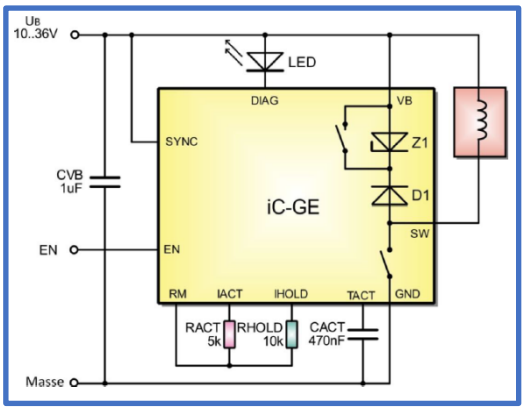

Figure 11.4. Current control with intelligent coil driver iC-GE. [73].

The resistor R_{act} helps set the activation current which is reduced to the holding current using R_{hold} typically after 65ms. The capacitor C_{act} defines the length of the activation phase. This design can be incorporated in our design for future prototypes. Additionally, Texas Instrument's solenoid driver board with plunger movement [Figure 11.5(c)] detection can help determine the amount of pressure we want to apply using our pump prototype [75]. Different plunger displacements imply variations of fluid pushed out of the pump, which results in different pressure readings. The driver

circuit utilizes the characteristics of the solenoid current [Figure 10.5(a)] in detecting movement of the plunger in a solenoid.

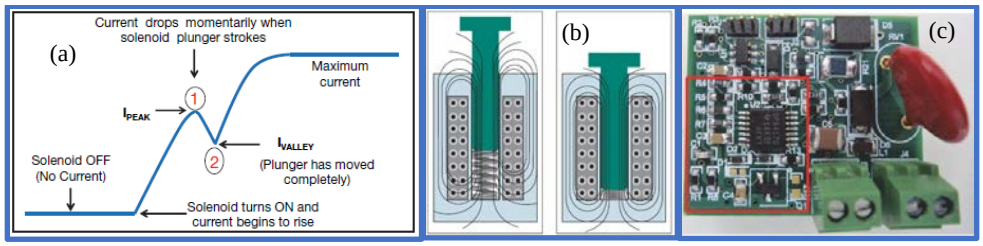

Figure 11.5. Plunger Movement detection circuit: (a) Excitation current characteristic of a solenoid; **(b)** Solenoid energized and the electromagnetic force is strong enough to move the plunger; **(c)** Solenoid driver board having plunger movement detection circuit [75].

11.3. Mini 5V Push/Pull Solenoid: Further Characterization

11.3.1. Solenoid Circuit 1 [64] (Appendix K)

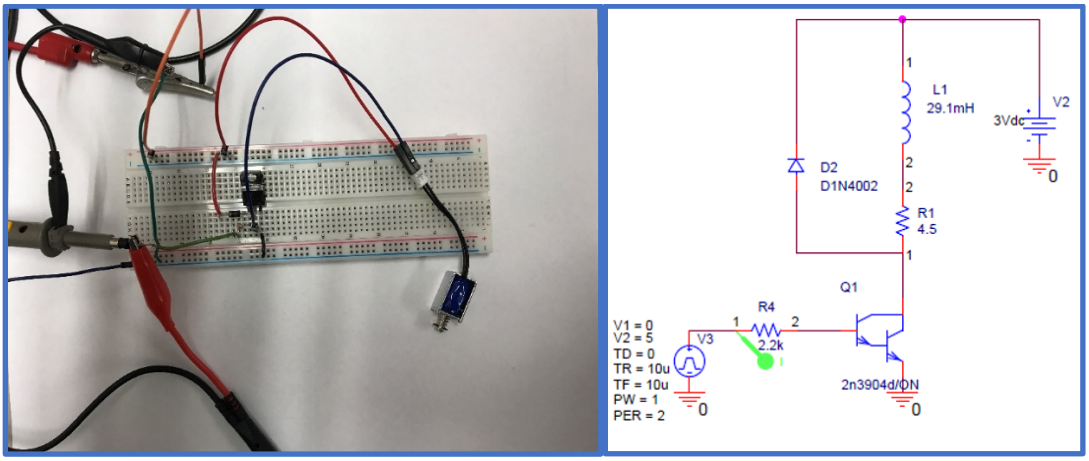

Figure 11.6. Solenoid Actuation Circuit 1 as recommended by Adafruit (Appendix K) [64] (Appendix K).

To power the solenoid, a basic circuit was designed consisting of the solenoid coil and a transistor TIP102 which acts as a switch. This circuit was used to test the functionality of the solenoid and for all testing purposes. However, in this circuit, the solenoid consumes constant rated current throughout the ON period which results in a higher power dissipation of the circuit.

11.3.2. Solenoid Circuit 2: Lowering Power Consumption (Appendix K)

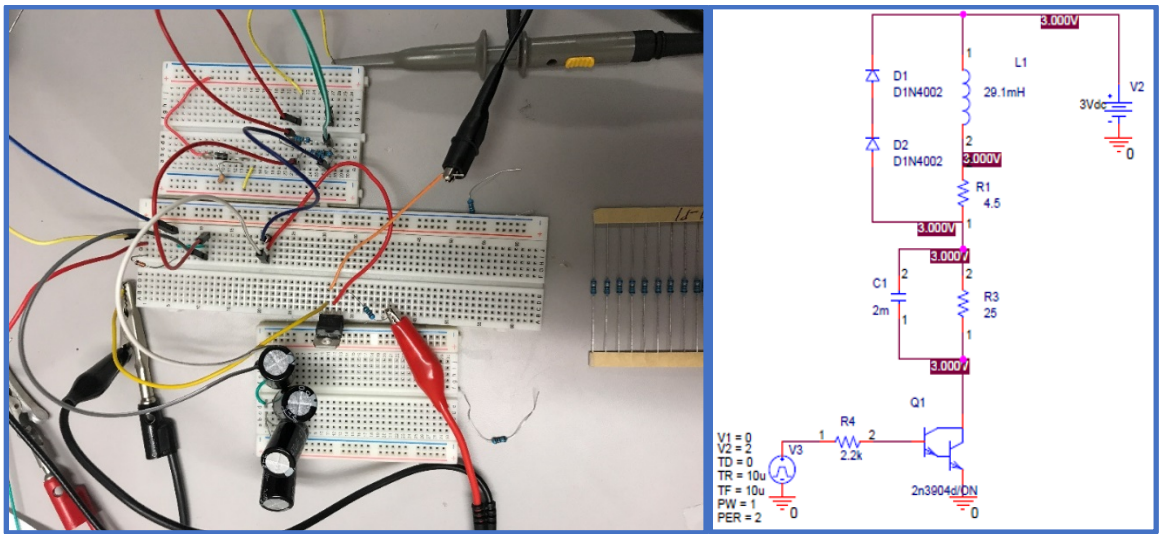

Figure 11.7. Solenoid Actuation Circuit 2 for Energy Saving [Appendix K].

A new and improved circuit is designed to reduce the current consumed during the ON period. This circuit consists of an additional parallel RC combination as shown in the figure (Figure 10.7). Here, the circuit operation can be differentiated in to 2 states namely the ON state and HOLD state. During the ON state, the initial pulse turns the Q1 on. This initial high frequency spike results in the C1 reducing to a short circuit for a brief instant of time i.e., t_{ON}. Now, the current follows through the path, L1-R1-C1-Q1. Following this t_{ON}, the pulse flattens out and the circuit now enters the HOLD state where C1 becomes an effective open circuit. Thus, a new path for the current is formed i.e., L1-R1-R3-Q1. It is apparent that this forms a resistive voltage divider with a hold voltage applied across the solenoid just sufficient to preserve the ON state and preventing the plunger from retracting back into the chassis. The current consumed by the solenoid in HOLD state is lower than

that of the ON state thereby reducing the effective power consumption of the circuit.

11.3.3. Solenoid Force Experiments

We calculated force generated by the solenoid using the setup shown in Figure 11.8. The actuation circuits used were: a simple connection of the solenoid to the power supply and the circuit shown in Schematic 1, which was also recommended by Adafruit [64].

Figure 11.8. Solenoid Force measurements setup

In the first setup, the solenoid was connected directly to the supply and this meant at a rated voltage of 5V and current rating of 1.1A.

We had to keep in mind that the solenoid would heat up and therefore, had to take quick results. There were three observations made which were integral to our idea's fast actuation system and uniform pressure distribution:

- When the solenoid was connected directly to the supply, it was basically shorted and this produced energy loss in the form of heat.
- The value of force obtained on the scale also varied with time as the coil heated up and began to lose its force.
- The force had a maximum value at impact and then fell and stabilized at a certain value. We ensure that we wait for a while before we took the force

readings at stead state. The maximum force at impact was a point in our design's favor since it allowed quick transfer of force from the solenoid plunger to the fluid in the pump.

Voltage (V)	Current (A)	Force (g)
5	0.97	76.5
4	0.72	78.2
3.3	0.58	74
3	0.53	75.1
2.8	0.5	74.1
2.7	0.47	73.4
2.6	0.47	73.6
2.5	0.47	72.2
2.4	0.47	72.5
2.3	0.47	73
2.1	0.47	75
2.05	0.47	74
2.03	0.45	74

Table 11.1. Solenoid Force measurements using a digital weighing scale when connected directly connected to the supply.

Table 11.1 shows the force produced at different values of voltage and the corresponding current. We found that the force remains relatively the same when the solenoid is connected directly to the supply. The region in orange depicts the working region of the solenoid such that we could save power by operating the solenoid at a lower voltage and current rating, thereby requiring less power. Therefore, we want to be in the 2.4-3.0V and 0.45-0.58A range. The results obtained from the experiment have been listed in Figure 10.9. The HOLD parameters are the minimum voltage and current required to hold the solenoid in its position. From the inductance and resistance values, we can calculate the time constant and frequency of the coil.

V_{rated}: 5V
I_{rated}: 1.1A
F_{rated}: 80gm
$V_{(ON)min}$: 2.6V
$I_{(ON)min}$: 0.5A
$V_{(HOLD)min}$: 0.95~1.0V
$I_{(HOLD)min}$: 80mA~0.1A
F_{expt}: 72~74 gm
L: 29.1mH
R: 4.5Ω

Figure 11.9. Solenoid Characteristics when connected to supply directly.

$$\tau = \frac{L}{R} = \frac{29.1mH}{4.5\Omega} = 6.46\ ms; f = 154.87\ Hz$$

Voltage (V)	Current (A)	Force (g)
5	0.87	72
4.5	0.77	60
4	0.67	45
3.5	0.57	31
3	0.47	19
2.5	0.38	8.2

Figure 11.10. Solenoid Characteristics when connected to Circuit 1 (Section 10.3.1).

Figure 11.10 gives the force measurements when connected to circuit 1 and the force versus voltage characteristic is shown in Graph 11.1 with a possible polynomial curve-fit.

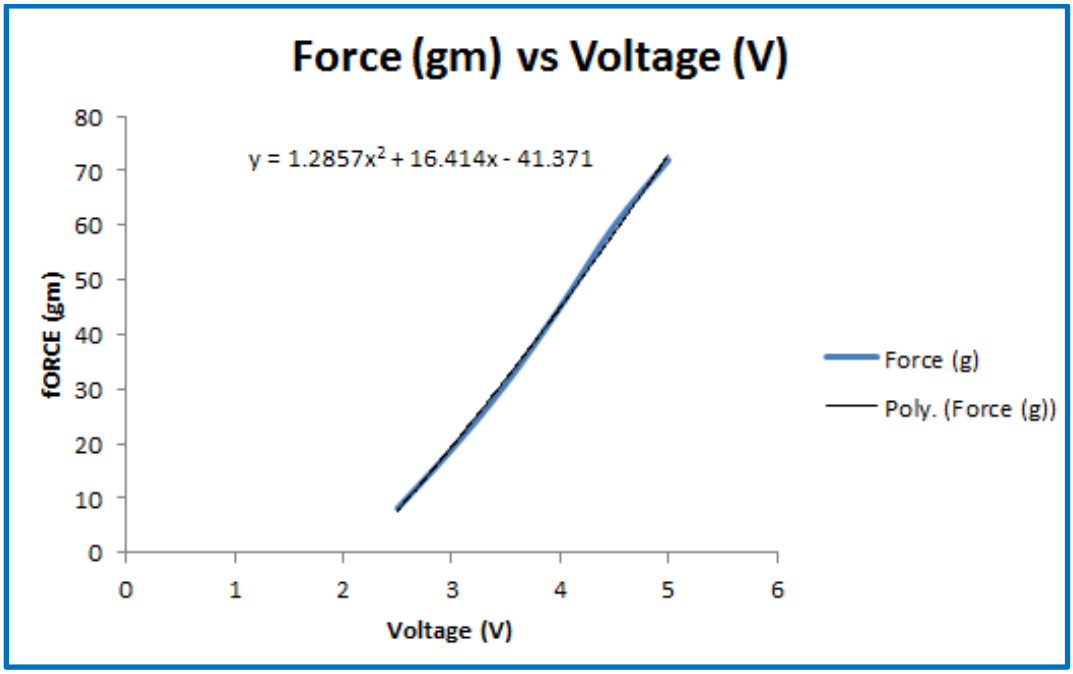

Graph 11.1. Force vs. Voltage of the solenoid with Circuit 1.

11.3.4. Energy: Possible Implantable Battery Technologies and Wireless Communication

Power calculations for our design are extrapolated from the battery technologies used in Medtronic's Interstim (Sacral Nerve Stimulator for Urinary Control) and Medtronic's Micra Pacing System [76], [77].

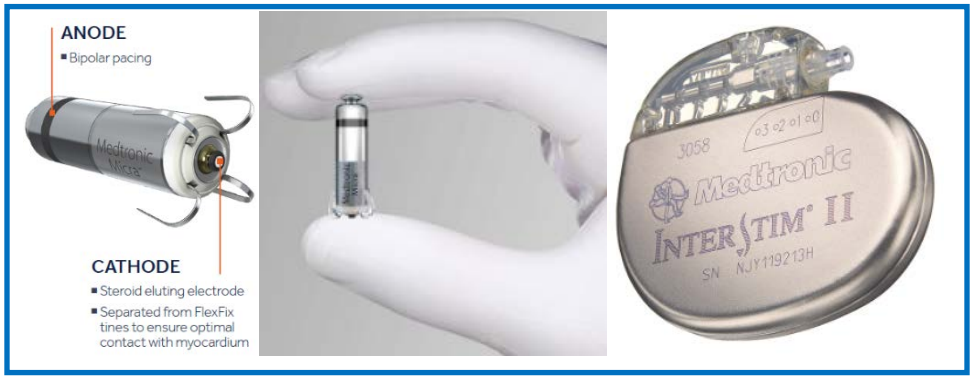

Figure 11.11. Medtronic's Micra Pacing System and the Sacral Interstim II Neurostimulator [67], [68].

From Figure 11.9, we calculate the solenoid's energy requirement and battery specifications using Medtronic's Micra pacing system, first. The coil inductor has a time constant of 6.46ms and since it takes some more time to actuate the plunger, we consider a total of 10ms to actuate the solenoid. $V_{(ON)min}$ and $I_{(ON)min}$ are considered (2.6V, 0.5A) since it's a lower voltage and current with the same amount of force which will be beneficial for power saving. Therefore, P_{ON} is 1.3 W which means the Energy is 13mJ. $V_{(HOLD)min}$ and $I_{(HOLD)min}$ are 1V and 0.1A, respectively which means that the energy required to hold the plunger at its position after actuation is 0.409J at a t_{HOLD} OF 4.09s. Total energy (E_{Tot}) required by solenoid is 0.422J/ cycle for every ON cycle. We assume that each cycle has a 5s duration.

The Micra pacemaker has a 3V and 120mAh battery which means the Energy (E_{Ba}) supplied by it is $E_{Ba} = 3 \times 120 \times 3600 = 1296Ws = 1296J$

$$Total\ number\ of\ Cycles = \frac{E_{Ba}}{E_{Tot}} = \frac{1296}{0.422} = 3071\ cycles$$

Assuming 20 cycles per day, we have 153.55 days (~ 5 months). Therefore, a battery of 3V, 150mAh can power the solenoid for 150 days at 20 cycles/ day. The Interstim II on the other hand uses a Lithium silver vanadium oxide hybrid that has a capacity of 1.3Ah at 3.2V. Using the same calculations as shown above, we get 11,090 cycles and on a 20 cycle/ day basis, we get 555 days (~1.5 years). This implies that our device would need an inductive wireless charging capability to allow patients to charge their device through the skin.

An additional capability that we tested was the ability of the solenoid to be actuated wirelessly using the Particle Photon Wi-Fi [78] enabled microcontroller with a robust cloud platform and a powerful STM32 arm Cortex M3 and a Cypress Wi-Fi chip as the brain of the microcontroller. We powered the Photon with a 5V supply and found that we could actuate the solenoid using our cell phone (Figure 10.12). The microcontroller can receive firmware updates wirelessly, and this will allow us to help adapt our device to a patient's level of activity in addition to other capabilities like plunger movement detection [75].

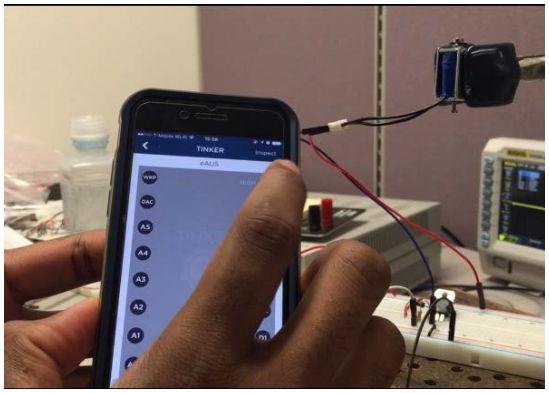

Figure 11.12. Wireless Communication with solenoid using Photon's cloud-based interface on a cell-phone.

12. Technical Specifications [71]

Table 12.1. Comparative study of features of our prototype and other similar work

Research Group	Lamraoui et al. [59], 2010	Ruthmann et al. [58] (2010)	Hached et al. [62] (2015)	This Work
Pumping System	Rolling Diaphragm	Piezoelectric Micropump	Centrifugal Pump	Solenoid Diaphragm Pump
Pumping Power Consumption	Pumping: 500 mW; Holding: 0mW	Pumping: 120 mW; Holding: 10mW	Pumping: 376 mW; Holding: 0mW	Pumping: 1.3W; Holding: 0.1W
Occlusive System	AMS 800 Cuff	Custom cuff	AMS 800 Cuff	AMS 800 Cuff
Pumping Flow	500-800 cmH_2O/s	2.23 mL/min	700 mL/min	Work to be done
Adaptability Features	With patient activity	No	With urethral morphology	With patient activity
Pressure Controller	PID	Yes, but not indicated	PID and adaptive	Solenoid Plunger Detection; Wireless Firmware upgrades
Batteries	Lithium	Lithium	Lithium and NiMH	Lithium oxide Vanadium Oxide Hybrid
Communication	Enhanced ShockBurst	MICS (403 MHz)	Bluetooth 4	Particle Photon (Wi-Fi)
Wireless Power Transfer	No	Inductive Link (125 KHz)	Qi Protocol	Work to be done

Based on Figure 8.9.
Maximum Diameter of Pump Body: 26 mm; Maximum Height: 9.86 mm
Volume within pump: 2 cc; Height of device (pump + solenoid): 35 mm

Current Status and Future Work

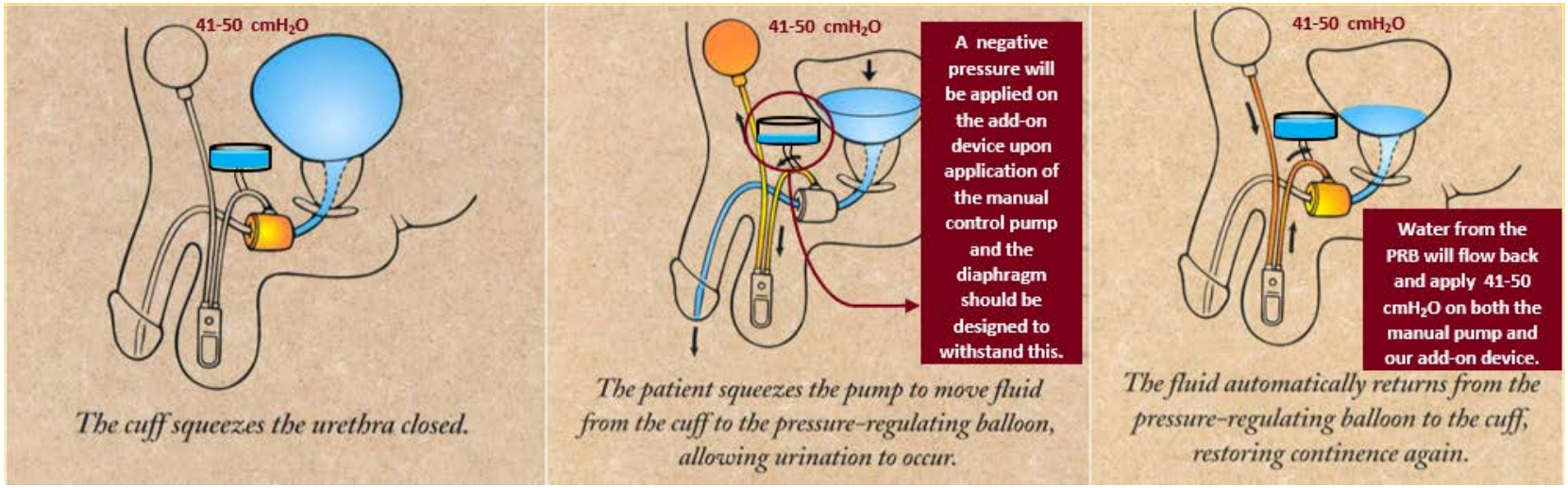

The diagrams above depict the working of our add-on device. The add-on device will complement the working of the existing AMS 800 and will apply a lower pressure on the urethra thereby reducing ischemia and erosion. At times of stress, the pressure will shoot up to 120 cmH_2O into the cuff. The manual control pump gives an additional back-up and maintains the integrity of the device. The add-on device will need to be designed to withstand negative pressure when fluid is pulled from the cuff while voiding. This aspect of device testing needs further experimentation and analysis and we are working at perfecting the device further from an implantable perspective by giving more attention to the power and energy requirements.

References

[1] A. Mangera, N. I. Osman, and C. R. Chapple, “Anatomy of the lower urinary tract,” *Surg. Oxf.*, vol. 31, no. 7, pp. 319–325, 2013.

[2] V. C. Scanlon and T. Sanders, *Essentials of anatomy and physiology*. FA Davis, 2014.

[3] J. Corcos, *The urinary sphincter*. CRC Press, 2001.

[4] R. P. Myers, D. R. Cahill, R. M. Devine, and B. F. King, “Anatomy of radical prostatectomy as defined by magnetic resonance imaging,” *J. Urol.*, vol. 159, no. 6, pp. 2148–2158, 1998.

[5] J. H. Dirckx, “Federative Committee on Anatomical Terminology (FCAT). Terminologia Anatomica. International Anatomical Terminology,” *Terminol. Int. J. Theor. Appl. Issues Spec. Commun.*, vol. 5, no. 2, pp. 279–283, 1998.

[6] M. M. Koraitim, “The male urethral sphincter complex revisited: an anatomical concept and its physiological correlate,” *J. Urol.*, vol. 179, no. 5, pp. 1683–1689, 2008.

[7] M. A. Ficazzola and V. W. Nitti, “The etiology of post-radical prostatectomy incontinence and correlation of symptoms with urodynamic findings,” *J. Urol.*, vol. 160, no. 4, pp. 1317–1320, 1998.

[8] J. E. McNeal, “The zonal anatomy of the prostate,” *The prostate*, vol. 2, no. 1, pp. 35–49, 1981.

[9] S. H. Selman, “The McNeal prostate: a review,” *Urology*, vol. 78, no. 6, pp. 1224–1228, 2011.

[10] J. E. Mcneal, “The prostate and prostatic urethra: a morphologic synthesis,” *J. Urol.*, vol. 107, no. 6, pp. 1008–1016, 1972.

[11] N. Yoshimura and W. C. de Groat, “Neural control of the lower urinary tract,” *Int. J. Urol.*, vol. 4, no. 2, pp. 111–125, 1997.

[12] F. Hinman Jr, G. M. Miller, E. Nickel, and E. R. Miller, “Vesical physiology demonstrated by cineradiography and serial roentgenography: preliminary report,” *Radiology*, vol. 62, no. 5, pp. 713–719, 1954.

[13] J. A. Gosling, J. S. Dixon, H. O. Critchley, and S.-A. THOMPSON, “A comparative study of the human external sphincter and periurethral levator ani muscles,” *BJU Int.*, vol. 53, no. 1, pp. 35–41, 1981.

[14] T. Bessede, P. Sooriakumaran, A. Takenaka, and A. Tewari, “Neural supply of the male urethral sphincter: comprehensive anatomical review and implications for continence recovery after radical prostatectomy,” *World J. Urol.*, vol. 35, no. 4, pp. 549–565, 2017.

[15] A. H. Sultan *et al.*, “An International Urogynecological Association (IUGA)/International Continence Society (ICS) joint report on the terminology for female anorectal dysfunction,” *Neurourol. Urodyn.*, vol. 36, no. 1, pp. 10–34, 2017.

[16] P. Abrams, J. G. Blaivas, S. L. Stanton, and J. T. Andersen, “Standardisation of terminology of lower urinary tract function,” *Neurourol. Urodyn.*, vol. 7, no. 5, pp. 403–427, 1988.

[17] P. Bates *et al.*, “Standardization of terminology of lower urinary tract function First and second reports: International Continence Society,” *Urology*, vol. 9, no. 2, pp. 237–241, 1977.
[18] T. Hald and W. E. Bradley, *The urinary bladder: neurology and dynamics*. Williams & Wilkins, 1982.
[19] E. H. Sonnenblick, “Force-velocity relations in mammalian heart muscle,” *Am. J. Physiol. Content*, vol. 202, no. 5, pp. 931–939, 1962.
[20] U. Nagavarapu, “PHM113B- Prevention and Treatment of Prostate Cancer Technologies and Global Markets,” *BCC Research*, 2017. [Online]. Available: https://www-bccresearch-com.ezp3.lib.umn.edu/market-research/pharmaceuticals/prostate-cancer-technologies-markets-report-phm113b.html. [Accessed: 30-Jul-2017].
[21] J. G. Blaivas, “Urinary incontinence after radical prostatectomy,” *Cancer*, vol. 75, no. S7, pp. 1978–1982, Apr. 1995.
[22] R. Chao and M. E. Mayo, “Incontinence after radical prostatectomy: detrusor or sphincter causes,” *J. Urol.*, vol. 154, no. 1, pp. 16–18, 1995.
[23] D. E. Chung, B. Dillon, J. Kurta, A. Maschino, A. Cronin, and J. S. Sandhu, “Detrusor underactivity is prevalent after radical prostatectomy: a urodynamic study including risk factors,” *Can. Urol. Assoc. J.*, vol. 7, no. 1–2, p. E33, 2013.
[24] M. Maffezzini and M. Maffezzini, “Evaluation of complications and results in a contemporary series of 300 consecutive radical retropubic prostatectomies with the anatomic approach at a single institution,” *Urology*, vol. 61, no. 5, pp. 982–986, 2003.
[25] K. Kobashi, “Stress Urinary Incontinence: A monograph from the Urology Care Foundation.” Urology Care Foundation, 2015.
[26] “Stress Urinary Incontinence: A Review of Treatment Options - AORN Journal.” [Online]. Available: http://www.aornjournal.org/article/S0001-2092(10)00155-9/fulltext. [Accessed: 02-Aug-2017].
[27] A. C. Kirby, J. Tan-Kim, and C. W. Nager, “Measurement of Dynamic Urethral Pressures with a High Resolution Manometry System in Continent and Incontinent Women,” *Female Pelvic Med. Reconstr. Surg.*, vol. 21, no. 2, p. 106, Apr. 2015.
[28] T. Spirka, K. Kenton, L. Brubaker, and M. Damaser, “Effect of Material Properties on Predicted Vesical Pressure During a Cough in a Simplified Computational Model of the Bladder and Urethra,” *Ann. Biomed. Eng.*, vol. 41, no. 1, pp. 185–194, Jan. 2013.
[29] G. Bunne and A. Öbrink, “Urethral closure pressure with stress — A comparison between stress-incontinent and continent women,” *Urol. Res.*, vol. 6, no. 3, pp. 127–134, Sep. 1978.
[30] N. Singla and A. K. Singla, “Post-prostatectomy incontinence: Etiology, evaluation, and management,” *Turk. J. Urol.*, vol. 40, no. 1, pp. 1–8, Mar. 2014.
[31] G. W. Timm and W. E. Bradley, “Electronic micturition reflex simulation,” *Proc 17th Spinal Cord Inj. Conf Veterans Adm.*, pp. 152–157, 1969.
[32] G. W. Timm and W. E. Bradley, “Electrical simulation of reflex function,” *Proc Brcing Child. Paraplegia Resulting Spina Bifida NRC*, 1969.

[33] G. W. Timm, D. C. Merrill, and W. E. Bradley, “Intermittent occlusion system,” *IEEE Trans. Biomed. Eng.*, no. 4, pp. 352–352, 1970.
[34] G. W. Timm, “An implantable incontinence device,” *J. Biomech.*, vol. 4, no. 3, pp. 213–219, 1971.
[35] G. W. Timm and W. E. Bradley, “Technologic and biologic considerations in neuro-urologic prostheses development,” *IEEE Trans. Biomed. Eng.*, no. 3, pp. 208–212, 1973.
[36] F. B. Scott, W. E. Bradley, and G. W. Timm, “Treatment of urinary incontinence by implantable prosthetic sphincter,” *Urology*, vol. 1, no. 3, pp. 252–259, 1973.
[37] F. B. Scott, W. E. Bradley, and G. W. Timm, “Treatment of urinary incontinence by an implantable prosthetic urinary sphincter,” *J. Urol.*, vol. 167, no. 2, pp. 1125–1129, 2002.
[38] G. W. Timm, D. A. Frohrib, and W. E. Bradley, “Genitourinary prosthetics of the present and future.,” in *Mayo Clinic proceedings*, 1976, vol. 51, pp. 346–350.
[39] J. H. Burton, M. A. Mikulich, G. W. Timm, F. B. Scott, S. L. Attia, and W. E. Bradley, “Development of urethral occlusive techniques for restoration of urinary continence.,” *Med. Instrum.*, vol. 11, no. 4, pp. 217–220, 1977.
[40] “AMS 800™ Urinary Control System For Male Patients: Operating Room Manual.” American Medical Systems, 2014.
[41] T. Hald, “Artificial sphincter,” *World J. Urol.*, vol. 4, no. 1, pp. 41–44, 1986.
[42] E. Chung, “A state-of-the-art review on the evolution of urinary sphincter devices for the treatment of post-prostatectomy urinary incontinence: past, present and future innovations,” *J. Med. Eng. Technol.*, vol. 38, no. 6, pp. 328–332, 2014.
[43] “FlowSecure - Artificial Urinary Sphincter,” *Endotherapeutics*. [Online]. Available: http://www.endotherapeutics.com.au/flowsecure.
[44] A. Mohammed, A. Khan, T. Shaikh, I. S. Shergill, and I. Junaid, “The artificial urinary sphincter,” *Expert Rev. Med. Devices*, vol. 4, no. 4, pp. 567–575, 2007.
[45] “Zephyr Surgical Implants - ZSI 375 Information.” [Online]. Available: https://www.zsimplants.ch/en/products-en/incontinence/zsi-375-en/zsi-375-information. [Accessed: 05-Aug-2017].
[46] “Urology,” *Silimed*. [Online]. Available: http://www.silimed.com.br/en/urology/. [Accessed: 05-Aug-2017].
[47] S. Crivellaro *et al.*, “Systematic review of surgical treatment of post radical prostatectomy stress urinary incontinence,” *Neurourol. Urodyn.*, vol. 35, no. 8, pp. 875–881, Nov. 2016.
[48] M. H. James and K. A. McCammon, “Artificial urinary sphincter for post-prostatectomy incontinence: A review,” *Int. J. Urol.*, vol. 21, no. 6, pp. 536–543, 2014.
[49] B. Brown and J. A. Brown, “Postprostatectomy Urinary Incontinence: A Comparison of the Cost of Conservative Versus Surgical Management,” *Urology*, vol. 51, no. 5, pp. 715–720, 1998.
[50] S. J. Hudak and A. F. Morey, “Impact of 3.5 cm artificial urinary sphincter cuff on primary and revision surgery for male stress urinary incontinence,” *J. Urol.*, vol. 186, no. 5, pp. 1962–1966, 2011.

[51] D. S. DiMARCO and D. S. Elliott, “Tandem cuff artificial urinary sphincter as a salvage procedure following failed primary sphincter placement for the treatment of post-prostatectomy incontinence,” *J. Urol.*, vol. 170, no. 4, pp. 1252–1254, 2003.
[52] M. L. Guralnick, E. Miller, K. L. Toh, and G. D. Webster, “Transcorporal artificial urinary sphincter cuff placement in cases requiring revision for erosion and urethral atrophy,” *J. Urol.*, vol. 167, no. 5, pp. 2075–2079, 2002.
[53] D. S. Aaronson, S. P. Elliott, and J. W. McAninch, “Transcorporal artificial urinary sphincter placement for incontinence in high-risk patients after treatment of prostate cancer,” *Urology*, vol. 72, no. 4, pp. 825–827, 2008.
[54] A. Saffarian, K. Walsh, I. K. Walsh, and A. R. Stone, “Urethral atrophy after artificial urinary sphincter placement: is cuff downsizing effective?,” *J. Urol.*, vol. 169, no. 2, pp. 567–569, 2003.
[55] “Toys from Trash.” [Online]. Available: http://www.arvindguptatoys.com/pumps-from-dump.php. [Accessed: 11-Aug-2017].
[56] S. Vaidyarajan, A. Gupta, and A. Deshpande, *PUMPS FROM THE DUMP*. New Delhi: Vigyan Prasar.
[57] “How Computer Keyboards Work,” 21-Nov-2000. [Online]. Available: http://computer.howstuffworks.com/keyboard.htm.
[58] “Keyboard technology,” *Wikipedia*. 17-Jul-2017.
[59] C. Berger, “Advantages and Disadvantages of Mechanical Keyboards,” *Mechanical-Keyboard.org*, 06-Dec-2015. .
[60] C. Stieger *et al.*, “Computer assisted optimization of an electromagnetic transducer design for implantable hearing aids,” *Comput. Biol. Med.*, vol. 34, no. 2, pp. 141–152, 2004.
[61] “How Solenoid Valve Works? Parts of Solenoid Valves,” *Brighthub Engineering*. [Online]. Available: http://www.brighthubengineering.com/manufacturing-technology/56397-parts-of-the-solenoid-valve-how-solenoid-valve-works/.
[62] C.-W. Song and S.-Y. Lee, “Design of a solenoid actuator with a magnetic plunger for miniaturized segment robots,” *Appl. Sci.*, vol. 5, no. 3, pp. 595–607, 2015.
[63] “DSMS-0730-05 Delta Electronics | Motors, Solenoids, Driver Boards/Modules | DigiKey.” [Online]. Available: https://www.digikey.com/product-detail/en/delta-electronics/DSMS-0730-05/1144-1315-ND/5214006. [Accessed: 12-Aug-2017].
[64] “Mini Push-Pull Solenoid - 5V ID: 2776 - $4.95 : Adafruit Industries, Unique & fun DIY electronics and kits.” [Online]. Available: https://www.adafruit.com/product/2776. [Accessed: 12-Aug-2017].
[65] M. Ahmadi, R. Rajamani, G. Timm, and S. Sezen, “Instrumented urethral catheter and its ex vivo validation in a sheep urethra,” *Meas. Sci. Technol.*, vol. 28, no. 3, p. 035702, 2017.
[66] “Tru-Wave® Pressure Transducer Kit | IV Accessories | IV Therapy | Moore Medical.” [Online]. Available: https://www.mooremedical.com/index.cfm?/Tru-Wave%AE-Pressure-Transducer-Kit/&PG=CTL&CS=HOM&FN=ProductDetail&PID=30450&spx=1. [Accessed: 13-Aug-2017].

[67] O. Ruthmann *et al.*, “The First Teleautomatic Low-Voltage Prosthesis With Multiple Therapeutic Applications: A New Version of the German Artificial Sphincter System,” *Artif. Organs*, vol. 34, no. 8, pp. 635–641, 2010.
[68] H. Lamraoui *et al.*, “Development of a novel artificial urinary sphincter: a versatile automated device,” *IEEEASME Trans. Mechatron.*, vol. 15, no. 6, pp. 916–924, 2010.
[69] M. V. Ramesh, D. Raj, N. Dilraj, and others, “Design of wireless real time artificial sphincter control system for urinary incontinence,” in *Technology Management and Emerging Technologies (ISTMET), 2014 International Symposium on*, 2014, pp. 44–49.
[70] S. Hached, O. Loutochin, J. Corcos, A. Garon, and M. Sawan, “Novel, remotely controlled, artificial urinary sphincter: a retro-compatible device,” *IEEEASME Trans. Mechatron.*, vol. 19, no. 4, pp. 1352–1362, 2014.
[71] S. Hached, Z. Saadaoui, O. Loutochin, A. Garon, J. Corcos, and M. Sawan, “Novel, wirelessly controlled, and adaptive artificial urinary sphincter,” *IEEEASME Trans. Mechatron.*, vol. 20, no. 6, pp. 3040–3052, 2015.
[72] T. Mazzocchi, L. Ricotti, N. Pinzi, and A. Menciassi, “Magnetically Controlled Endourethral Artificial Urinary Sphincter,” *Ann. Biomed. Eng.*, vol. 45, no. 5, pp. 1181–1193, 2017.
[73] “WP8en_Flexible Low Power Driving of Solenoid Coils.pdf.” .
[74] S. Kartmann, “A Disposable Dispensing Valve for Non-Contact Microliter Applications in a 96-Well Plate Format,” *Micromachines*, vol. 6, no. 4, pp. 423–436, 20150401.
[75] “Detection of Plunger Movement in DC Solenoids- Texas Instruments.” .
[76] “InterStim II Neurostimulator Sacral Neuromodulation.” [Online]. Available: http://www.medtronic.com/us-en/healthcare-professionals/products/urology/sacral-neuromodulation-systems/interstim-ii.html. [Accessed: 14-Aug-2017].
[77] “Micra Transcatheter Pacing System | Medtronic.” [Online]. Available: http://www.medtronic.com/us-en/healthcare-professionals/products/cardiac-rhythm/pacemakers/micra-pacing-system.html. [Accessed: 14-Aug-2017].
[78] “Photon - Particle Retail.” [Online]. Available: https://store.particle.io/products/photon. [Accessed: 14-Aug-2017].
[79] G. Singh and D. G. Thomas, “Artificial urinary sphincter for post-prostatectomy incontinence,” *BJU Int.*, vol. 77, no. 2, pp. 248–251, 1996.
[80] S. E. Litwiller, K. B. Kim, P. D. Fone, R. W. deVere White, and A. R. Stone, “Post-prostatectomy incontinence and the artificial urinary sphincter: a long-term study of patient satisfaction and criteria for success,” *J. Urol.*, vol. 156, no. 6, pp. 1975–1980, 1996.
[81] F. Haab, B. A. Trockman, P. E. Zimmern, and G. E. Leach, “Quality of life and continence assessment of the artificial urinary sphincter in men with minimum 3.5 years of followup,” *J. Urol.*, vol. 158, no. 2, pp. 435–439, 1997.
[82] D. S. Elliott and D. M. Barrett, “Mayo Clinic long-term analysis of the functional durability of the AMS 800 artificial urinary sphincter: a review of 323 cases,” *J. Urol.*, vol. 159, no. 4, pp. 1206–1208, 1998.

[83] S. N. Venn, T. J. Greenwell, and A. R. Mundy, “The long-term outcome of artificial urinary sphincters,” *J. Urol.*, vol. 164, no. 3, pp. 702–707, 2000.
[84] J. Q. Clemens, T. G. Schuster, J. W. Konnak, E. J. McGUIRE, and G. J. Faerber, “Revision rate after artificial urinary sphincter implantation for incontinence after radical prostatectomy: actuarial analysis,” *J. Urol.*, vol. 166, no. 4, pp. 1372–1375, 2001.
[85] A. E. Gousse, S. Madjar, M.-M. Lambert, and I. J. Fishman, “Artificial urinary sphincter for post-radical prostatectomy urinary incontinence: long-term subjective results,” *J. Urol.*, vol. 166, no. 5, pp. 1755–1758, 2001.
[86] G. V. Raj, A. C. Peterson, K. L. Toh, and G. D. Webster, “Outcomes following revisions and secondary implantation of the artificial urinary sphincter,” *J. Urol.*, vol. 173, no. 4, pp. 1242–1245, 2005.
[87] G. V. Raj, A. C. Peterson, and G. D. Webster, “Outcomes following erosions of the artificial urinary sphincter,” *J. Urol.*, vol. 175, no. 6, pp. 2186–2190, 2006.
[88] H. H. Lai, E. I. Hsu, B. S. Teh, E. B. Butler, and T. B. Boone, “13 years of experience with artificial urinary sphincter implantation at Baylor College of Medicine,” *J. Urol.*, vol. 177, no. 3, pp. 1021–1025, 2007.
[89] S. P. Kim, Z. Sarmast, S. Daignault, G. J. Faerber, E. J. McGuire, and J. M. Latini, “Long-term durability and functional outcomes among patients with artificial urinary sphincters: a 10-year retrospective review from the University of Michigan,” *J. Urol.*, vol. 179, no. 5, pp. 1912–1916, 2008.
[90] R. C. O’Connor, M. B. Lyon, M. L. Guralnick, and G. T. Bales, “Long-term follow-up of single versus double cuff artificial urinary sphincter insertion for the treatment of severe postprostatectomy stress urinary incontinence,” *Urology*, vol. 71, no. 1, pp. 90–93, 2008.
[91] F. T. Rocha, C. M. Gomes, A. I. Mitre, S. Arap, and M. Srougi, “A prospective study evaluating the efficacy of the artificial sphincter AMS 800 for the treatment of postradical prostatectomy urinary incontinence and the correlation between preoperative urodynamic and surgical outcomes,” *Urology*, vol. 71, no. 1, pp. 85–89, 2008.
[92] D. K. Montague, “Artificial urinary sphincter: long-term results and patient satisfaction,” *Adv. Urol.*, vol. 2012, 2012.
[93] “Anaesthesia UK : The invasive arterial system and Wheatstone bridge.” [Online]. Available: http://www.frca.co.uk/article.aspx?articleid=336. [Accessed: 13-Aug-2017].

Appendix A: Findings about AMS 800 Complications from Literature Publications (1996-2016)

Reference Nos.	Authors	Journal	Year
[79]	G. Singh, D.G. Thomas	British Journal of Urology	1996

Number of Patients: 28 with Post-Prostatectomy Incontinence
Mean Age: 71 years
Mean Follow-Up: 41 months

	Primary bulbar	*Primary membranous*
Complication		
Infection	1	1
Persistent stress	6	–
System failure	2	–
Re-operation		
Higher pressure balloon	5	
Smaller cuff	1	
Revision of bulbar cuff	2	
Revision to membranous cuff	1	
Total	9	1
Third operation (revision to membranous cuff)	3	–

Figure A.1. (Left) Number of complications and reoperations after implanting AUS; **(Bottom)** Outcome after AUS implantation

Status	*Primary bulbar*	*Primary membranous*	*All*
Total	21	7	28
Continent	18	6	24
Occasional stress (1–2 pads)	2	1	3
Permanent catheter	1	–	1

The reoperation rate of 57% was considered very high when compared to prior literature with a mean of 27% for reoperation rate.
Conclusion: 95% continence rate can be achieved with the AUS implantation.

[80]	S. E. Litwiller, K. B. Kim, P. D. Fone, R. W. deVere White, and A. R. Stone	The Journal of Urology	1996

Number of Patients: 65 (50 patients participated in the survey)
Median Follow-up: 23.4 months
Mean Age:71
Preoperative incontinence in the patients was severe.
90% patients reported continuous leakage; 70% wore on an average 6 pads per day; 24% wore 7.4 pads daily
96% would recommend the AUS to a friend with continence issues.
Despite the successes of the AUS, physicians and patients were worried about infection and erosion- adverse post-operative complications.

[81]	F. Haab, B. A. Trockman, P. E. Zimmern, and G. E. Leach	The Journal of Urology	1997

Number of patients: 68
Mean Follow-up: 7.2 years
Pad score reduced after AUS implantation: 2.75 PPD to 0.97 PPD
AUS permanently removed in 4 patients due to urethral erosion.
Revisions for mechanical failure or urethral atrophy required in 25% of the patients.
Mechanical Failure: 17 of 68
Urethral Atrophy: 6 of 68
80% of patients were socially continent at mean follow-up.
Design modifications made to the AUS in 1987 drastically reduced mechanical failure (Figure A.2).
51-60 cmH_2O balloon was used more often compared to higher pressure balloons which reduced urethral erosion and atrophy rate.

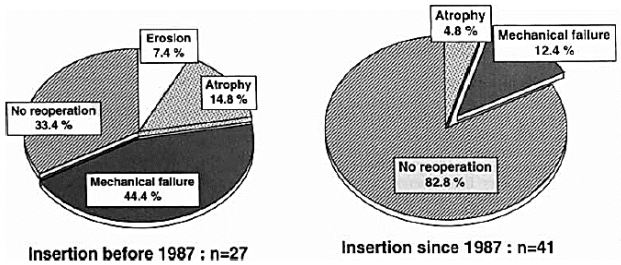

Figure A.2. Mechanical failure rate significantly reduced after improvement of the device in 1987 [40].

[82]	D. S. Elliott and D. M. Barrett	The Journal of Urology	1998

Mechanical vs. non-mechanical failure and reoperation rates from 1983-1987 and 1988- present
Number of patients: 400 (323 patients met survey criteria)
Mean Age: 60.4 years
Mean Follow-up: 68.8 months
Patients with minimum 18 months of follow-up were included in the study
AUS implanted at urethra in 272 patients and bladder neck in 52.
437 operations were required in 323 patients.
Mechanical failure: fluid leaks, tube kinking, pump malfunction, connector separations
Non-Mechanical failure: cuff erosion, infection, atrophy, pimp malposition
1983-1987: Non-narrow backing design cuff (139 cuffs places)
1988- present: narrow backing cuff (184 cuffs placed)
Non-mechanical failure rate in the non-narrow backing cuff patient portfolio was 17% and mechanical failure was 21%. On the other hand, in the narrow backing

cuff patient portfolio, non-mechanical failure rate was 9% and mechanical failure rate was 7.6%.

[83]	S. N. Venn, T. J. Greenwell, and A. R. Mundy	The Journal of Urology	2000

Review of AUSs inserted more than 10 years ago
Number of patients: 100
Median follow-up: 11 years
84 patients were continent- 27 patients had device replaced due to mechanical failure; 21 patients had device removed due to erosion or infection or reimplantation.

Device survival was 66% at 10 years.
Over the 10 years, 37% devices were removed due to erosion or infection with the highest risk in females.

Early revision for mechanical problems involved replacement of the defective component or device. Early explantation due to erosion or infection followed by a recovery period and implantation was another revision procedure. Device removal due to infection or erosion was commonly caused by introduction of infection during surgery.
In some patients, device was removed because of urethral atrophy caused by cuff pressure. This is attributed to a high balloon pressure that cannot be controlled. Instances where the device is unable to compensate for the increase in intra-abdominal pressure, patients tend to experience stress incontinence.

[84]	J. Q. Clemens, T. G. Schuster, J. W. Konnak, E. J. McGUIRE, and G. J. Faerber	The Journal of Urology	2001

Revision rate for AUS implanted post-RP
Number of patients: 70 (showed signs of incontinence post-RP)
66 patients had postoperative data: 24 required reoperations (36.4% rate), cuff revision was 60%
At 36.4% revision rate, of the 54 procedures- 5 were due to mechanical failure.
Cuff revision rates in cases of erosion or atrophy were 89% and 60% for 1 and 5 years, respectively.

[85]	A. E. Gousse, S. Madjar, M.-M. Lambert, and I. J. Fishman	The Journal of Urology	2001

Number of patients: 71 (29 had earlier version of AMS 800^{TM}; 42 had the newer narrow-back cuff)
Mean follow-up: 7.7 years
Surgical revision required in 29% of the cases due to complications: 25% of which were mechanical failure, 4% were erosion, and 1.4% was infection. Device was removed from 2 patients due to mechanical failure.

The narrow-back cuff of the AMS 800 has helped reduce the incidence of erosion and need for revision.

[86]	G. V. Raj, A. C. Peterson, K. L. Toh, and G. D. Webster	The Journal of Urology	2005

Comparative study of outcomes after primary and secondary procedures
Number of patients: 554
119 patients underwent 159 secondary procedures.
31 revisions were due to mechanical failure and 88 due to non-mechanical failure.
Non-mechanical failure included 63 cases of urethral atrophy, 21 cases of erosion.
Total device replacement was carried out in 75 cases.
Of the 119 patients who underwent secondary revisions, 91 needed no additional surgical intervention, and 28 needed 40 interventions for mechanical and non-mechanical failures.
Urethral sub-cuff atrophy was the most common non-mechanical failure and cuff leakage was the most common mechanical failure. In sub-cuff atrophy cases, the procedure involved downsizing of the cuff and reimplantation. The decision to replace the whole device or components of the device lies solely on the physician's discretion based on the condition of the device and health of the urethra. The health of the urethra is the most limiting factor in secondary revisions. In such situations, physicians chose to place the new cuff distal or proximal to the primary site. However, as one moves distal to the primary site, the urethral circumference reduces and the spongy surround decreases.

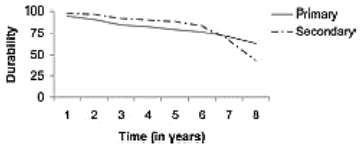

Figure A.3. Durability of primary and secondary AUS implantations [45].

5-year durability outcomes for primary and secondary AUS implantations were at 80% and 88% respectively (Figure A.3). Continence outcomes were 80% and 82% in primary and secondary procedures, respectively.

[87]	G. V. Raj, A. C. Peterson, and G. D. Webster	The Journal of Urology	2006

Understanding the eroded AUS from a preoperative perspective
Number of patients: 637
54 explantations in 46 patients because of erosions. The institution erosion rate was 2.2%. Erosions were linked to certain comorbidities like hypertension, coronary artery disease, prior radiation therapy and prior AUS revisions. Majority of the patients who underwent revisions for erosion had mild incontinence and with reimplantations, these patients had a significantly higher rate of second erosions with an average of 6.7 months.

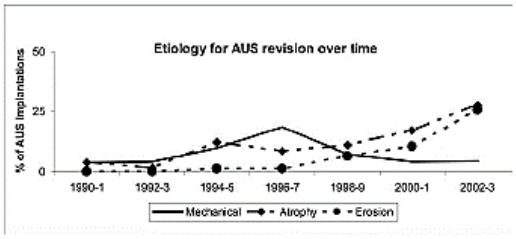

Figure A.4. Revisions due to Mechanical failure vs Non-mechanical failure in the last 12 years [46].

Stemming from [86], here Raj et al. looked at secondary revisions due to erosions and involved removal of components of the AUS.
Of the 637 patients, 591 patients underwent primary AUS implantation and 112 underwent secondary revisions.

Within the 112 patients, 72 patients had sub-cuff urethral atrophy and 40 mechanical causes. There has been a significant increase in the number of erosion cases (Figure A.4). The paper also looked at durability of the device over time in patients undergoing revisions for erosions and other reasons, and found that the durability of the device in erosions cases was much lower and patients would be prone to another erosion. The study conclusively showed that the number of patients undergoing AUS revisions is increasing.

[88]	H. H. Lai, E. I. Hsu, B. S. Teh, E. B. Butler, and T. B. Boone	The Journal of Urology	2007

Outcomes from the narrow-backed cuff AUS at Baylor College of Medicine
Number of patients: 270 (Follow-up data on 218 [Figure A.5] patients were available)
Mean Follow-up: 36.4 months
Infection rate: 5.5%; Erosion: 6%; Urethral atrophy: 9.6%; mechanical failure: 6%; surgical removal/ revision: 27.1%
Median time for complications: 3.7 months for infection, 19.8 months for erosion, 29.6 months for atrophy, 68.1 months for failure and 14.4 months for surgery.
After 5 years, 75% of the patients were free from any revision and 10% did not have a functional AUS. The study finds that the risks from infection and erosions plateaued by 48 months, unlike risks from atrophy and mechanical failure which continued to increase throughout the study. Cuff atrophy was the most common complication.

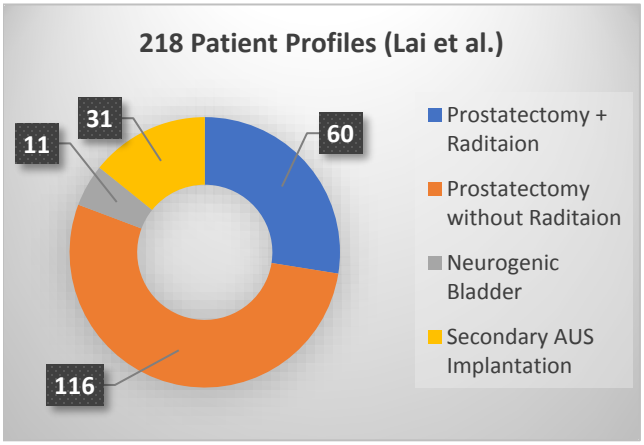

Figure A.5. Patient profiles of 218 patients with available follow-up data.

[89]	S. P. Kim, Z. Sarmast, S. Daignault, G. J. Faerber, E. J. McGuire, and J. M. Latini	The Journal of Urology	2008

The study highlights AUS complication rates, associated risk factors, quality and durability.
Number of patients: 124
Mean Follow-up: 6.8 years

Overall complication rate: 37%
Most common complication: Mechanical failure (29 patients)
36% experienced complications within 10 years with most events occurring in the first 48 months. 10 patients had erosion, 7 had infection.
12 patients required removal of the device due to infection and erosion.

[90]	R. C. O'Connor, M. B. Lyon, M. L. Guralnick, and G. T. Bales	Urology	2008

Effectiveness and complications of single and double cuff AUS
Number of patients: 56 (single cuff- 28 and double cuff- 28)
Data available for 47 men (25 single cuff and 22 double cuff)
Mean Age: 67 years
Mean Follow-up: 74.1 months for single cuff and 58 months for double cuff
The double cuff placement is also referred to as tandem-cuff placement. The incidence of complications in tandem cuff cases was higher. The double cuff did not provide any significant change in continence rates when compared to single cuff. For double cuff, social continence rate was 72%.

Of the 22 patients who received tandem cuff placements, 55% reported complications that required surgical revisions. Complications in both the single and double cuff patient cohort ranged from urethral atrophy, erosion, mechanical failure. In tandem cuff cases, the cuff sizes were downsized to reduce atrophy and erosion.

[91]	F. T. Rocha, C. M. Gomes, A. I. Mitre, S. Arap, and M. Srougi	Urology	2008

Evaluation of long term efficacy of the AUS
Number of patients: 40
Mean age: 68.3 ± 6.3 years
Mean Follow-up: 27 to 132 months
Surgical revision rate was 20%
3 cases of prosthetic infections followed by erosions. 4 patients lost continence after two years of implantation because of mechanical failure which required device replacement. Continence rate obtained was 90% and there was a significant impact on the quality of life of patients when they were no longer incontinent.

[92]	D. K. Montague	Advances in Urology	2012

This paper highlights the fact that majority of the patients who undergo AUS implantation have satisfactory results. This review paper lists the following rates for complications:
Infection: 0.465 to 7%
Cuff erosion: 3.8% to 10%
Urethral atrophy: 9.6% to 11.4%
Figure A.6 below summarizes 4 papers that have been discussed earlier and the findings have been averaged to give us a better idea on the incidences of complications post-implantation.

Reference	*N*	Mean followup (months)	Infection (%)	Cuff erosion (%)	Urethral atrophy (%)	Device failure (%)	Removal/revision (%)
Lai et al. [15]	176	36.5	5.5	6.0	9.6	6.0	27.1
Kim et al. [12]	124	81.6	7	10		29	37
Raj et al. [11]	554	68	0.46	3.8	11.4	5.6	21.4
Gousse et al. [13]	71	92.4	1.4	4		25	29

Figure A.6. Complications rates from 4 references.

Freedom from mechanical failure was 79% at 5 years and 72% at 10 years
Most men need 0-1 pad per day and AUSs are susceptible to revision and replacement in the future.

Appendix B: Comparison of Literature eAUS Prototypes [71]

Research group	Lamraoui et al.[13]	Ruthmann et al. [14]	This work
Pumping system	Rolling Diaphragm	piezoelectric micropump	Centrifugal micropump
Pumping power consumption	Pumping: 500mW Holding: 0mW	Pumping: 120mW Holding:10mW	Pumping: 376mW Holding: 0mW
Occlusive system	AMS800 cuff	Custom cuff geometry	AMS800 cuff
Pumping flow	500 to 800 cmH_2O/s	2.23 ml/min	700ml/min
Adaptability features	With patient activity	No	With urethral morphology
Pressure controller	PID	Yes but not indicated	PID and adaptive
Control performance	PID: $\pm 1 cmH_2O$	not indicated	PID: $\pm 1 cmH_2O$ Adaptive : $\pm$ $3 cmH_2O$
Standby power consumption	$\geq$40 µW, without the transceiver	10 mW	26.33 µW
Batteries	Lithium	Lithium	Lithium and NiMH
Communication protocol	Enhanced ShockBurst	MICS (403 MHz)	Bluetooth 4
Wireless power transfer	No	Inductive link (125KHz)	Qi Protocol
Volume	60 cm^3	100 cm^3	50 cm^3

Appendix C: Patent Survey (Courtesy Innography)

Item	Number	Inventor(s)	Assignee	Title
1	US201720157759	Wirbisky, Alan G Vandeweghe, Andrew P	Boston Scientific Scimed, Inc.	Artificial Sphincter system and method

Abstract:
The present invention provides an artificial sphincter employing an easily controlled electro-mechanical pump system. The artificial sphincter includes an inflatable cuff a control pump fluidly coupled to the inflatable cuff and an electro-mechanical pump system. The inflatable cuff is adapted to surround a urethra or rectum of the patient to facilitate continence. An inflation element or balloon can be included to further control pressure to the cuff.

Claims:
An electro-mechanical artificial sphincter system, comprising:

an adjustable cuff adapted to apply pressure to a bladder neck or a urethra to promote continence;

a fluid reservoir portion; and

a centrifugal pump device in fluid communication with the cuff and the fluid reservoir portion, with the centrifugal pump capable of forcing fluid to the cuff to inflate the cuff.

an electro-mechanical pump device in operable communication with the fluid chamber to displace fluid within the chamber upon actuation to selectively control inflation or deflation of the cuff.

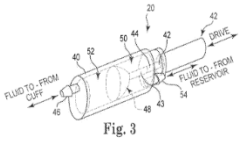

Fig. 3

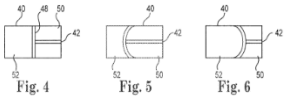

Fig. 4 Fig. 5 Fig. 6

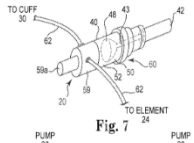

Fig. 7

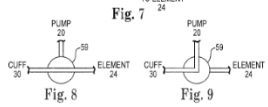

Fig. 8 Fig. 9

2	**US8801594 B2**	Fogarty, Terence M.	Fogarty Terence M.	Fluid control system for inflatable sphincter prosthese

Abstract:
A fluid transfer system for an inflatable sphincter prosthesis is disclosed. The implantable inflatable sphincter prosthesis may include a fluid transfer system and at least one inflatable cuff for occluding a body channel. The fluid transfer system may include an inflate pump a deflate pump and three one-way valves.

Claims:
An implantable sphincter prosthesis comprising a fluid transfer system and an inflatable cuff for occluding a body channel, said fluid transfer system comprising:

an inflate pump having a first elastomeric pump bulb, said first elastomeric pump bulb being volitionally deformable to create positive intraluminal pump pressure that forces fluid to be exhausted from the inflate pump, wherein, subsequent to volitional deformation, said first elastomeric pump bulb is incapable of imposing a negative intraluminal inflate pump pressure;

a deflate pump having a second elastomeric pump bulb, said second elastomeric pump bulb being volitionally deformable to create a positive intraluminal pump pressure that forces fluid to be exhausted from the deflate pump, wherein, subsequent to volitional deformation, said second elastomeric pump bulb imposes a negative intraluminal deflate pump pressure to cause fluid to fill the deflate pump;

a first one-way valve located between said inflate pump and said inflatable cuff with a first fluid flow through said first one-way valve directed from said inflate pump to said inflatable cuff;

a second one-way valve located between said deflate pump and said inflate pump with a second fluid flow through said second one-way valve directed from said deflate pump to said inflate pump, the second one-way valve having a backpressure corresponding to a desired intraluminal pressure of the inflatable cuff in an inflated state, the first one-way valve having a backpressure greater than the backpressure of the second one-way valve; and

a third one-way valve located between said inflatable cuff and said deflate pump with a third fluid flow through said third one-way valve directed from said inflatable cuff to said deflate pump, the third one-way valve having at least substantially zero backpressure,

wherein said fluid transfer system enables fluid to flow from said inflate pump to said inflatable cuff when said inflate pump is volitionally deformed to provide patient continence, and wherein said third fluid flow enables fluid to flow from said inflatable cuff to said deflate pump and said inflate pump upon activation of said deflate pump to

permit patient voiding.

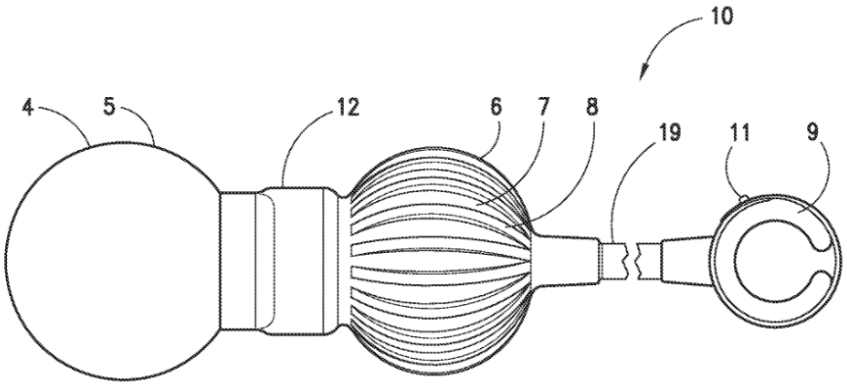

3	**US6319191B1**	Global Medical Devices	Peter H. Sayet, Lloyd A. Sutherland, Victor Politano	Implantable body fluid flow control device

Abstract

An apparatus for controlling fluid flow within a host body has a first shell and a second shell for coupling with the second shell to form a cylindrical object suitable for engaging and surrounding a selected canal with the host body. The cylindrical object is open at both ends and has an interior diameter of a dimension making it suitable for fitting over the selected host body's canal such as the urethra. The apparatus also includes a plunger for constricting the fluid flow when activated. The plunger may be activated by an electrical solenoid or hydraulic or pneumatic activation to move from a free-flow position into a constricting position wherein the fluid flow though the canal is substantially prevented or reduced. The apparatus can be used for controlling incontinence or restricting fluid flow in other body canals. The host-user can activate the apparatus with a remote-control device outside the body which communicates with the implanted apparatus by means of any wireless communication that transmits a signal to the device causing the solenoid to move the plunger into the constricting position. A second signal causes the plunger to retract into a free-flow position when the user no longer feels the urge to urinate.

Claims

An implantable incontinence apparatus for selectively controlling urine flow from a bladder through an urethra having internal and external walls and diameters, respectively, in a host body without having to sever the urethra to implant said implantable apparatus in the host body or to operate said implantable device following implantation thereof, said implantable apparatus comprising:

a hollow housing, wherein said hollow housing has a plurality of portals for permitting fluid from outside of the urethra to flow into said hollow housing to promote tissue growth and anchor said implantable incontinence device following implantation thereof,

a stop device within said hollow housing and positioned adjacent a selected portion of the external wall of the urethra through which urine flows following implantation of said implantable incontinence apparatus into the body host;

an electrically operated constricting piston having a sliding shaft connected to a plunger for engaging a certain area of the external wall of the urethra which is opposite the selected area of the external wall of the urethra against which said stop device is located when said electrically operated constricting piston is activated, said plunger having a front on which more than one ridge is formed to create separate pressure points against the urethra when the plunger engages the urethra;

a control device for selectively activating said constricting piston;

whereby, when said control device is activated, the plunger when retracted extends to an extended position to restrict to restrict the certain area of the exterior wall of the urethra against said stop device to reduce the internal diameter of the urethra located between the plunger and said stop device to reduce or stop urine flow through the urethra, and the plunger when extended retracts to a retracted position to open the urethral to permit urine flow there through.

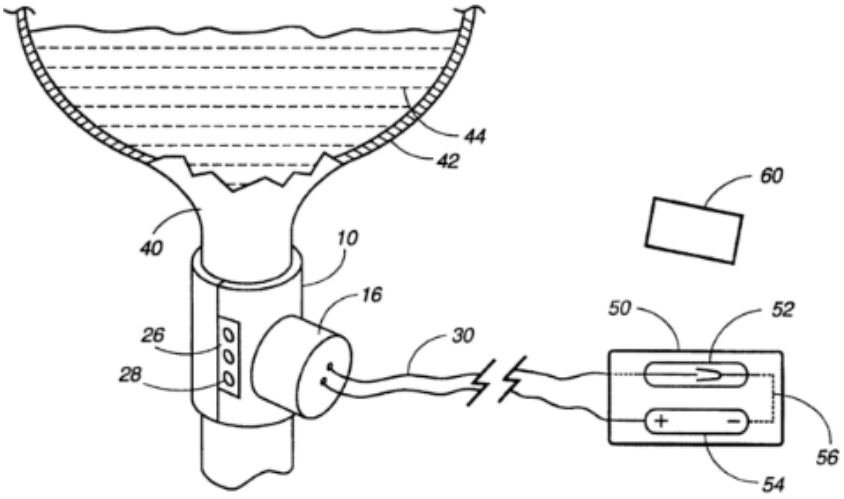

Appendix D: Other Designs

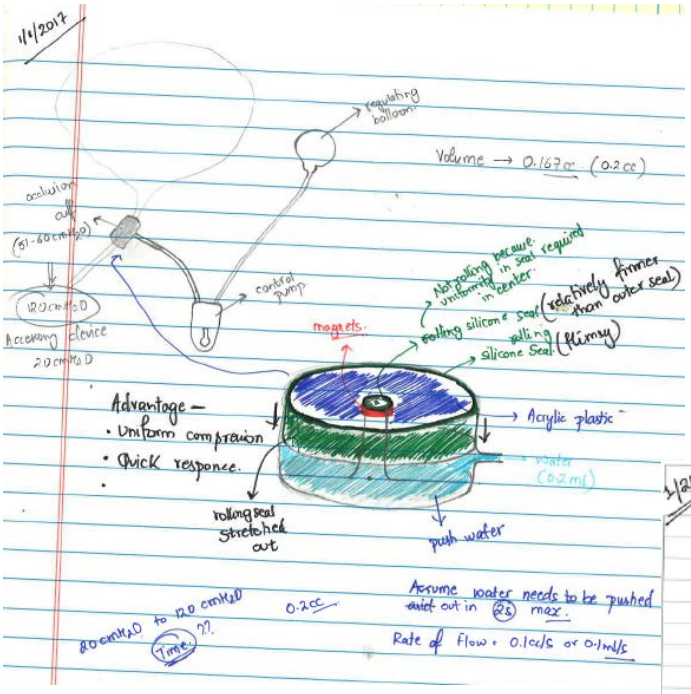

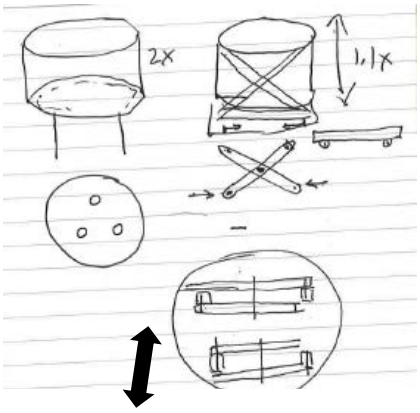

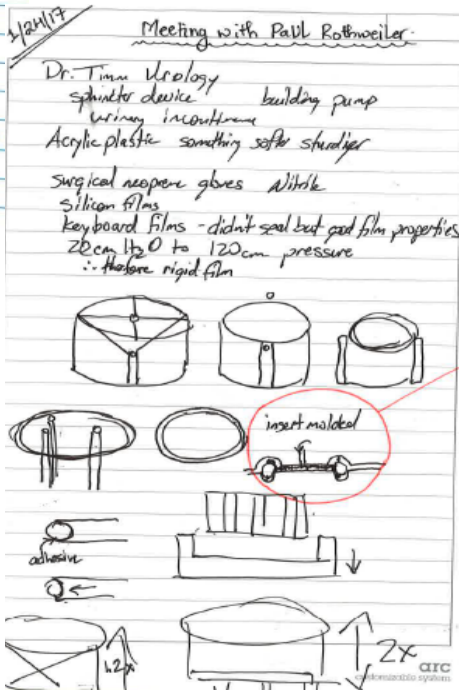

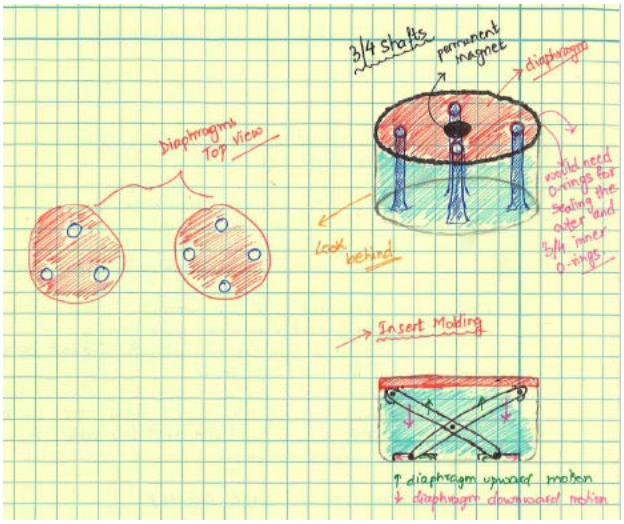

Appendix E: Onshape Designs for 3-D Printing

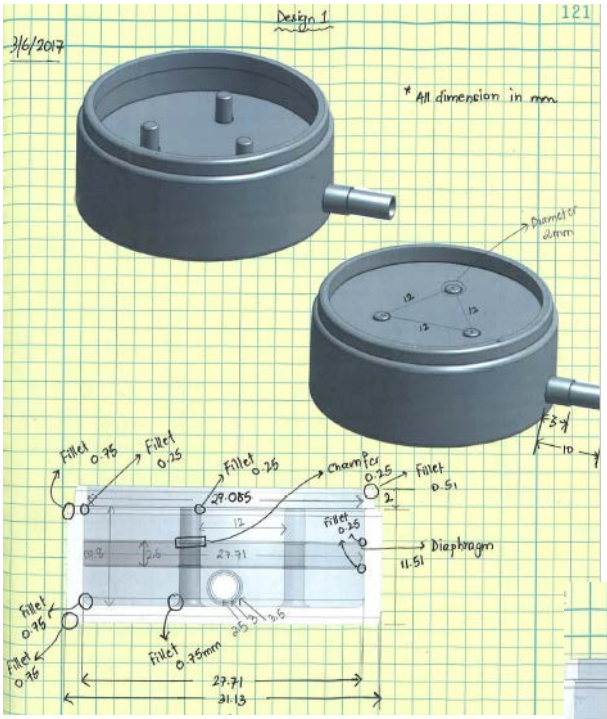

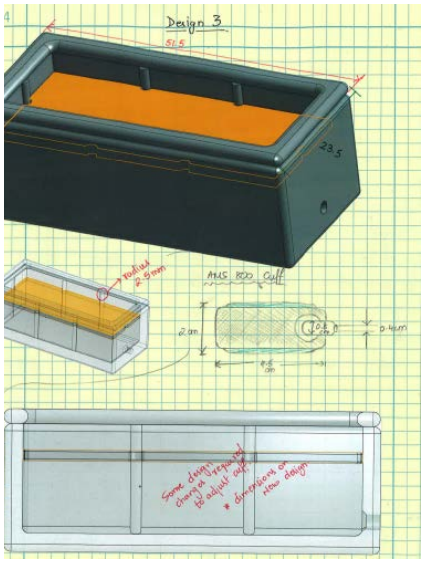

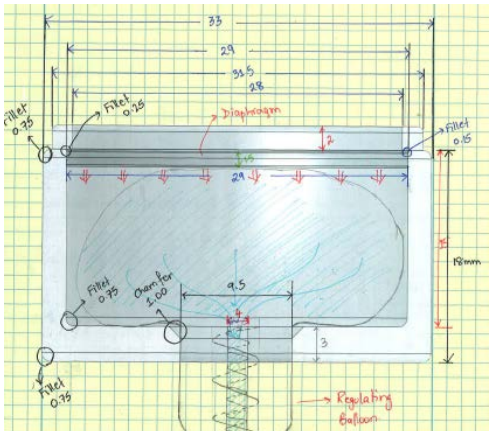

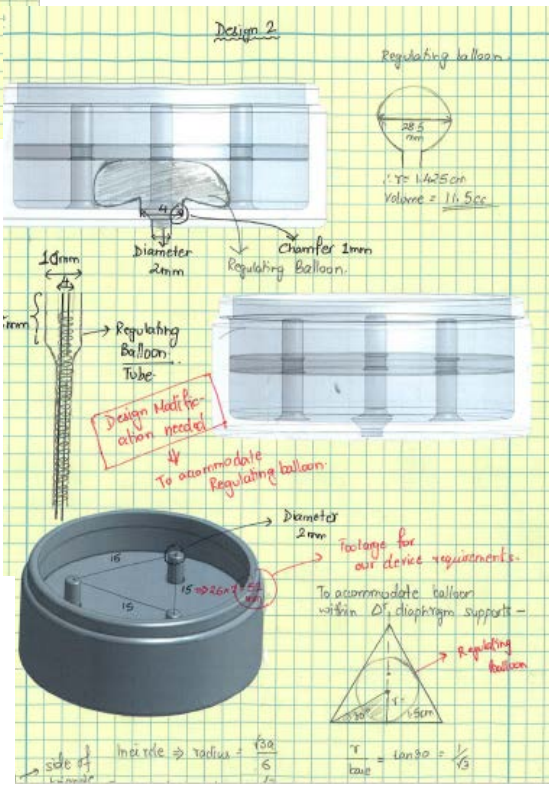

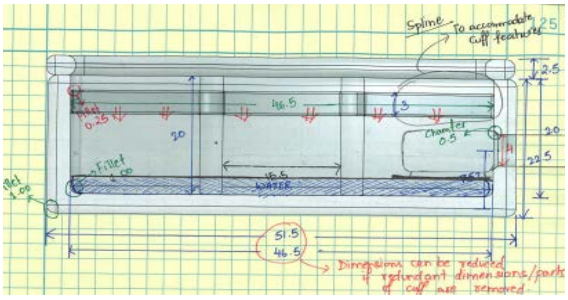

Push Pull 5V Latching Solenoid

RoHS Compliant

Website: www.deltaww.com

No. 252 SHANG YING ROAD.
GUI SHAN INDUSTRIAL ZONE, 33341,TAO
YUAN COUNTLY, TAIWAN
Tel: 886-3-3591968
Fax: 886-3-3591991

SOLENOID PRODUCT SPECIFICATION

PART No.	VOLTAGE	DUTY CYCLE	POWER (W)	CURRENT (A)	DCR (Ω) *
DSMS-0730-24	24 VDC	2%, 45msec On	35	1.5	16
DSMS-0730-18	18 VDC	2%, 45msec On	34	1.92	9.4
DSMS-0730-12	12 VDC	2%, 45msec On	32	2.67	4.5
DSMS-0730-09	9 VDC	2%, 45msec On	30	3.35	2.7
DSMS-0730-05	5 VDC	2%, 45msec On	30	5.9	0.85

* OPERATION: POWER TO PUSH AND RELEASE, BUILT-IN RETURN SPRING.

* DCR VALUES ARE ±10% AT 25°C
* WEIGHT ARE 38 GRAMS ±10%

1. MECHANICAL DIMENSIONS :

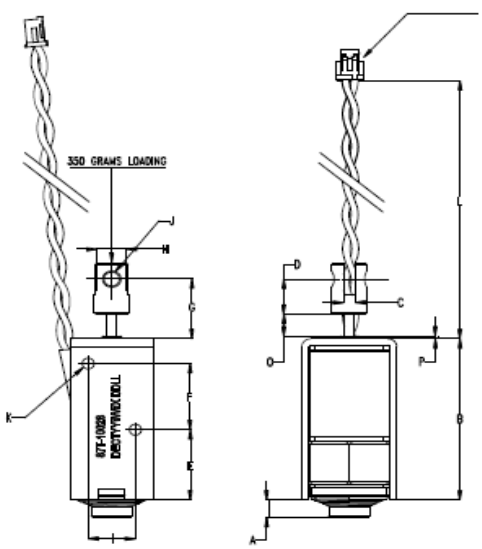

UNIT : mm.

A	=	3.40 ± 0.2
B	=	30.00 ± 0.25
C	=	2.00 ± 0.1
D	=	6.50 ± 0.1
E	=	13.20 ± 0.2
F	=	12.20 ± 0.2
G	=	10.5 ± 0.1
H	=	ø6.0 ± 0.1
I	=	8.00 ± 0.1
J	=	ø2.6 ± 0.1
K	=	4-M2.6x0.45
L	=	180 MIN.
M	=	14.00 ± 0.2
N	=	16.00 ± 0.2
O	=	3.50 ± 0.1
P	=	0.50 ± 0.1

UNLESS TOLERANCES.

X.X	=	±0.2
X.XX	=	±0.1
ANGLES	=	±1°

EXTENT POSITION.

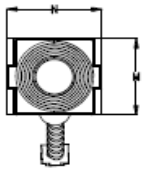

2. SCHEMATIC AND CONSTRUCTION :

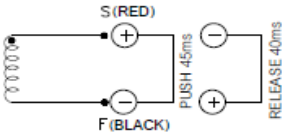

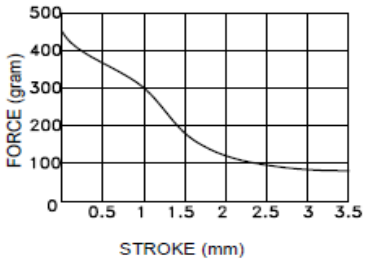

TEST CONDITION	FORCE TEST
0 Vdc.	450 GRAMS MIN. (MAGNET HOLDING WITHOUT SPRING)
NOMINAL VOLTAGE @25°C, 45±10ms PULSE WIDTH.	350 GRAMS MIN. (PLUNGER PULL-IN FORCE)
NOMINAL VOLTAGE @25°C, 40±5ms PULSE WIDTH.	350 GRAMS LOADING (DURING PLUNGER RELEASE)

* NOMINAL OPERATION DUTY CYCLE: POWER ON 40ms / OFF 2 SEC

INSULATION MATERIALS: UL CONSTRUCTION, CLASS B 130°C
LIFE EXPECTANCY: 100K CYCLES OPERATIONS

LAYER TEST	IR. @500 Vdc.	HI-POT
(S-F) 500Vp. MIN.	COIL TO FRAME	@50/60Hz.,2mA
TEST ONLY COIL	50 MOHM MIN.	COIL TO FRAME
		1200Vac.,1s

Appendix G: Mini 5V Push-Pull Solenoid from Adafruit Industries LLC [64]

TECHNICAL DETAILS

- Rated Voltage: 5V
- Current (at DC 5V): 1.1A
- DC Resistance: 4.5 ± 5% Ω
- Throw (at DC 5V): 3mm / 80g
- Lead Length: ~57mm / 2.2"
- Weight: 12.6g

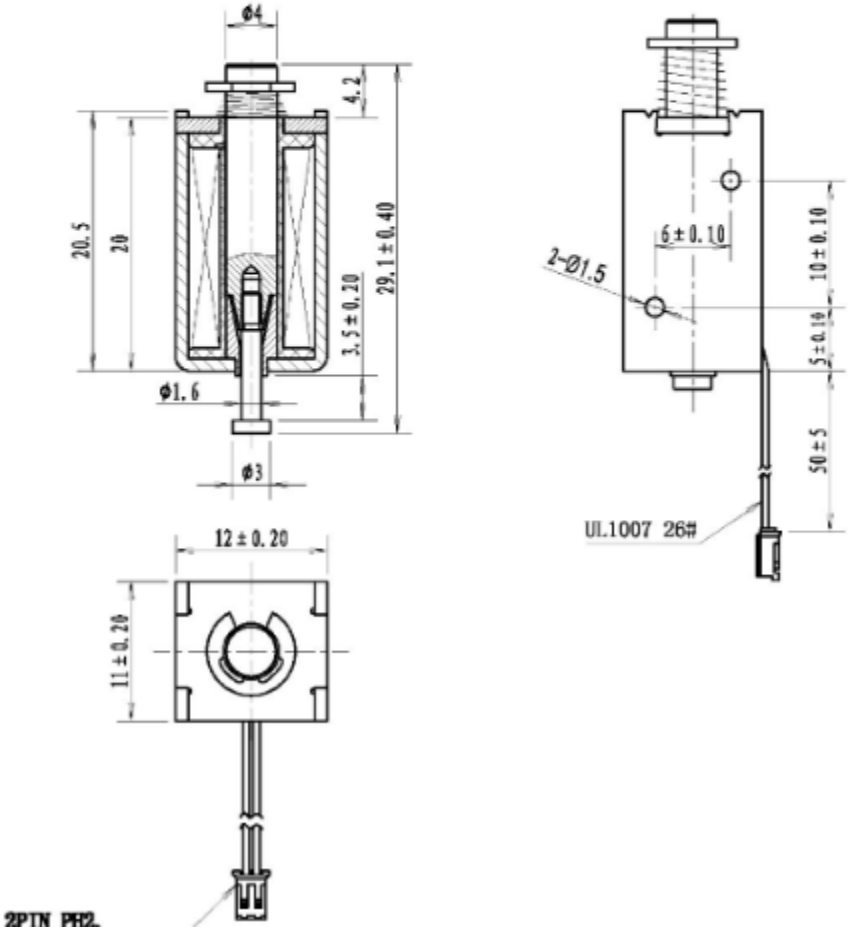

Appendix H: Edward LifeSciences TruWave Pressure Transducer [93]

(Images reproduced with kind permission from Edwards Lifesciences)

The cannula is connected to a transducer (a transducer converts one form of energy to another) via a column of heparinised saline at a pressure of 300 mmHg. The saline passes through a drip chamber adjusted to allow a flow of 4 ml/hour. This continuously flushes the tubing and cannula. The ideal solution for use is dextrose, since a non-electrical conducting fluid avoids current passing down the catheter into the heart. The transducer is a strain gauge variable transducer. If a wire is stretched it becomes longer and thinner and thus its resistance increases. This is known as a strain gauge. This is connected to an amplifier and oscilloscope.

Appendix I: TIP 102 (Complementary Silicon Power Darlington Transistors)- STMicroelectronics

TIP102
TIP107

COMPLEMENTARY SILICON POWER DARLINGTON TRANSISTORS

- STMicroelectronics PREFERRED SALESTYPES
- COMPLEMENTARY PNP - NPN DEVICES
- INTEGRATED ANTIPARALLEL COLLECTOR-EMITTER DIODE

APPLICATIONS
- LINEAR AND SWITCHING INDUSTRIAL EQUIPMENT
- AUDIO POWER AMPLIFIER
- GENERAL POWER SWITCHING
- DC-AC CONVERTER
- EASY DRIVER FOR LOW VOLTAGE DC MOTOR

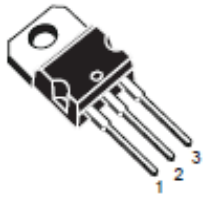

TO-220

DESCRIPTION

The TIP102 is a silicon Epitaxial-Base NPN power transistor in monolithic Darlington configuration mounted in TO-220 plastic package. It is intented for use in power linear and switching applications.

The complementary PNP type is TIP107.

INTERNAL SCHEMATIC DIAGRAM

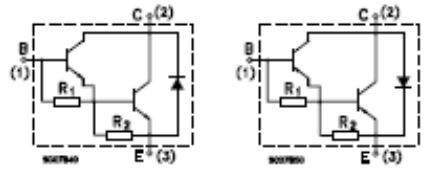

R_1 Typ. = 5 KΩ R_2 Typ. = 150 Ω

ABSOLUTE MAXIMUM RATINGS

Symbol	Parameter		Value	Unit
		NPN	TIP102	
		PNP	TIP107	
V_{CBO}	Collector-Base Voltage (I_E = 0)		100	V
V_{CEO}	Collector-Emitter Voltage (I_B = 0)		100	V
V_{EBO}	Emitter-Base Voltage (I_C = 0)		5	V
I_C	Collector Current		8	A
I_{CM}	Collector Peak Current		15	A
I_B	Base Current		1	A
P_{tot}	Total Dissipation at $T_{case} \leq 25$ °C $T_{amb} \leq 25$ °C		80 2	W W
T_{stg}	Storage Temperature		-65 to 150	°C
T_j	Max. Operating Junction Temperature		150	°C

* For PNP types voltage and current values are negative.

THERMAL DATA

$R_{thj\text{-}case}$	Thermal Resistance Junction-case	Max	1.56	°C/W
$R_{thj\text{-}amb}$	Thermal Resistance Junction-ambient	Max	62.5	°C/W

ELECTRICAL CHARACTERISTICS (T_{case} = 25 °C unless otherwise specified)

Symbol	Parameter	Test Conditions		Min.	Typ.	Max.	Unit
I_{CEO}	Collector Cut-off Current (I_B = 0)	V_{CE} = 50 V				50	µA
I_{CBO}	Collector Cut-off Current (I_E = 0)	V_{CB} = 100 V				50	µA
I_{EBO}	Emitter Cut-off Current (I_C = 0)	V_{EB} = 5 V				8	mA
$V_{CEO(sus)}$*	Collector-Emitter Sustaining Voltage (I_B = 0)	I_C = 30 mA		100			V
$V_{CE(sat)}$*	Collector-Emitter Saturation Voltage	I_C = 3 A I_C = 8 A	I_B = 6 mA I_B = 80 mA			2 2.5	V V
V_{BE}*	Base-Emitter Voltage	I_C = 8 A	V_{CE} = 4 V			2.8	V
h_{FE}*	DC Current Gain	I_C = 3 A I_C = 8 A	V_{CE} = 4 V V_{CE} = 4 V	1000 200		20000	
V_F*	Forward Voltage of Commutation Diode (I_B = 0)	I_F = - I_C = 10 A				2.8	V

* Pulsed: Pulse duration = 300 µs, duty cycle 1.5 %
For PNP types voltage and current values are negative.

Safe Operating Area

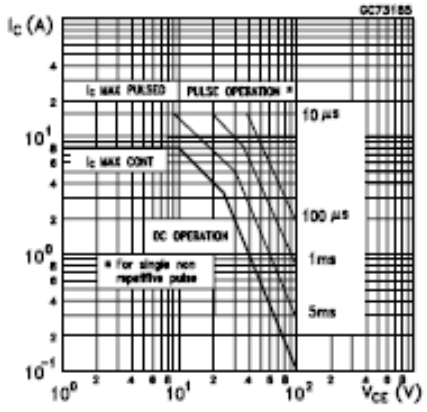

TO-220 MECHANICAL DATA

DIM.	mm			inch		
	MIN.	TYP.	MAX.	MIN.	TYP.	MAX.
A	4.40		4.60	0.173		0.181
C	1.23		1.32	0.048		0.052
D	2.40		2.72	0.094		0.107
E	0.49		0.70	0.019		0.027
F	0.61		0.88	0.024		0.034
F1	1.14		1.70	0.044		0.067
F2	1.14		1.70	0.044		0.067
G	4.95		5.15	0.194		0.202
G1	2.40		2.70	0.094		0.106
H2	10.00		10.40	0.394		0.409
L2		16.40			0.645	
L4	13.00		14.00	0.511		0.551
L5	2.65		2.95	0.104		0.116
L6	15.25		15.75	0.600		0.620
L7	6.20		6.60	0.244		0.260
L9	3.50		3.93	0.137		0.154
M		2.60			0.102	
DIA.	3.75		3.85	0.147		0.151

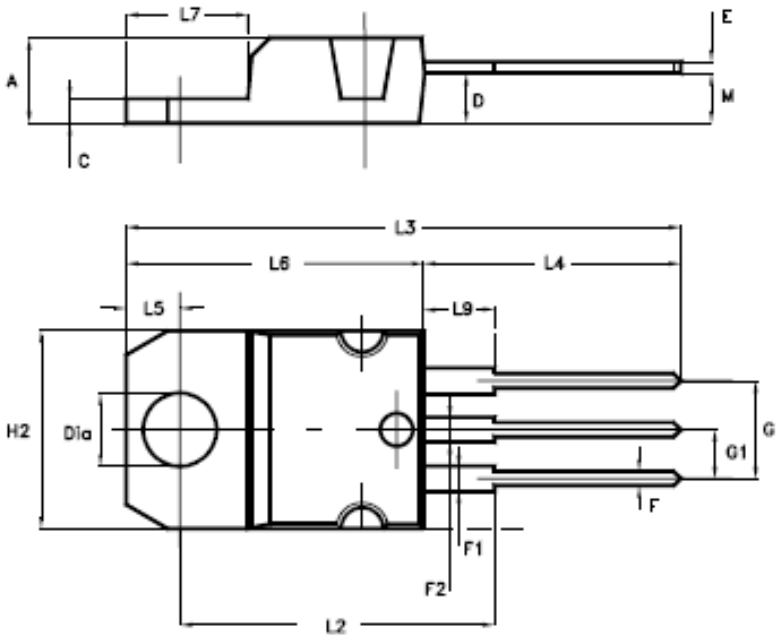

Appendix J: iC-GE PWM Relay/ Solenoid Driver IC (1A)

DRIVER iCs › Relay/Solenoid Drivers › iC-GE

iC-GE PWM Relay/Solenoid Driver for a Wide Operating Voltage Range (1 A)

Applications
- PWM driver for inductive loads (e.g. relays, electrovalves)
- Relay low-/high-side switch

Features
- Current control for inductive actuators at 24 V (10 to 36 V)
- High efficient current control up to 1 A
- Switching with power saving and reduced power dissipation
- Individual setting of energising and hold current
- Contact conserving switching of relays synchronous to the mains
- Monitoring of coil current, supply voltage and temperature
- Shutdown with overtemperature and undervoltage
- Status indication via LED or logic output
- Fast demagnetising due to 15 V countervoltage
- High PWM frequency with frequency spreading for low EMI
- Energising time of 50 ms prolongable with external capacitor

Packages

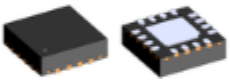

QFN16 4x4

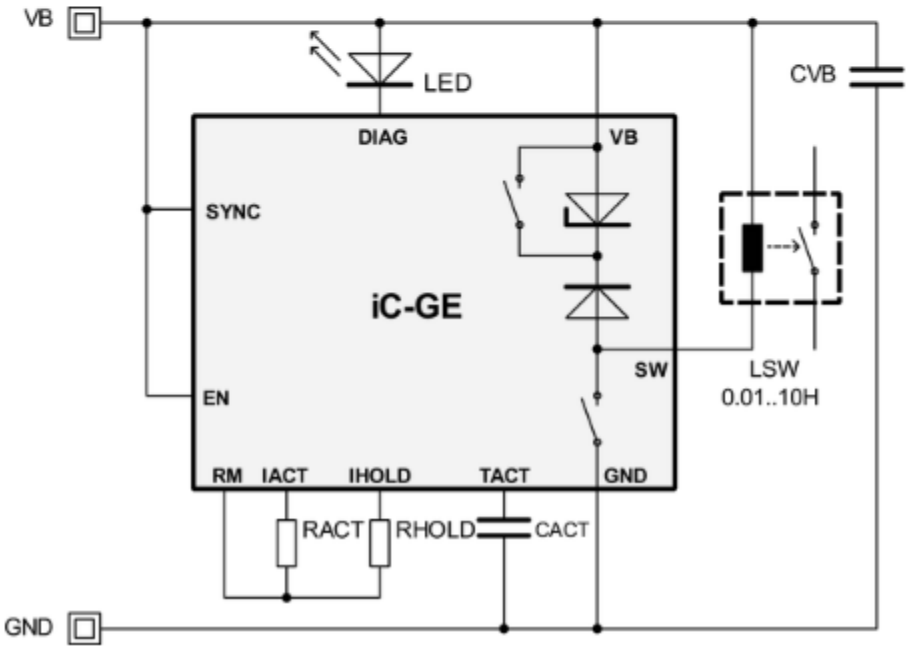

Appendix K: OrCAD Circuit Schematics

Schematic 1: Adafruit recommended Circuit [64]

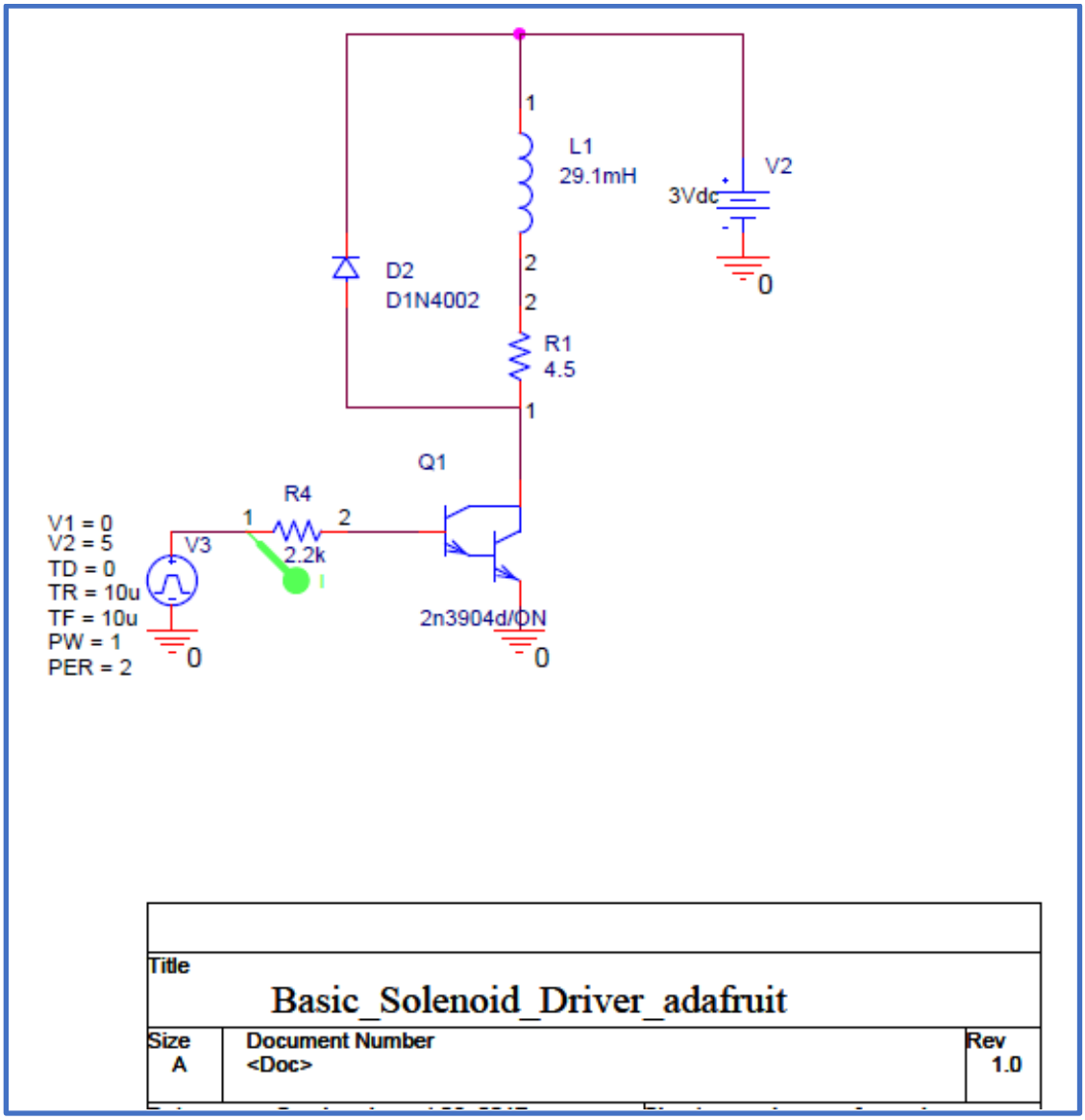

Schematic 2: Power Reduction Circuit

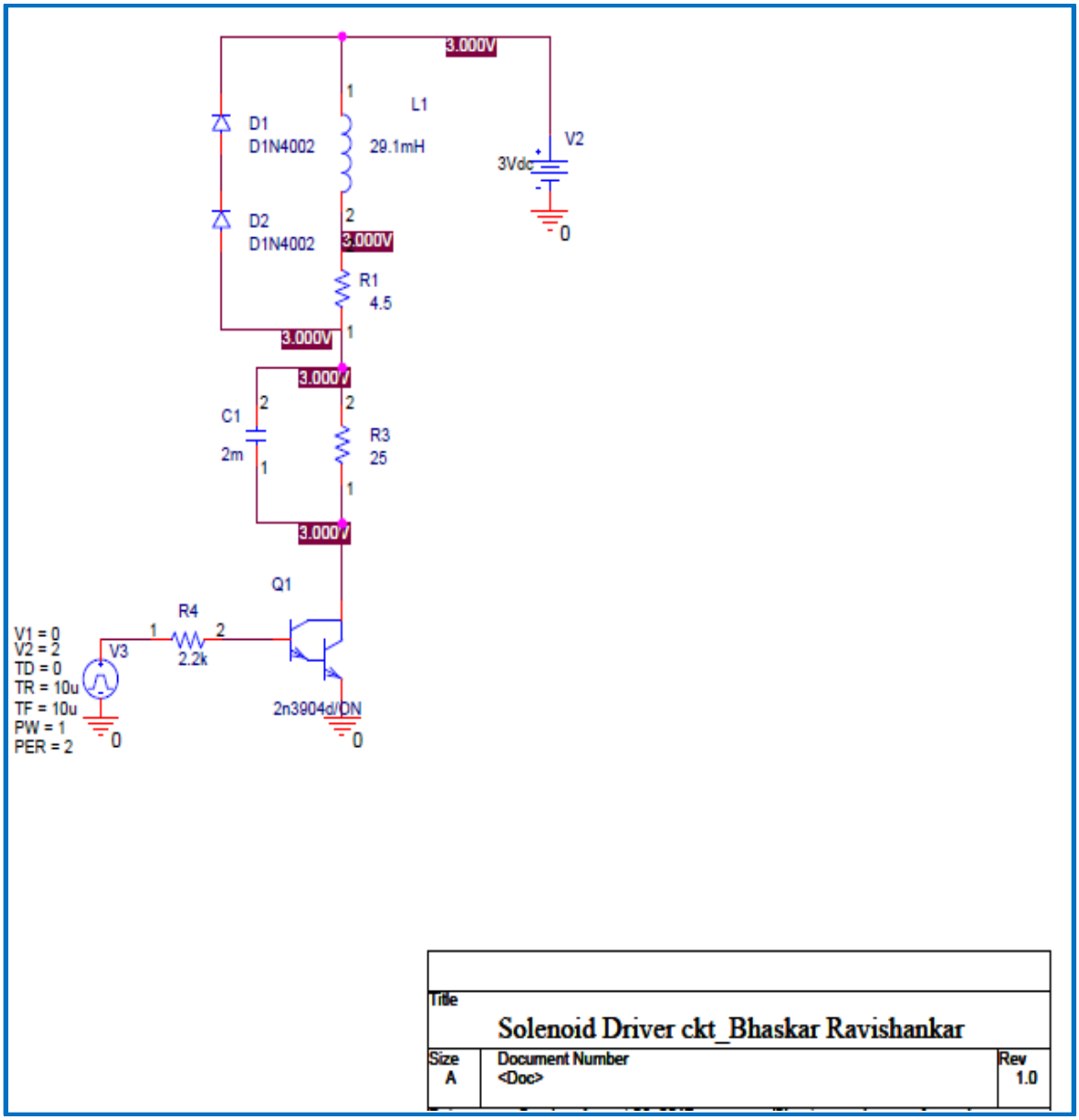

Appendix L: Particle Photon Wi-Fi Module for Wireless Communication [78]

Photon $19.00

A tiny, reprogrammable Wi-Fi development kit for prototyping and scaling your Internet of Things product

Photon with headers - $19.00

ADD TO CART

SEE MORE

The Photon is a $19 tiny Wi-Fi development kit for creating connected projects and products for the Internet of Things. It's easy to use, it's powerful, and it's connected to the cloud.

The tools that make up the Photon's ecosystem (and come along with the board) are designed to let you build and create whether you're an embedded engineer, web developer, Arduino enthusiast or IoT entrepreneur. You'll be able to write your firmware in our web or local IDE, deploy it over the air, and build your web and mobile apps with ParticleJS and our Mobile SDKs.

The board itself uses a Cypress wi-fi chip (one that can be found in Nest Protect, LIFX, and Amazon Dash) alongside a powerful STM32 ARM Cortex M3 microcontroller. It's like the Spark Core. But better.

Does not ship with breadboard or USB cable. This board can ship with or without headers. Photons with headers are great for using with breadboards; Photons without headers are best for surface mounting and special applications.

Buying more than 50? See our Wholesale store.

SPECS:

- Particle P0 Wi-Fi module
- Cypress BCM43362 Wi-Fi chip
- STM32F205 120Mhz ARM Cortex M3
- 1MB flash, 128KB RAM
- 802.11b/g/n
- Soft AP setup
- FCC/CE/IC certified
- Full specs here